



Mapping the blazar radiation zone with X-ray polarization and TeV gamma-ray observations

Manel Errando
Washington University in St Louis

on behalf of the VERITAS Collaboration

Polarization measures B field geometry

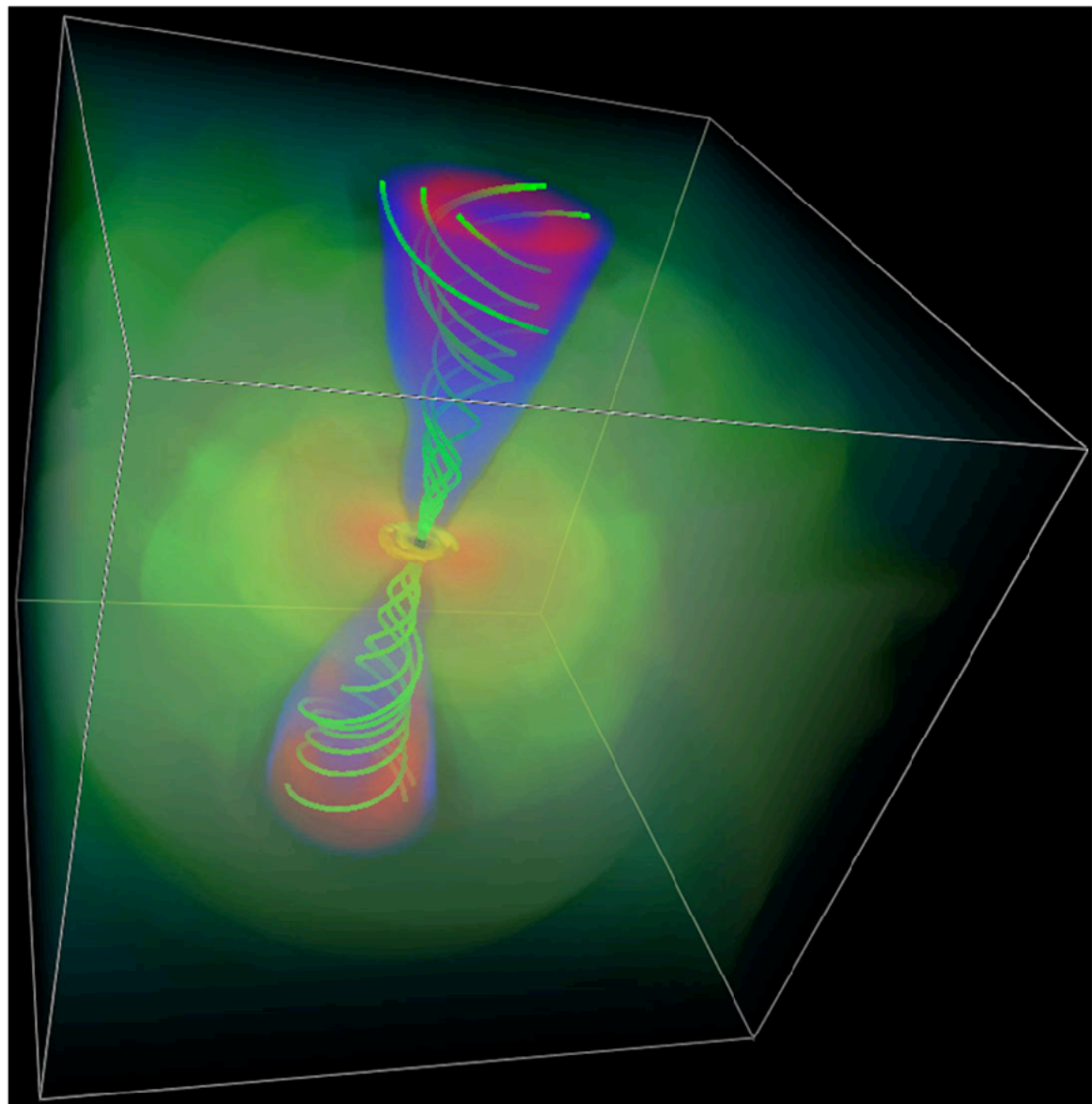


X-rays
Reveal skeleton

Polarization measures B field geometry



X-rays
Reveal skeleton

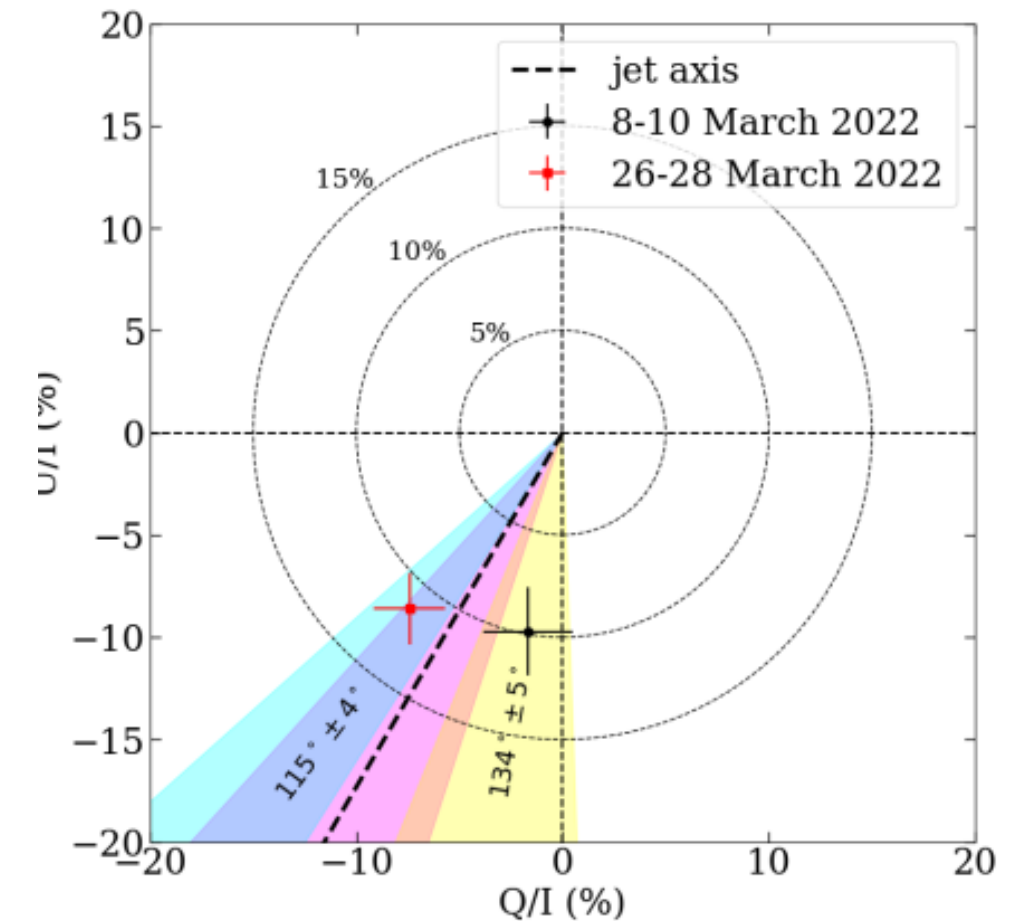
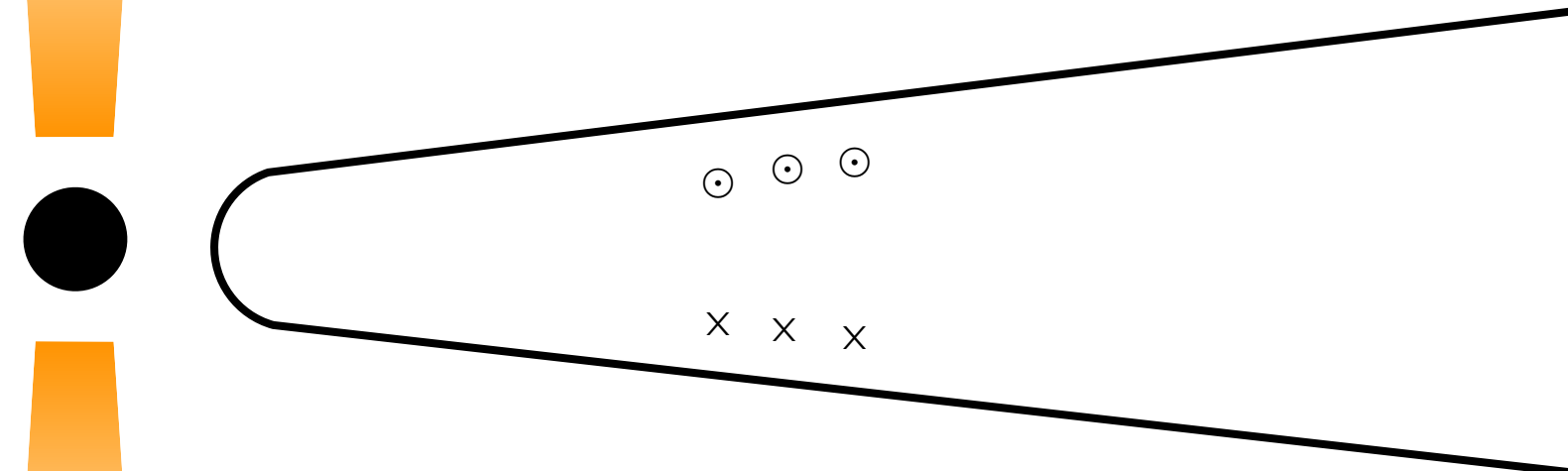


X-ray polarization
Reveals magnetic field structure in
astrophysical objects

McKinney + Blandford 2009

First blazar observation: Mrk 501

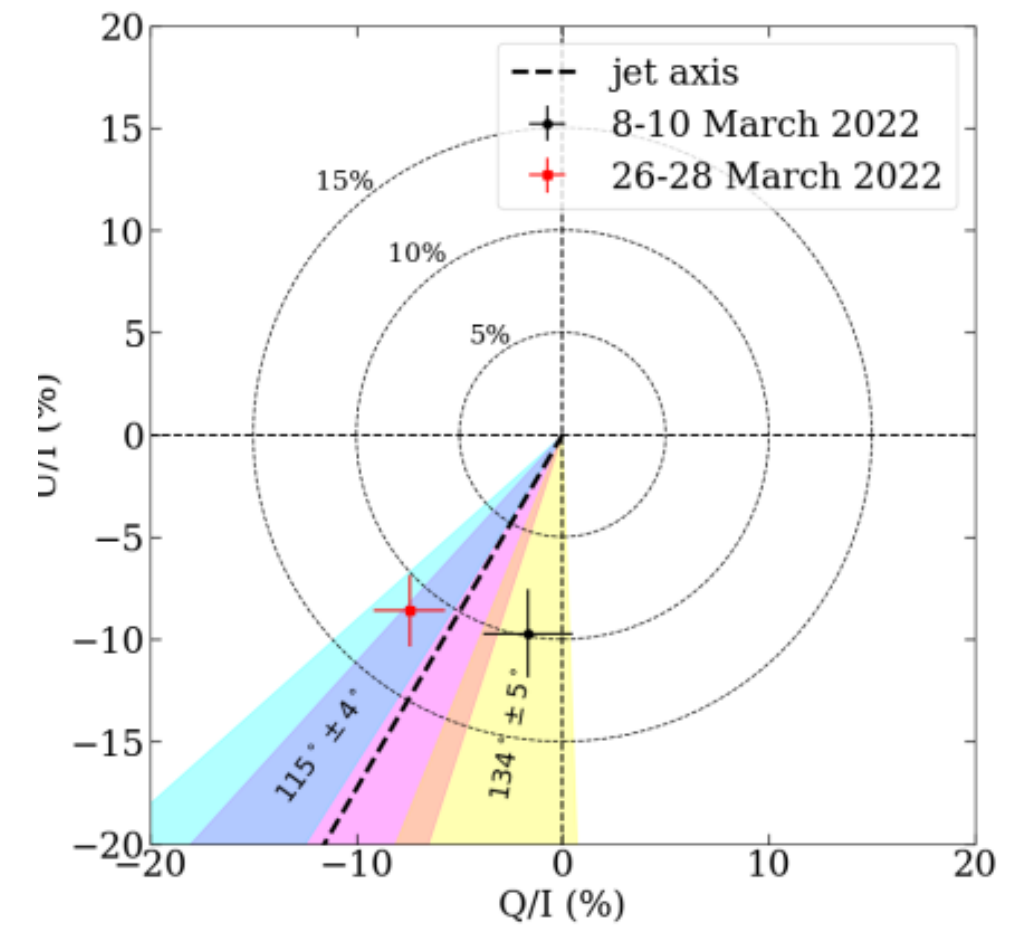
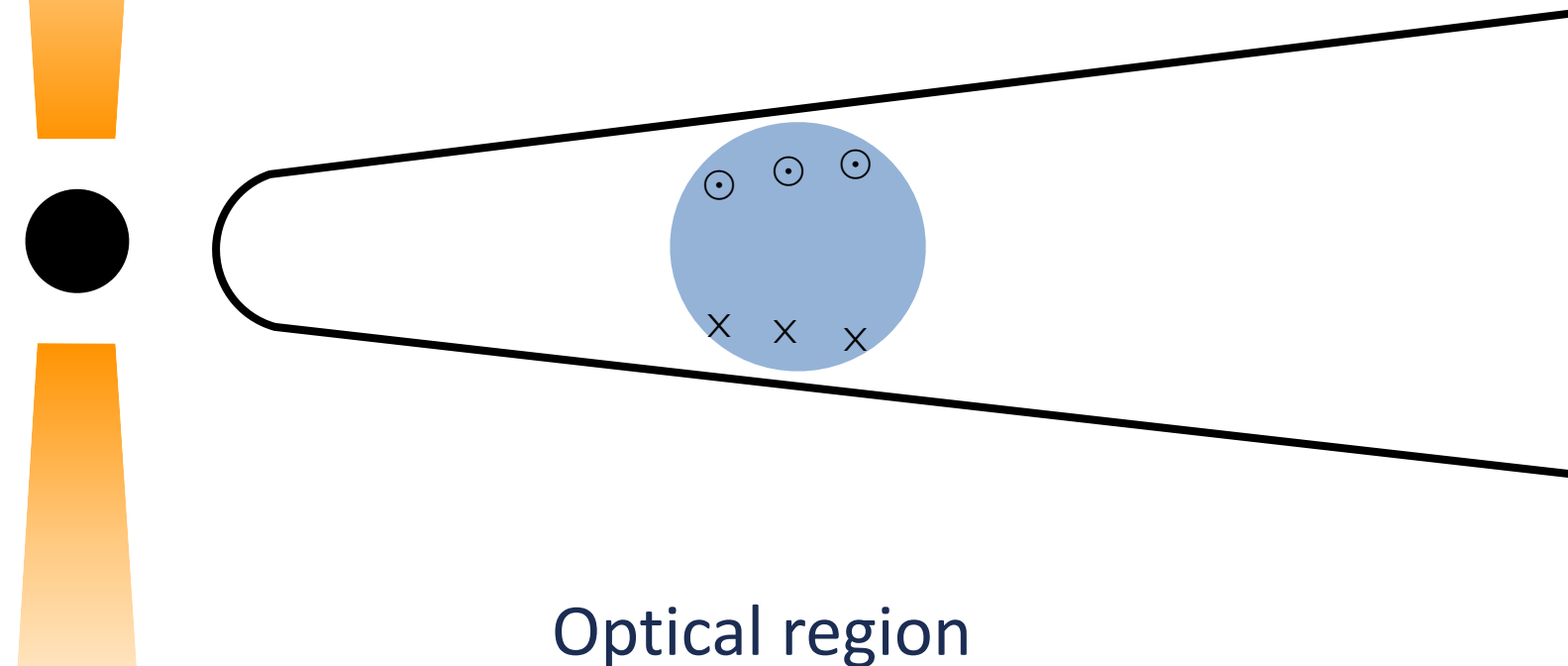
- X-ray polarization $11\% \pm 2\%$
- Optical polarization $4\% \pm 1\%$



Liodakis, et al. (2022) Nature, 611, 677

First blazar observation: Mrk 501

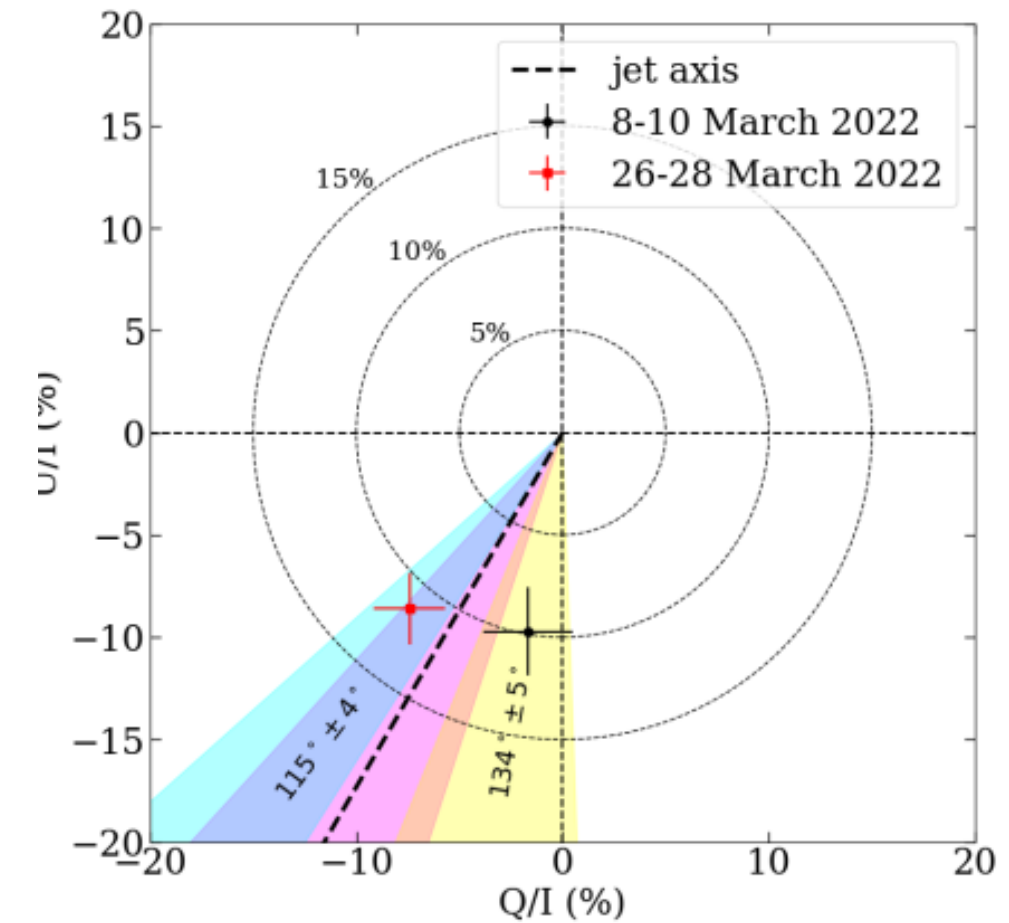
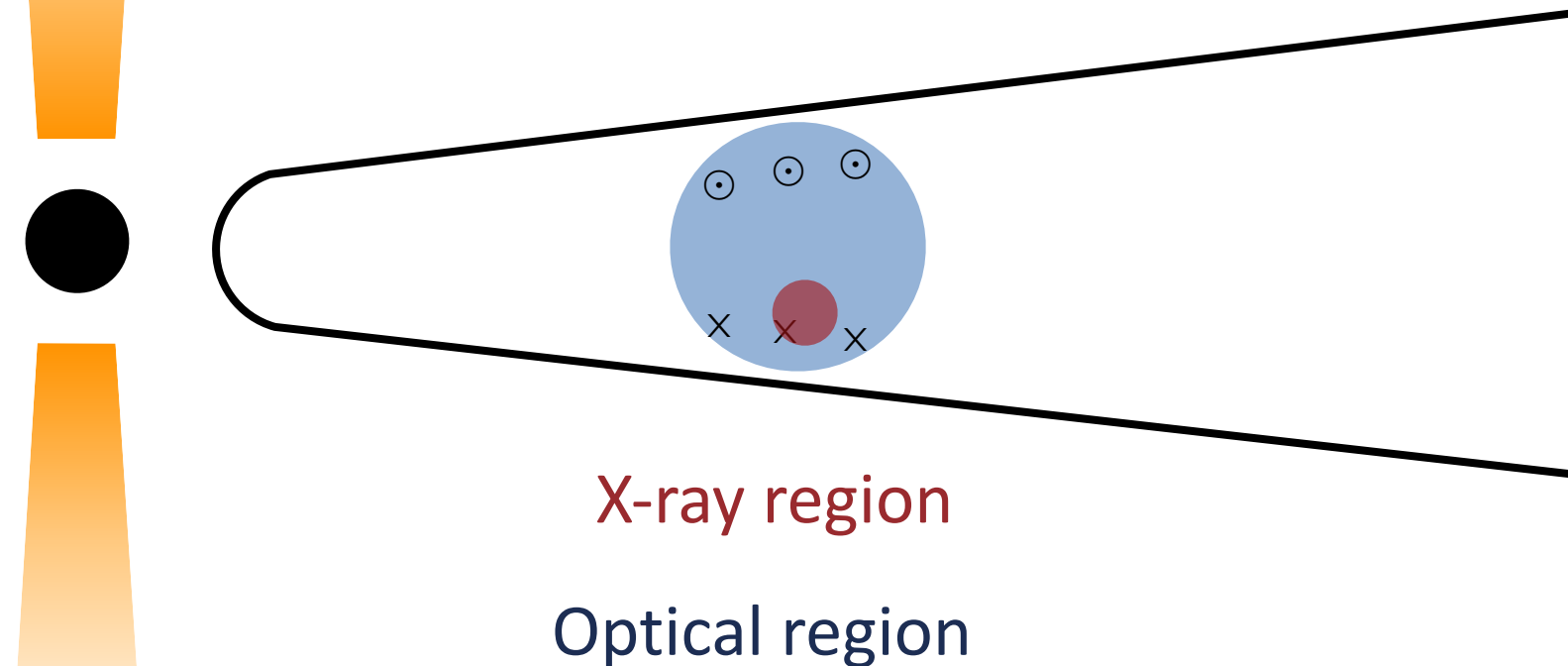
- X-ray polarization $11\% \pm 2\%$
- Optical polarization $4\% \pm 1\%$



Liodakis, et al. (2022) Nature, 611, 677

First blazar observation: Mrk 501

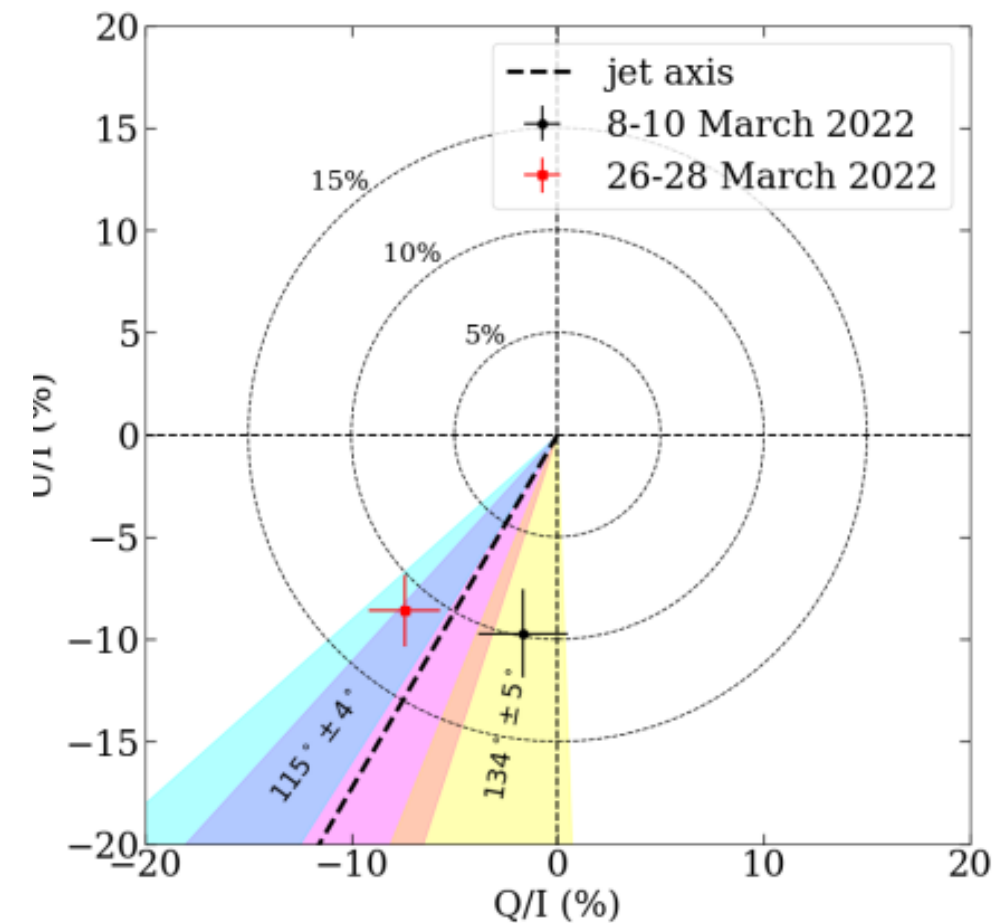
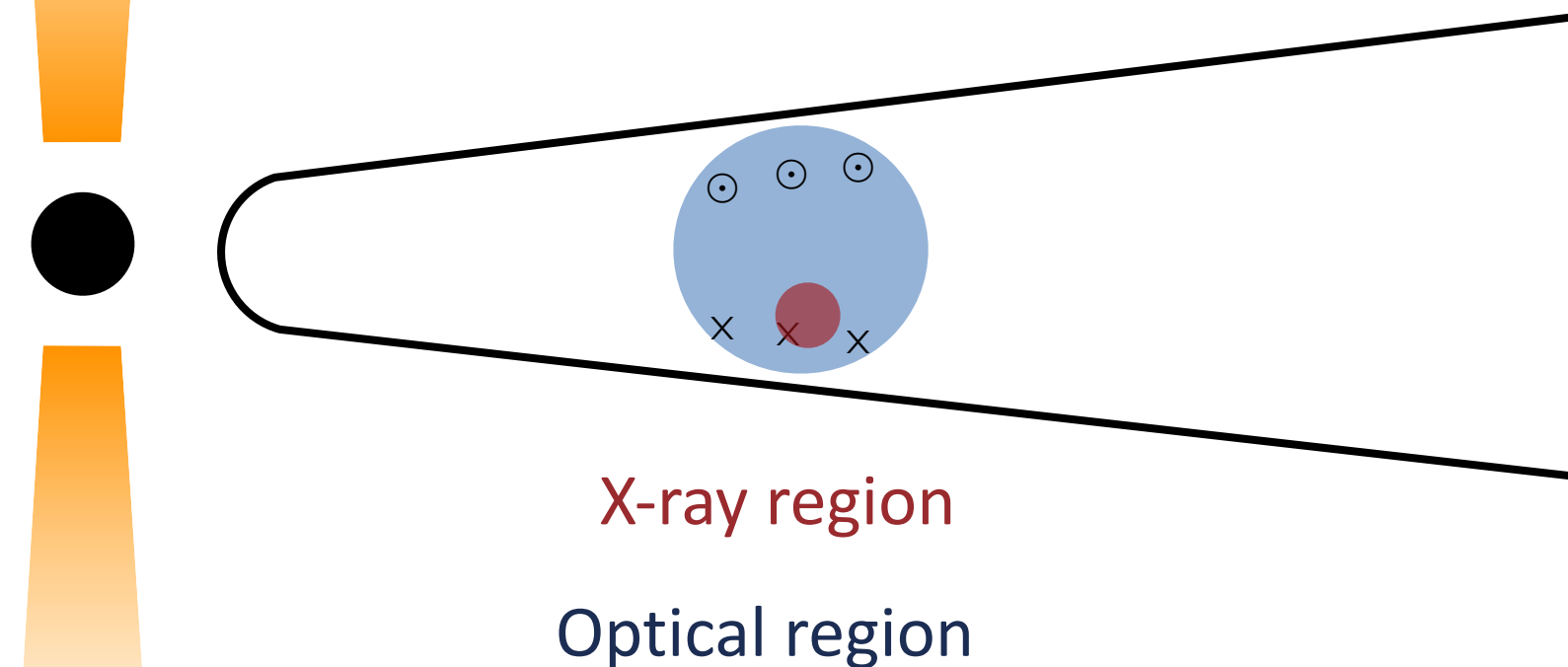
- X-ray polarization $11\% \pm 2\%$
- Optical polarization $4\% \pm 1\%$



Liodakis, et al. (2022) Nature, 611, 677

First blazar observation: Mrk 501

- X-ray polarization $11\% \pm 2\%$
- Optical polarization $4\% \pm 1\%$



Liodakis, et al. (2022) Nature, 611, 677

The X-ray emitting region in relativistic jets is more compact than the that at longer wavelengths. The highest-energy particles occupy a small volume and radiate quickly.

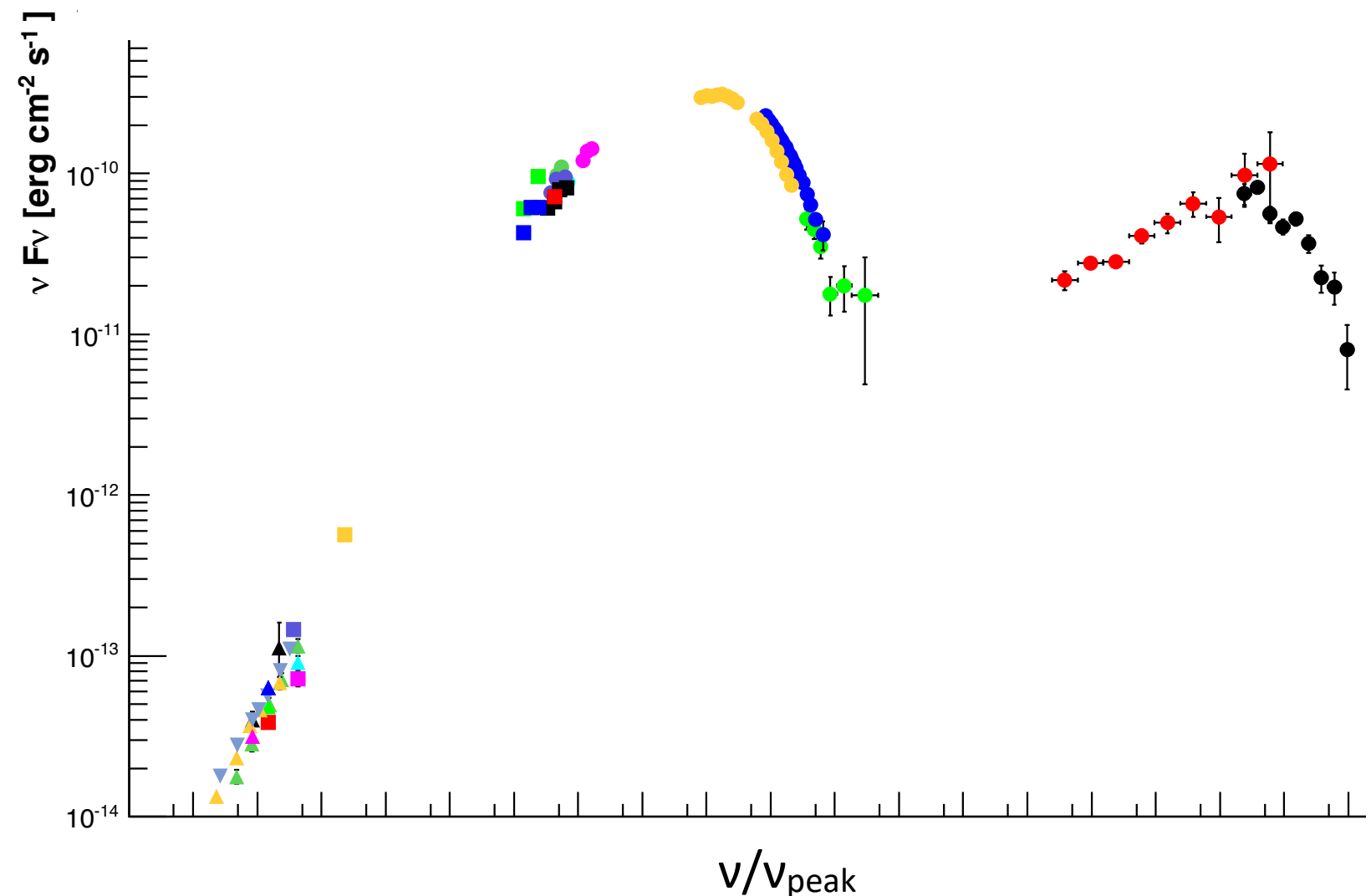
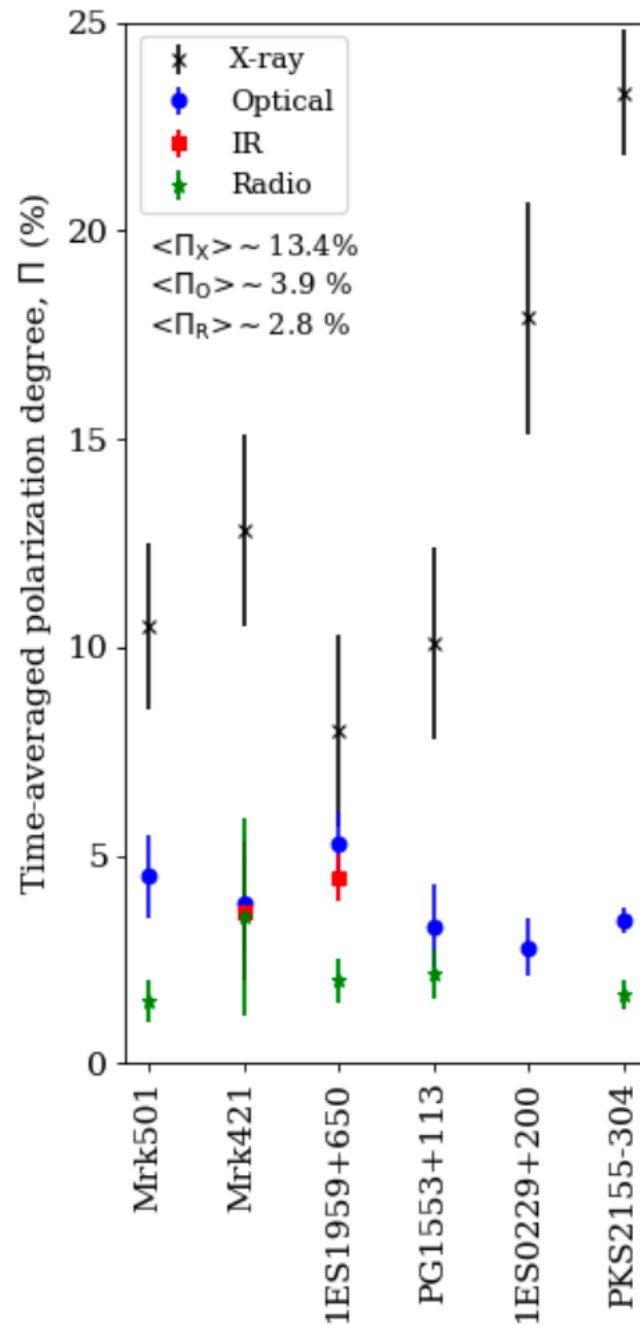
Summary of X-ray polarization results

Source	Reference	X-ray polarization
Mrk 421	Di Gesu+ 2022	~15%
Mrk 501	Liodakis+ 2022	~10%
BL Lac	Middei+ 2023	< 12.6% (UL)
BL Lac flare	Peirson+ 2023	~22%
PG 1553+113	Middei+ 2023	~10%
Mrk 421	Di Gesu+ 2023	~10%, rotation
1ES 0229+200	Ehlert+ 2023	~18%
Mrk 421	Kim+ 2024	~14%
1ES 1959+650	Errando+ 2024	~8%, <5% (UL)
PKS 2155-304	Kouch+, 2024	~30%, ~15%
Mrk 501	Chen+ 2024	~9%, ~6%, ~18%
3C 273, 3C 279, 3C 454.3, S5 0716+714	Marshall+ 2024	<10-30% (UL)

Summary of X-ray polarization results

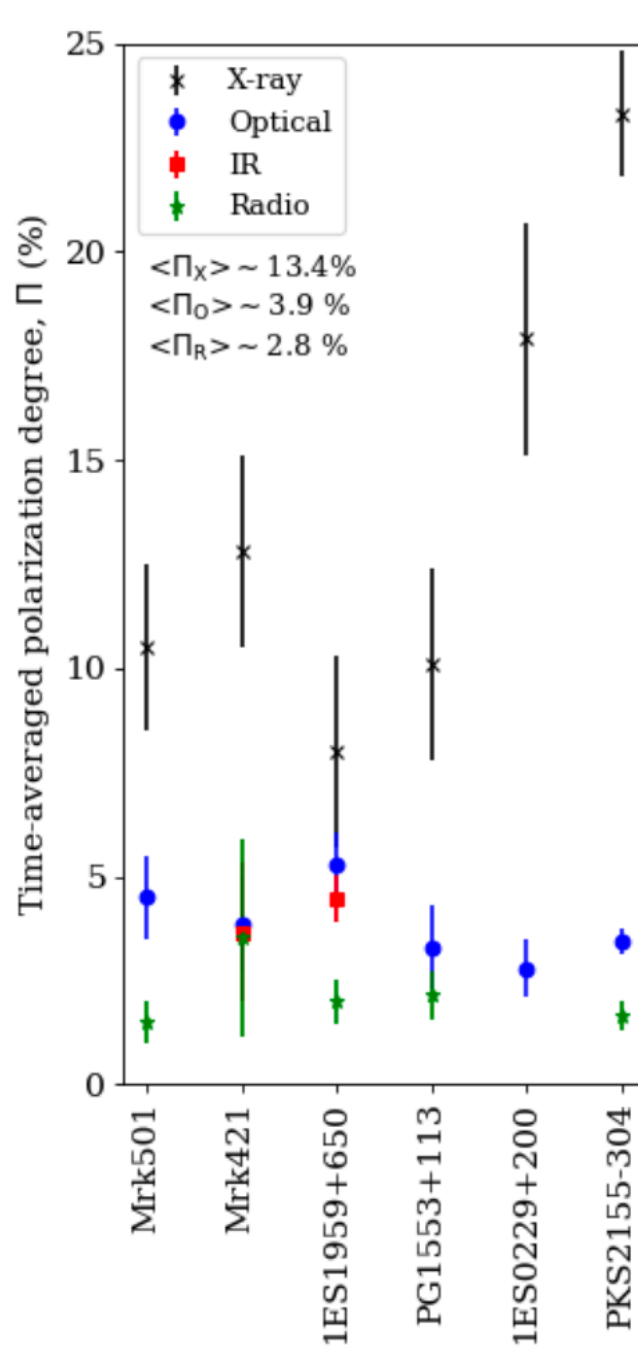
Source	Reference	X-ray polarization	TeV (VERITAS)
Mrk 421	Di Gesu+ 2022	~15%	✓
Mrk 501	Liodakis+ 2022	~10%	✓
BL Lac	Middei+ 2023	< 12.6% (UL)	✓
BL Lac flare	Peirson+ 2023	~22%	✓
PG 1553+113	Middei+ 2023	~10%	
Mrk 421	Di Gesu+ 2023	~10%, rotation	✓ (not rotation)
1ES 0229+200	Ehlert+ 2023	~18%	UL
Mrk 421	Kim+ 2024	~14%	
1ES 1959+650	Errando+ 2024	~8%, <5% (UL)	✓
PKS 2155-304	Kouch+, 2024	~30%, ~15%	
Mrk 501	Chen+ 2024	~9%, ~6%, ~18%	✓
3C 273, 3C 279, 3C 454.3, S5 0716+714	Marshall+ 2024	<10-30% (UL)	0716+714 (UL)

Polarization, blazar jets

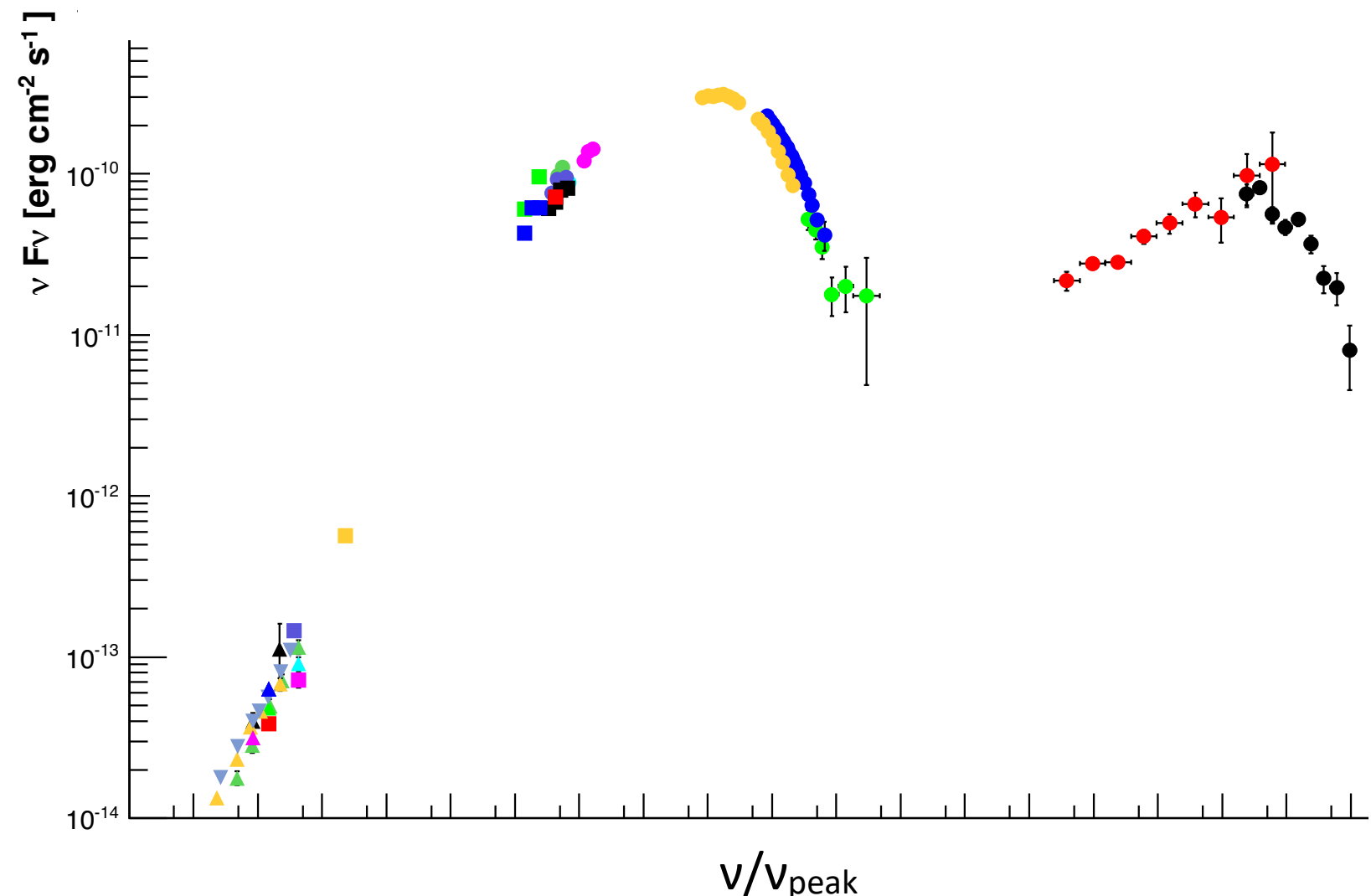


More often than not:
EVPA is aligned with the jet direction
X-ray polarization is higher than optical polarization

Polarization, blazar jets

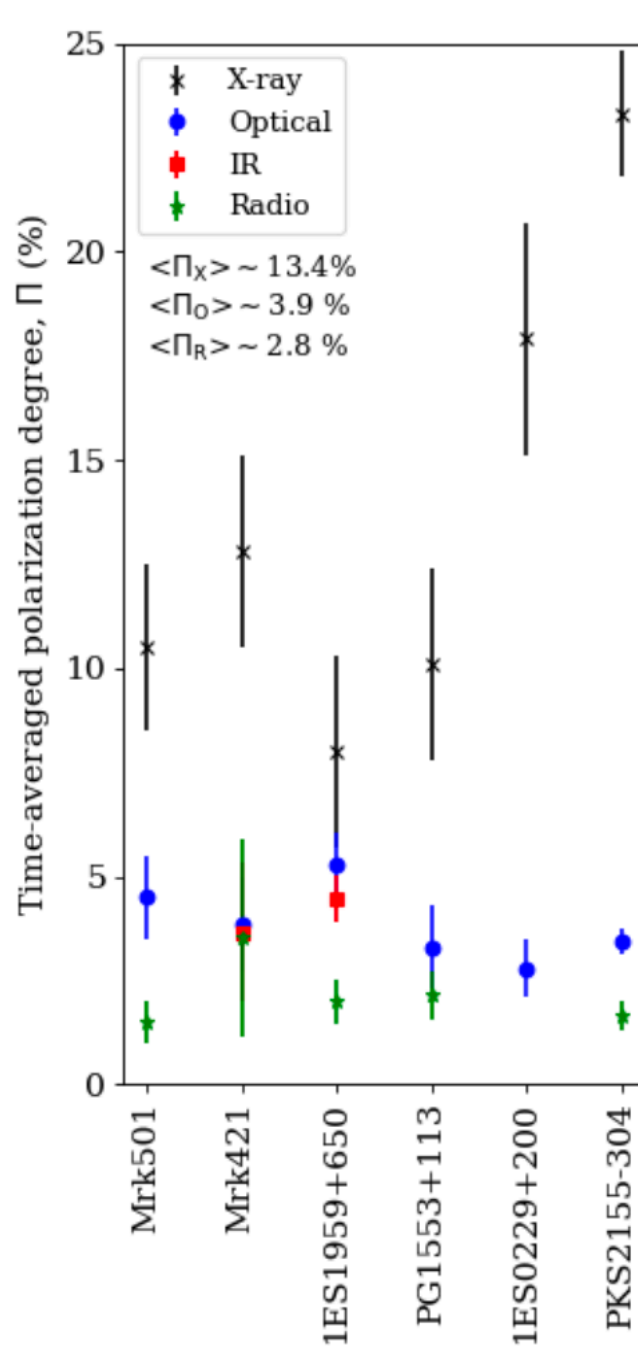


Increasing polarization → Ordered B → More compact region

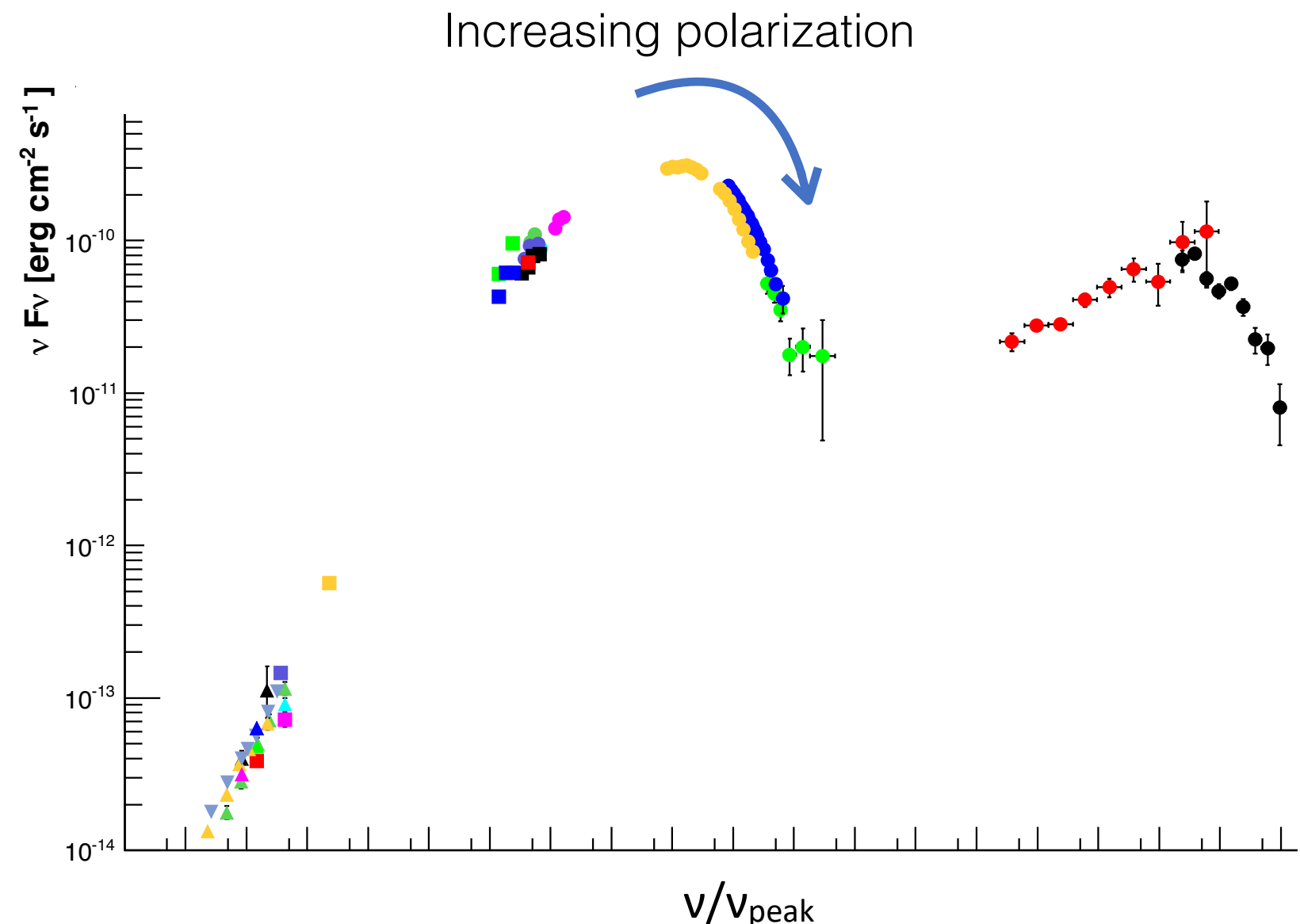


More often than not:
EVPA is aligned with the jet direction
X-ray polarization is higher than optical polarization

Polarization, blazar jets

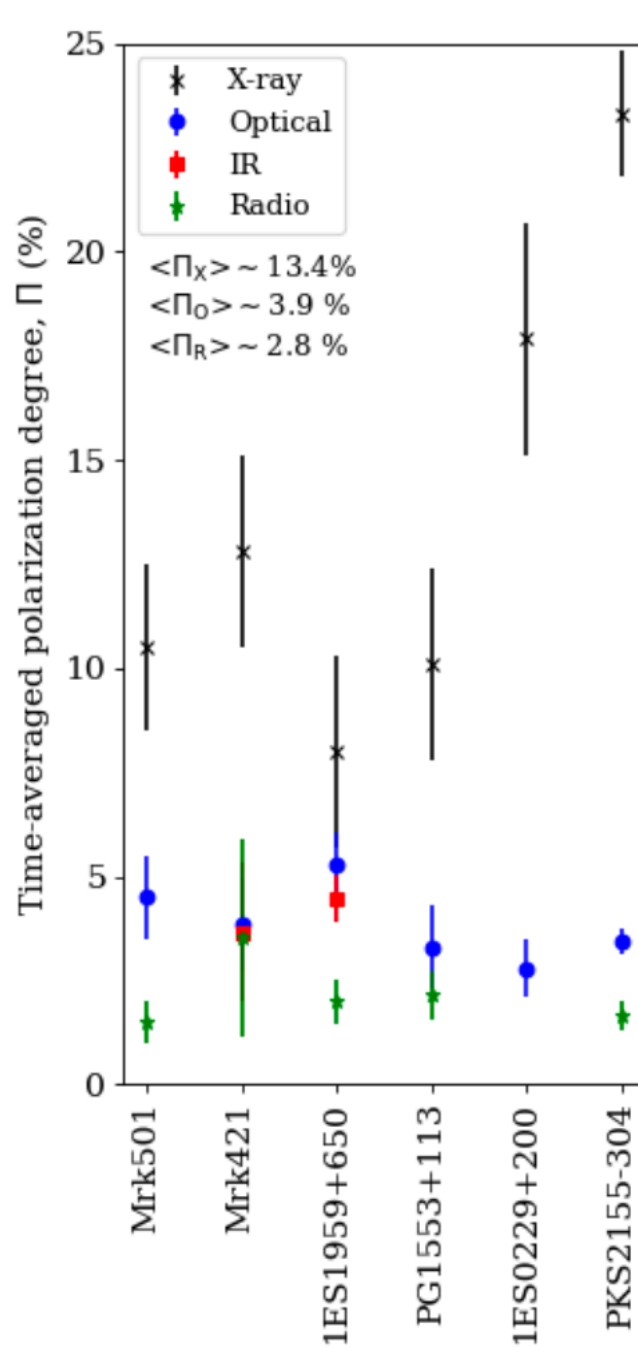


Increasing polarization \rightarrow Ordered B \rightarrow More compact region

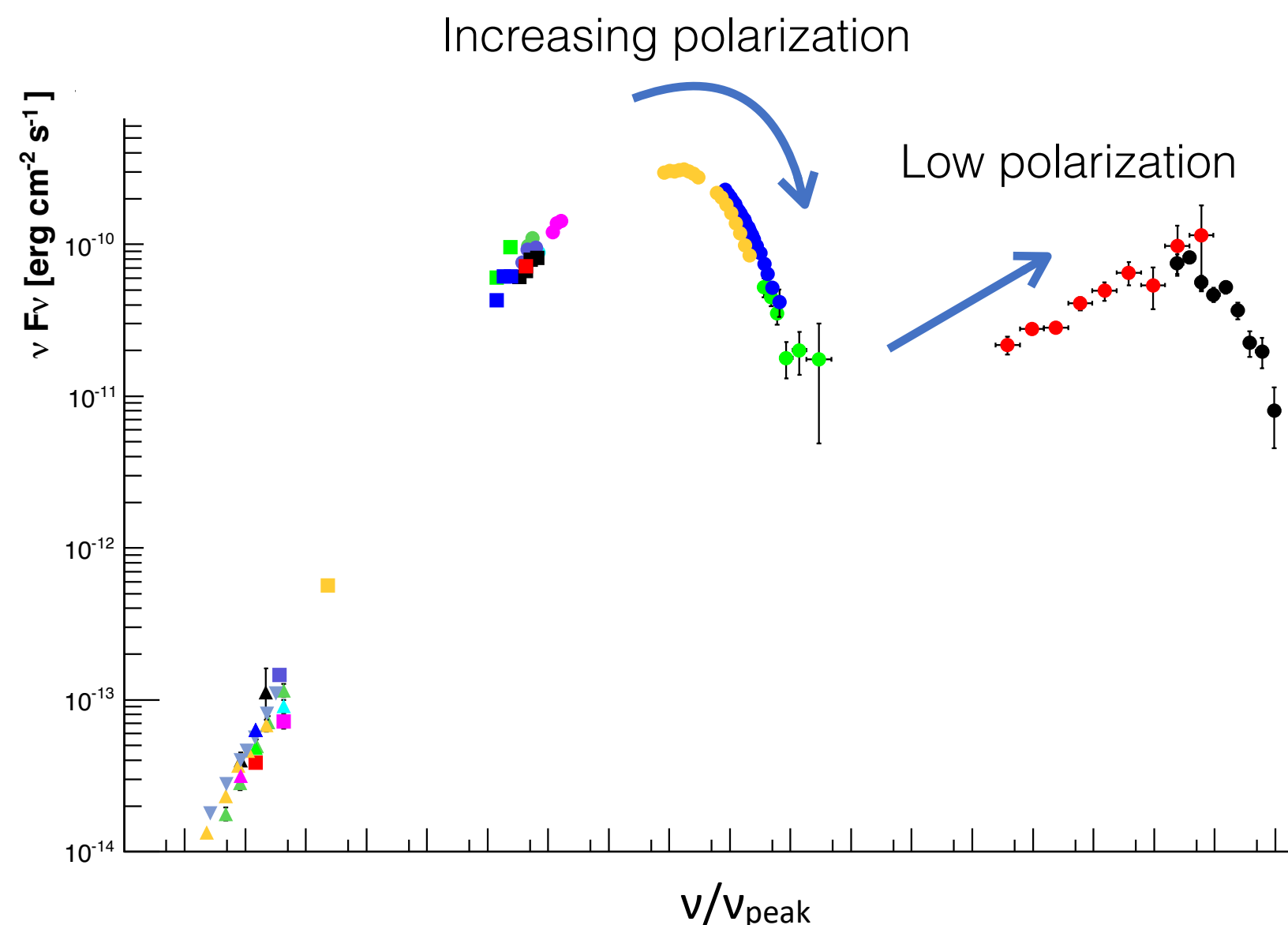


More often than not:
EVPA is aligned with the jet direction
X-ray polarization is higher than optical polarization

Polarization, blazar jets



Increasing polarization \rightarrow Ordered B \rightarrow More compact region

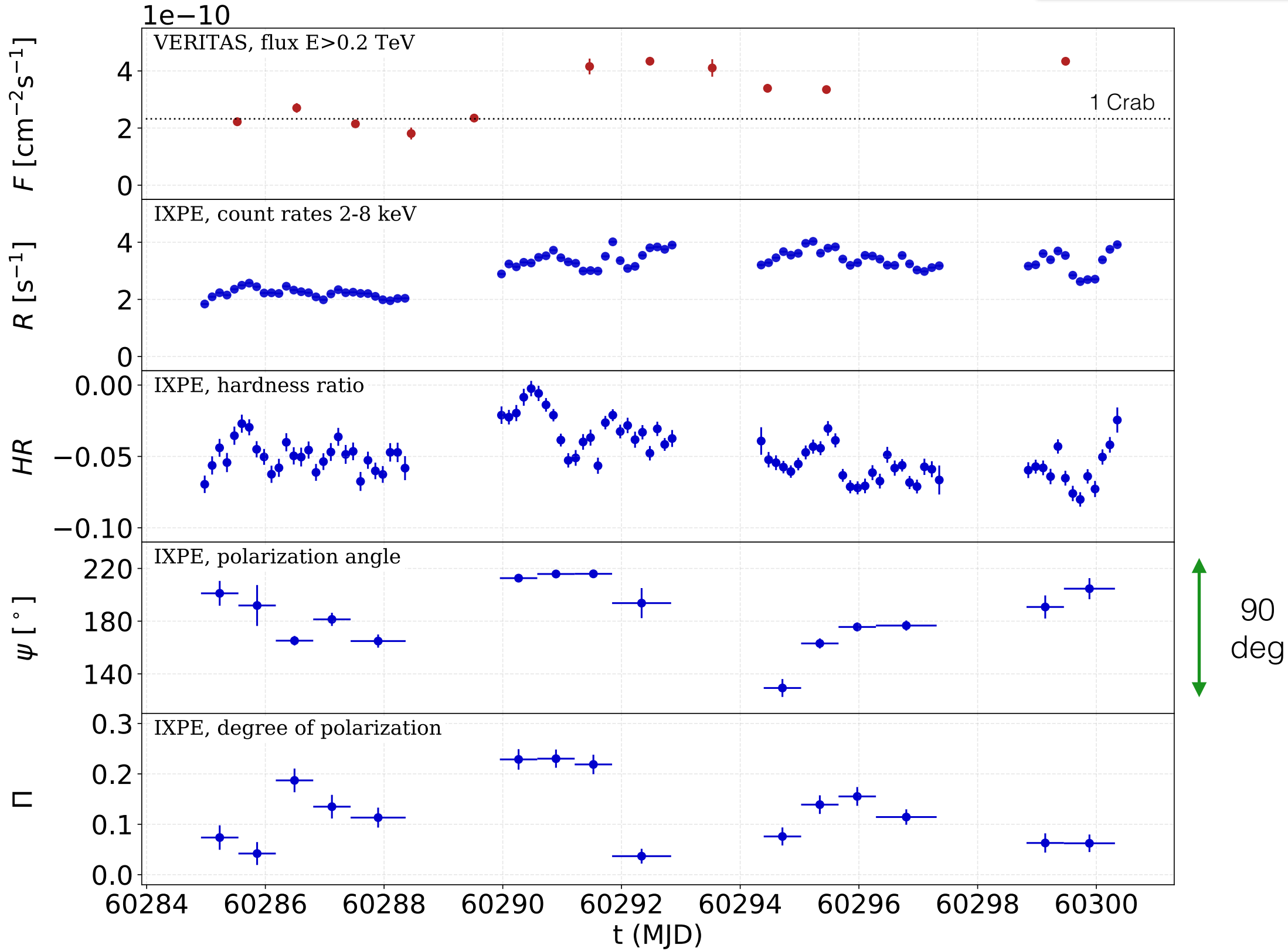


More often than not:
EVPA is aligned with the jet direction
X-ray polarization is higher than optical polarization

Jet dynamics: Mrk 421 with VERITAS

Mrk 421, 7-22 Dec 2023

VERITAS coll., in prep

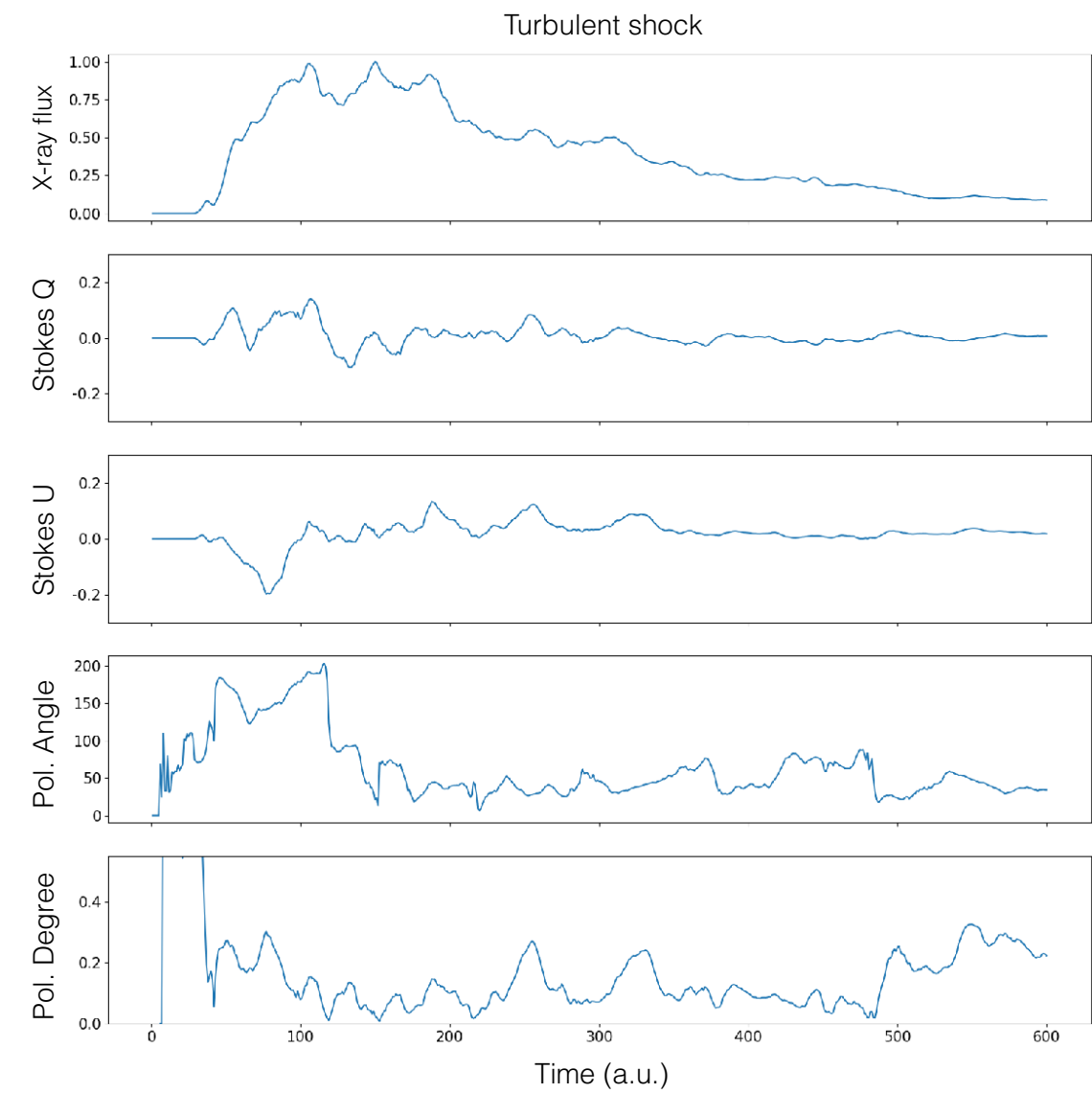
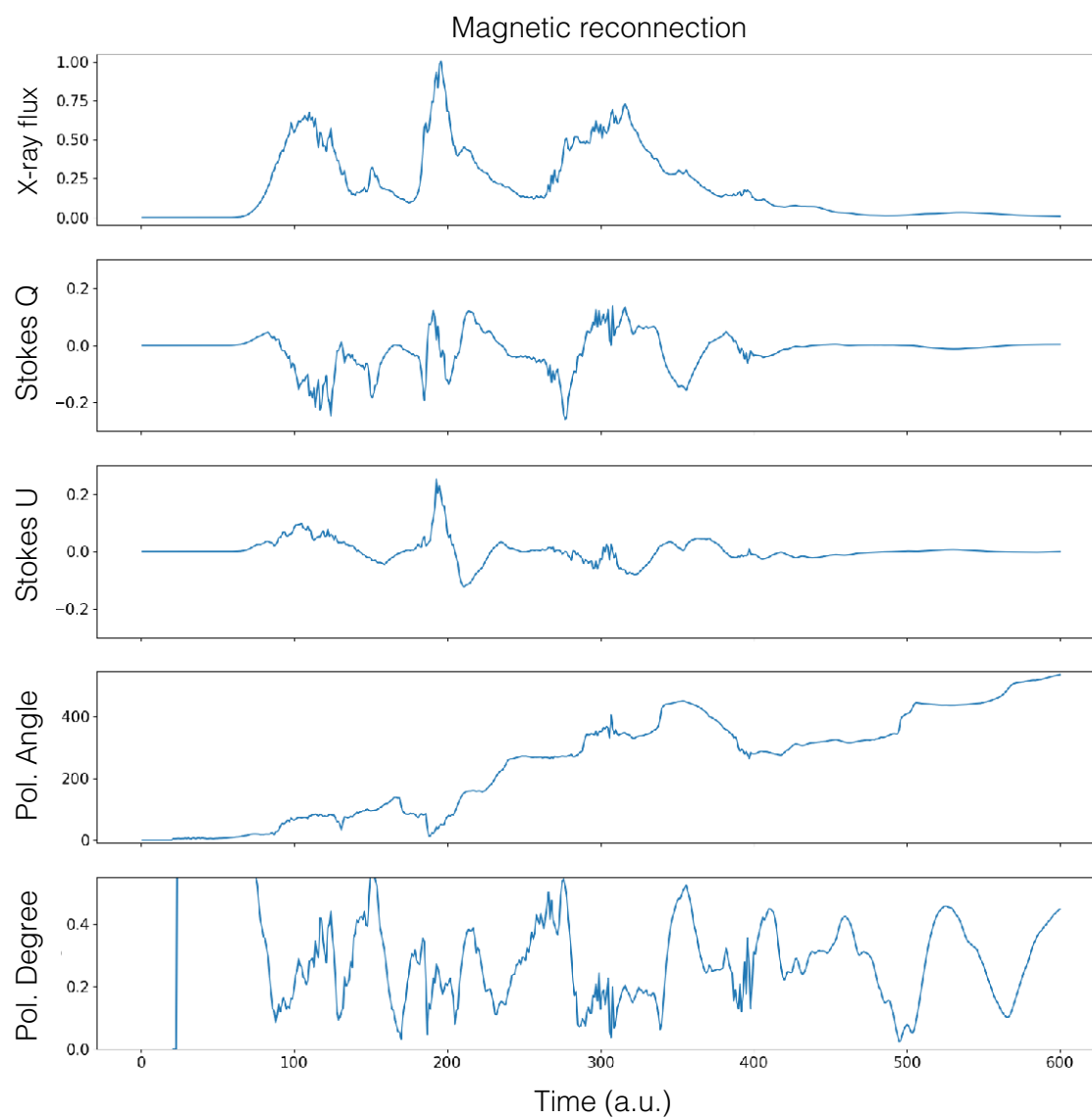


Particle-in-cell simulations

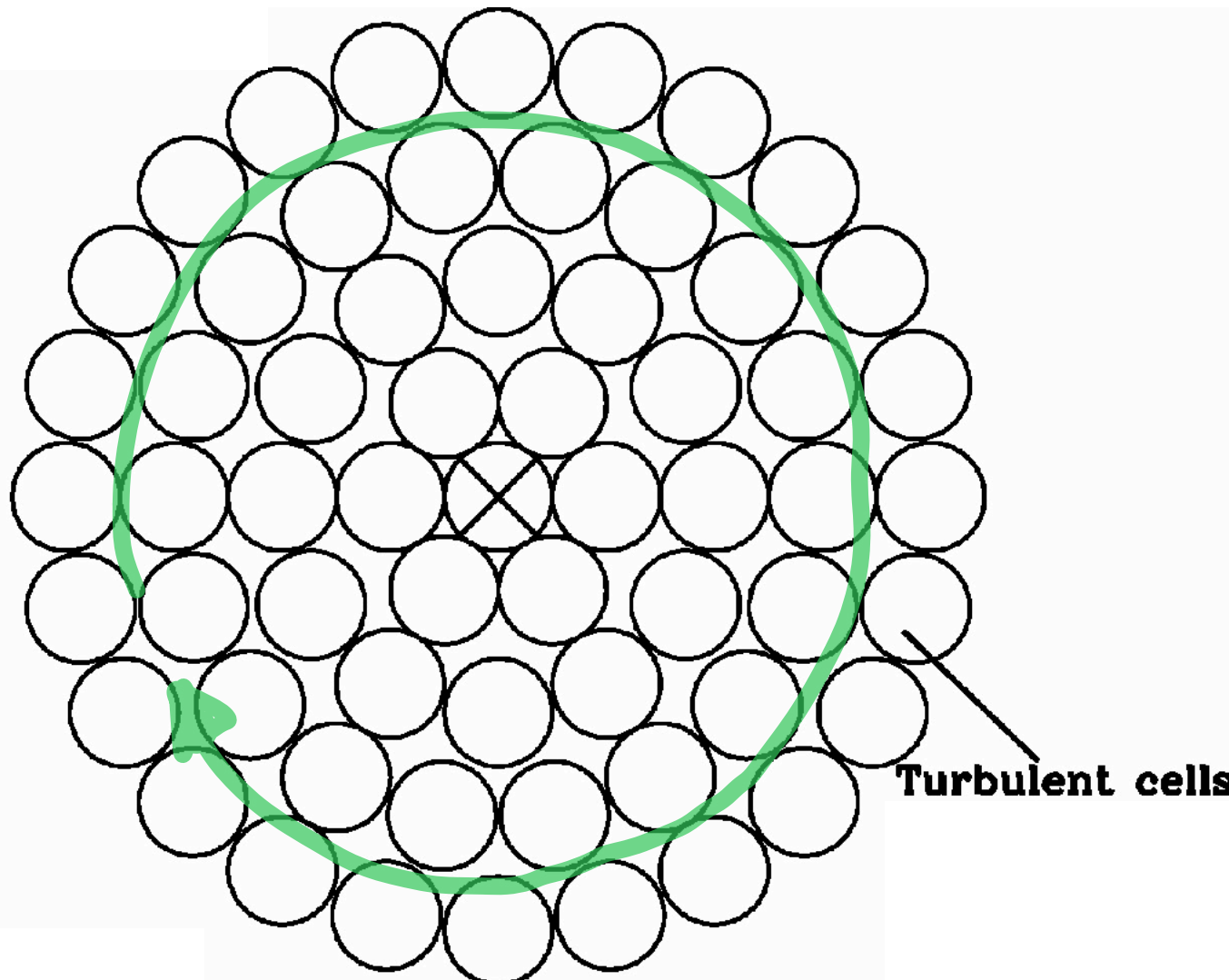


In collaboration with Haocheng Zhang
(NASA Goddard)

Zhang+ 2018



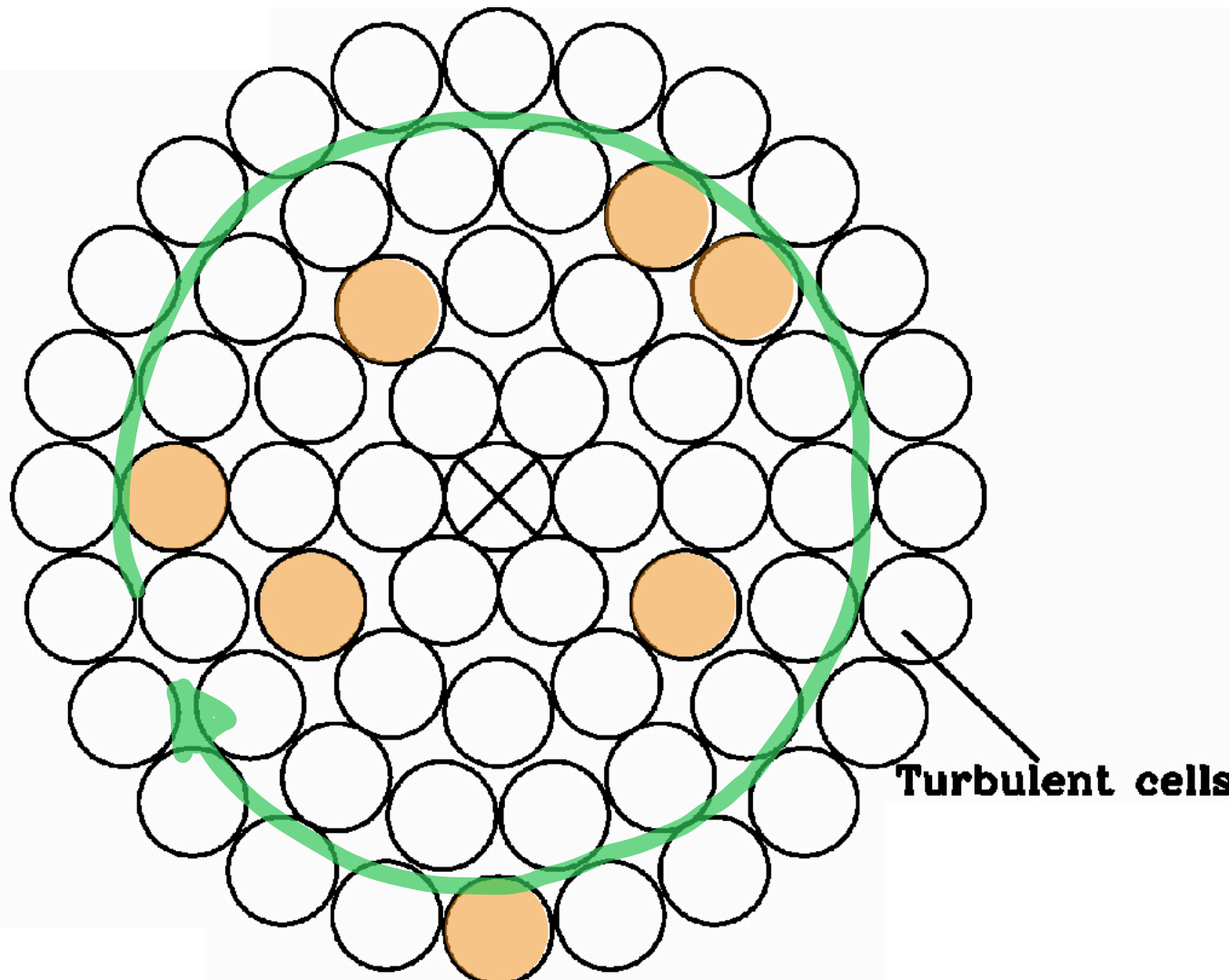
Particle-in-cell simulations



Toroidal B field

- Match simulation cooling time to observed flux variability timescale.
- Add emission from multiple cells.
- Explore parameter space:
 - Shocks vs mag. reconnection
 - Number of cells
 - Compactness of cell cluster
 - Cell brightness distribution: equal, power law.
- Calculate metrics: Polarization degree, pol. angle, variability timescales and range

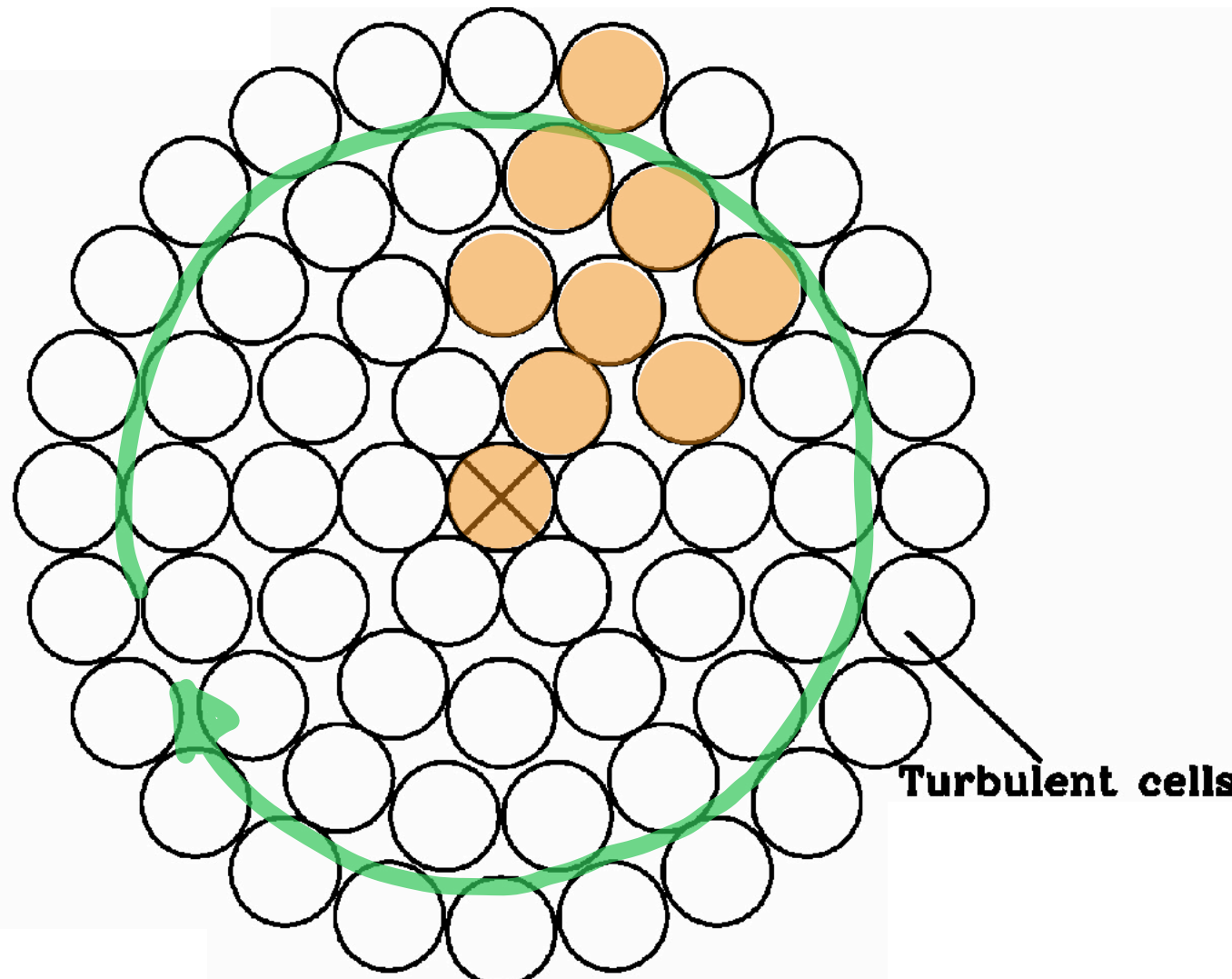
Particle-in-cell simulations



Toroidal B field

- Match simulation cooling time to observed flux variability timescale.
- Add emission from multiple cells.
- Explore parameter space:
 - Shocks vs mag. reconnection
 - Number of cells
 - Compactness of cell cluster
 - Cell brightness distribution: equal, power law.
- Calculate metrics: Polarization degree, pol. angle, variability timescales and range

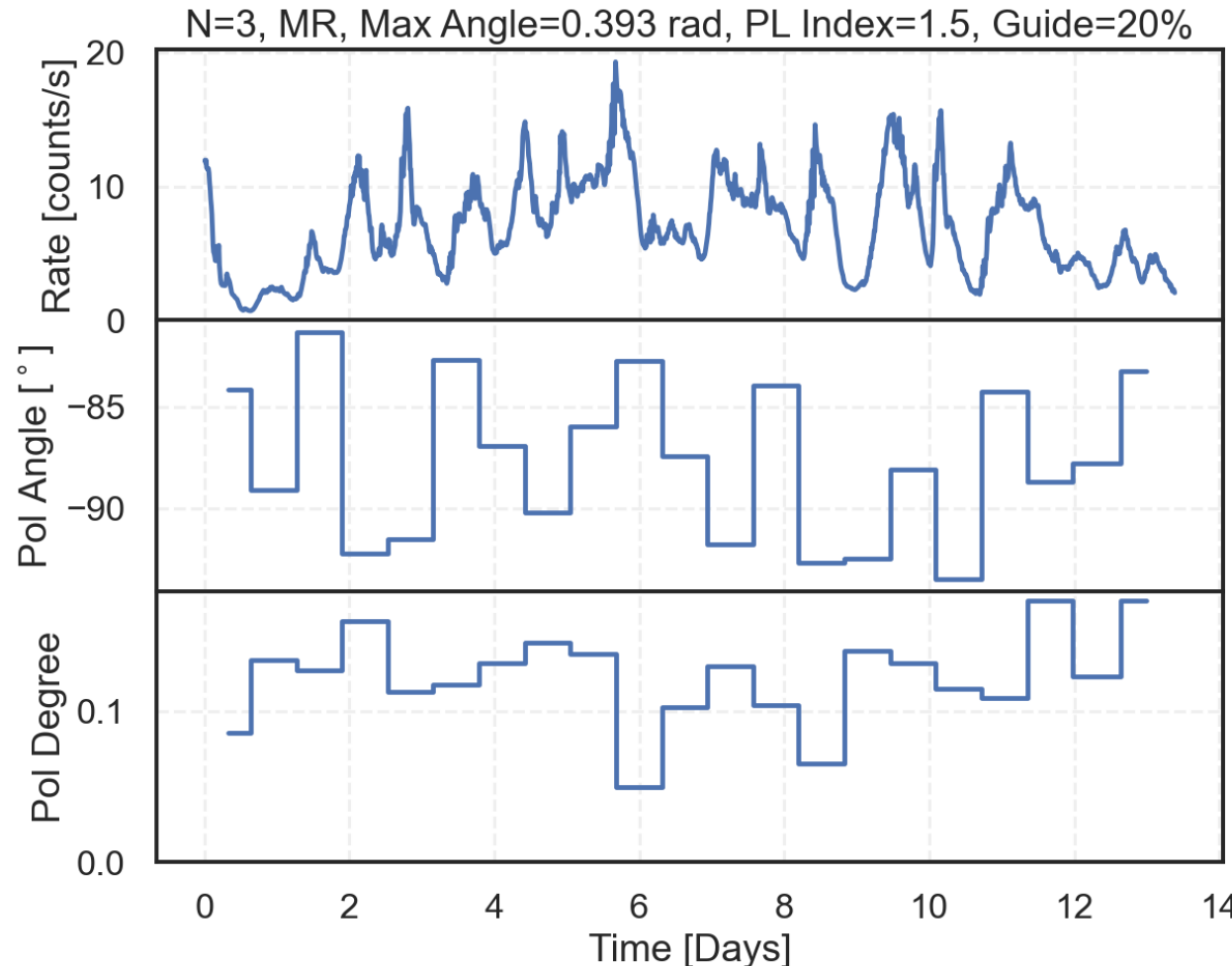
Particle-in-cell simulations



Toroidal B field

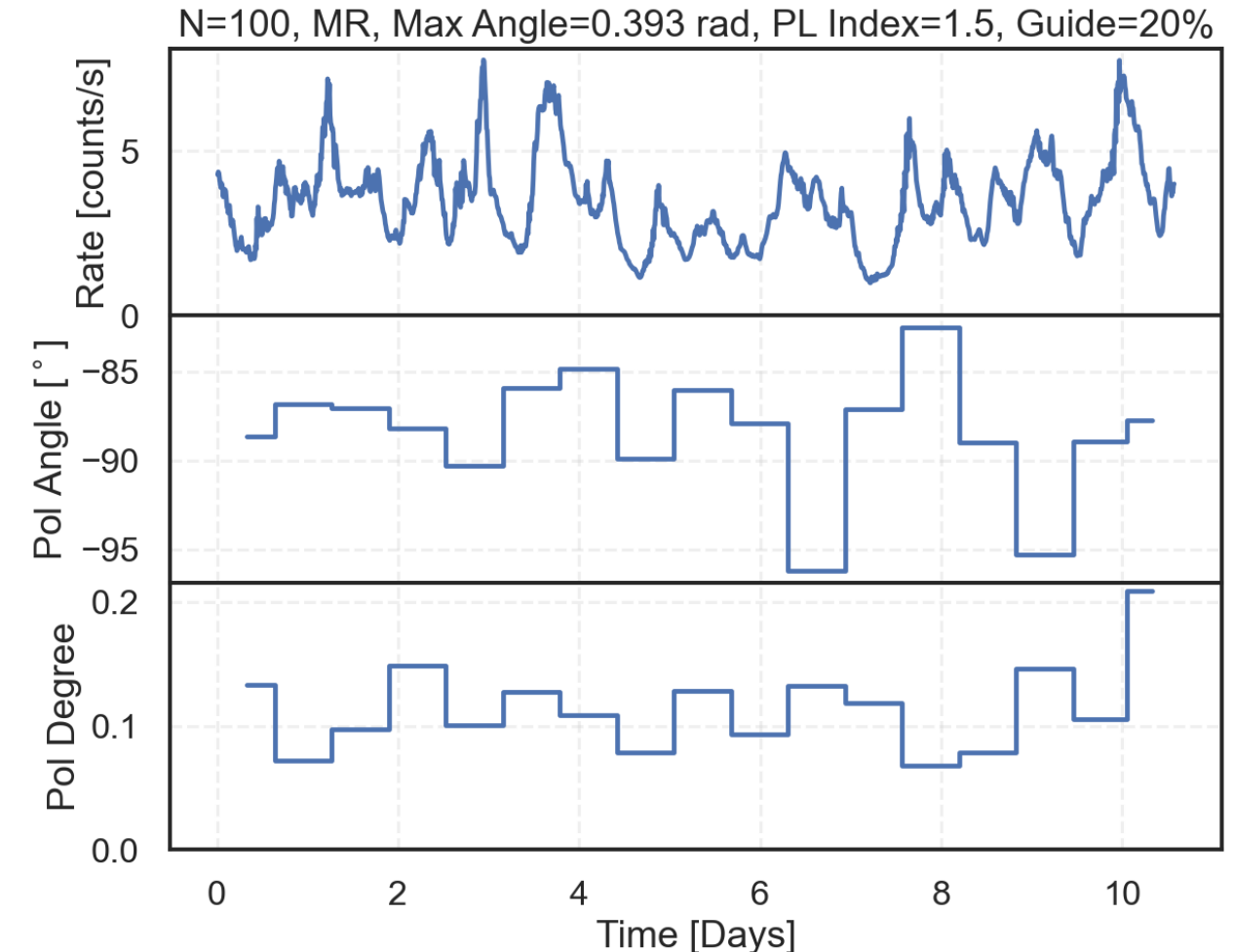
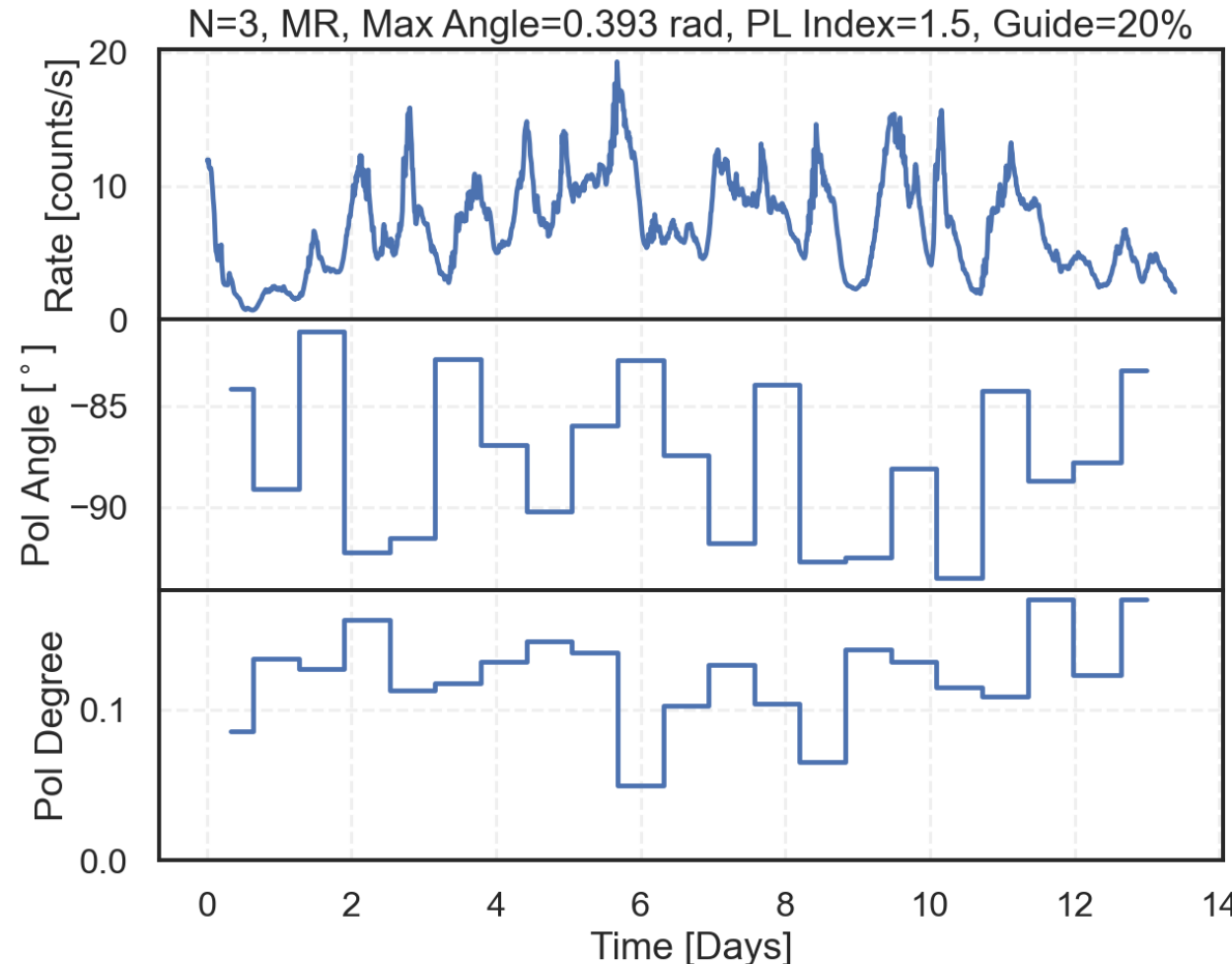
- Match simulation cooling time to observed flux variability timescale.
- Add emission from multiple cells.
- Explore parameter space:
 - Shocks vs mag. reconnection
 - Number of cells
 - Compactness of cell cluster
 - Cell brightness distribution: equal, power law.
- Calculate metrics: Polarization degree, pol. angle, variability timescales and range

Mag. reconnection multi-cell simulation



- Small number of cells, compact
- Can produce 10% polarization
- Too much flux variability

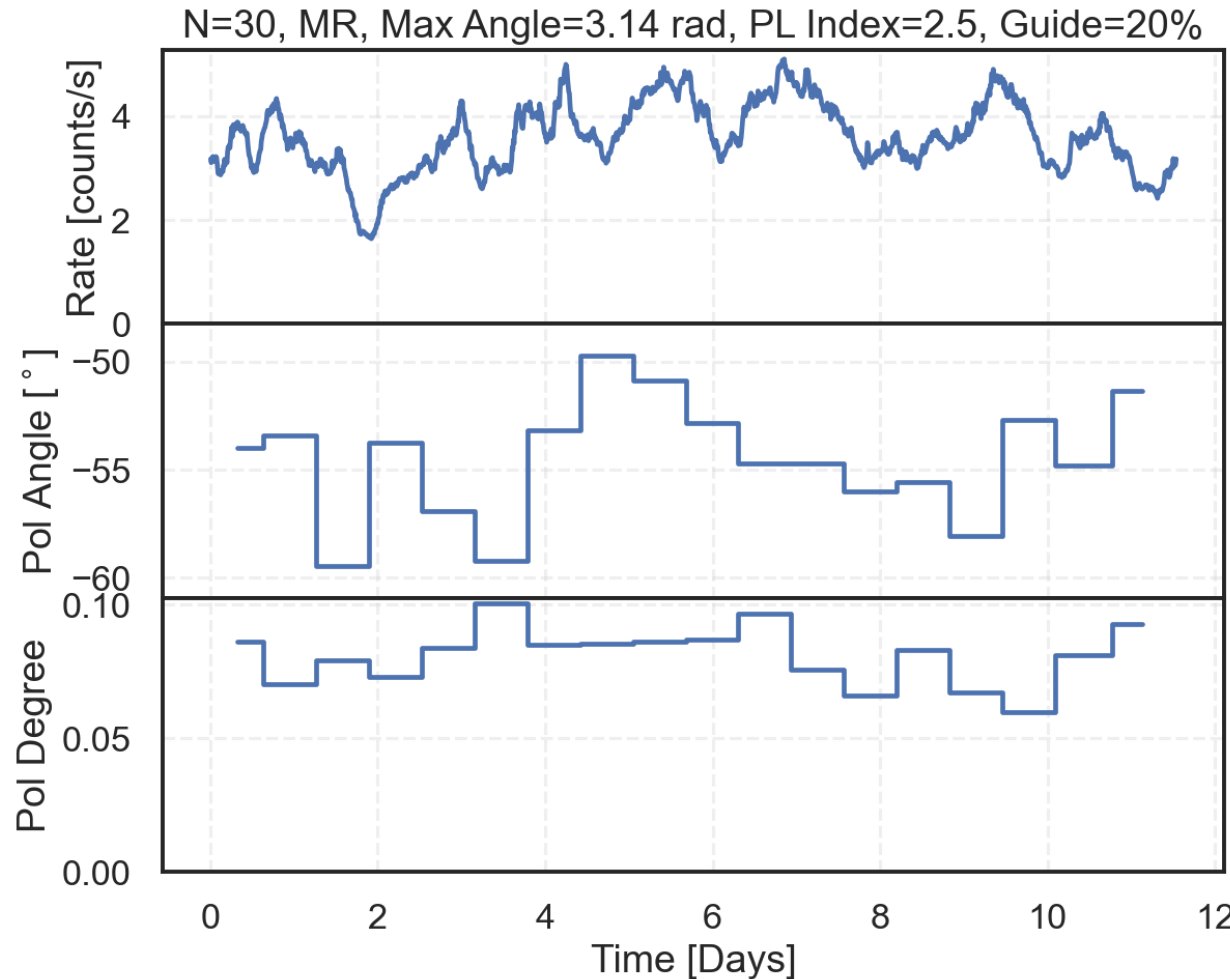
Mag. reconnection multi-cell simulation



- Small number of cells, compact
- Can produce 10% polarization
- Too much flux variability

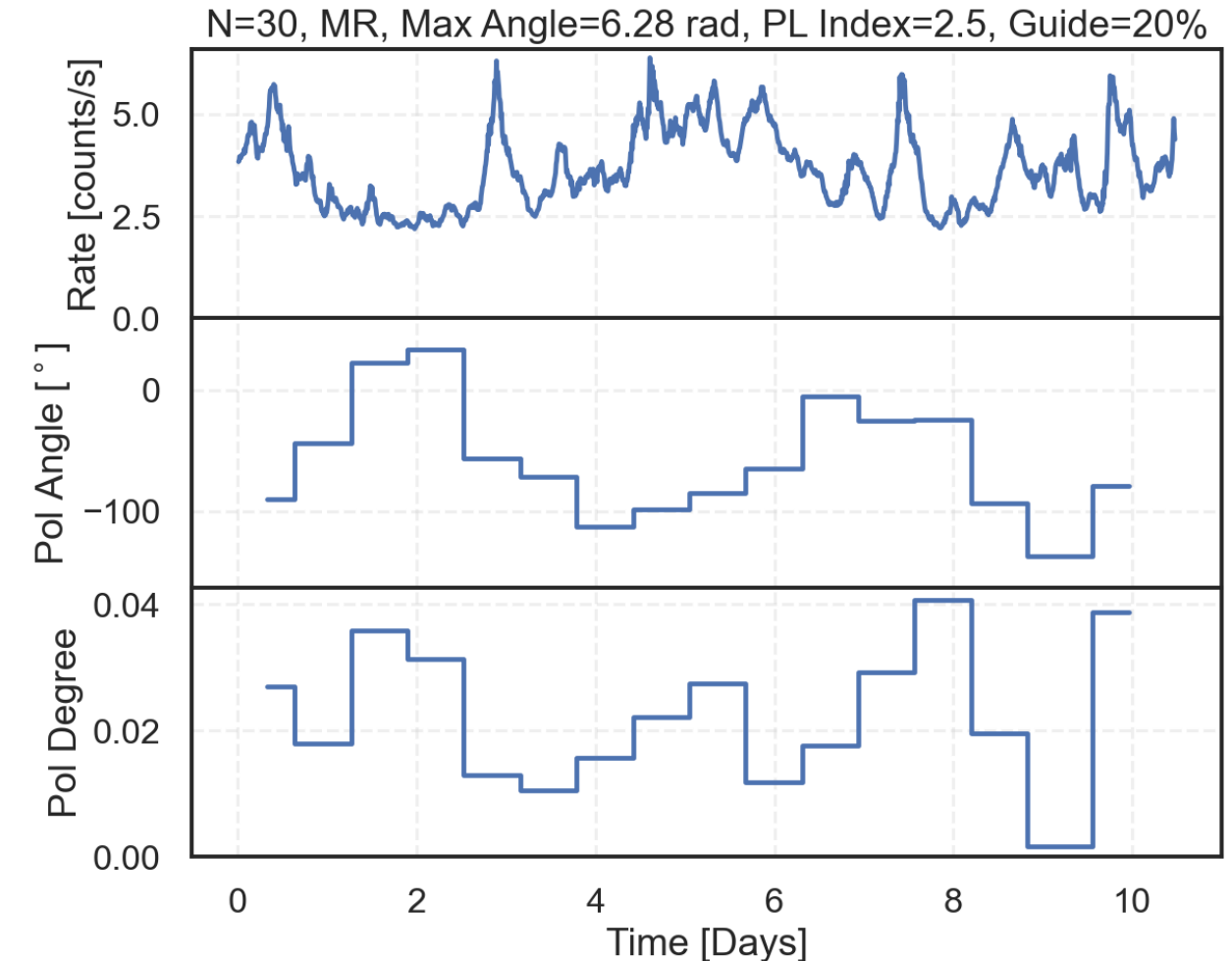
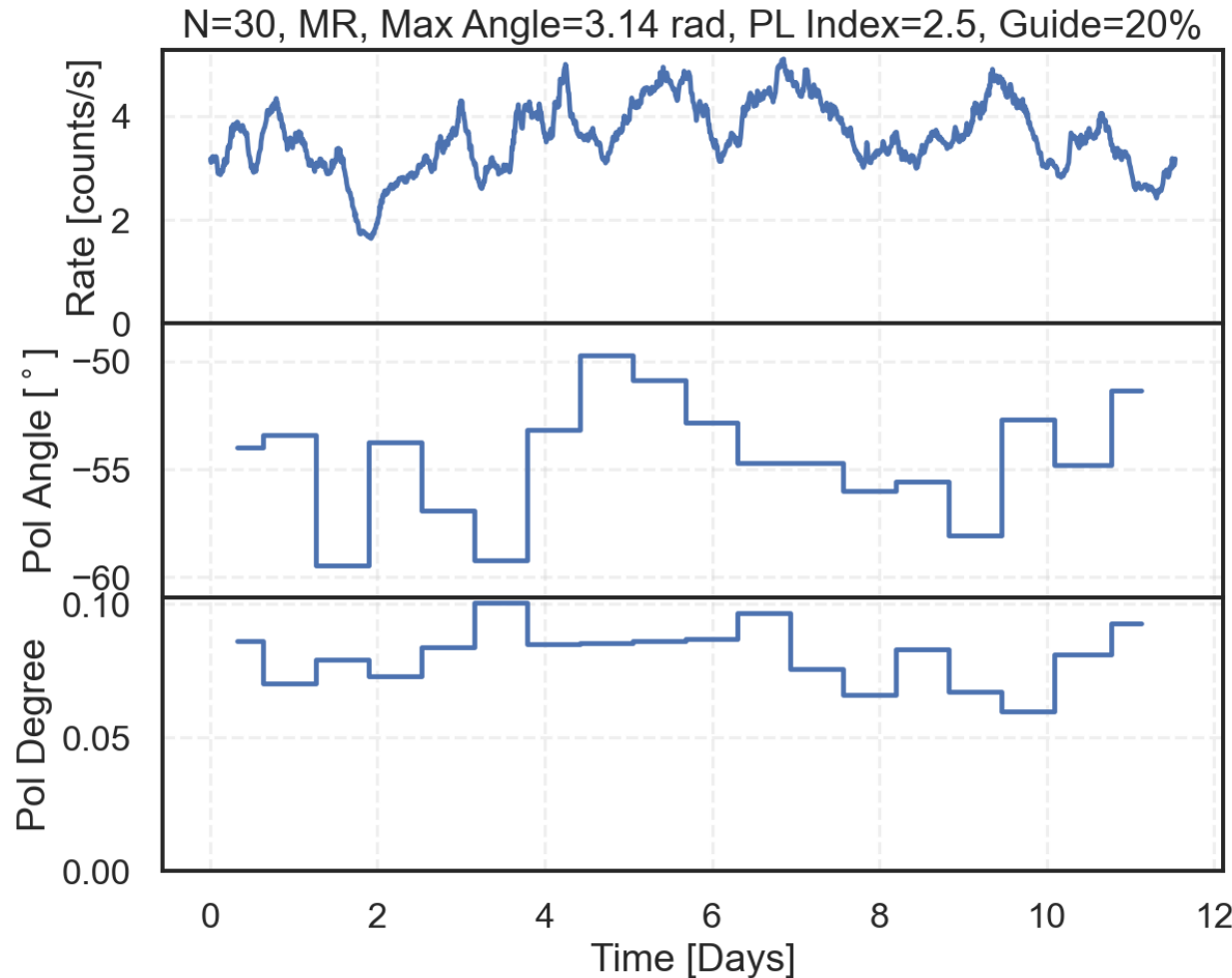
- Increase number of cells
- Flux variability closer to data
- Pol. deg and angle too steady

Mag. reconnection multi-cell simulation



- Less compact cluster, 1/4 jet
- Reproduces light curve and pol. deg
- Pol. Angle still too steady

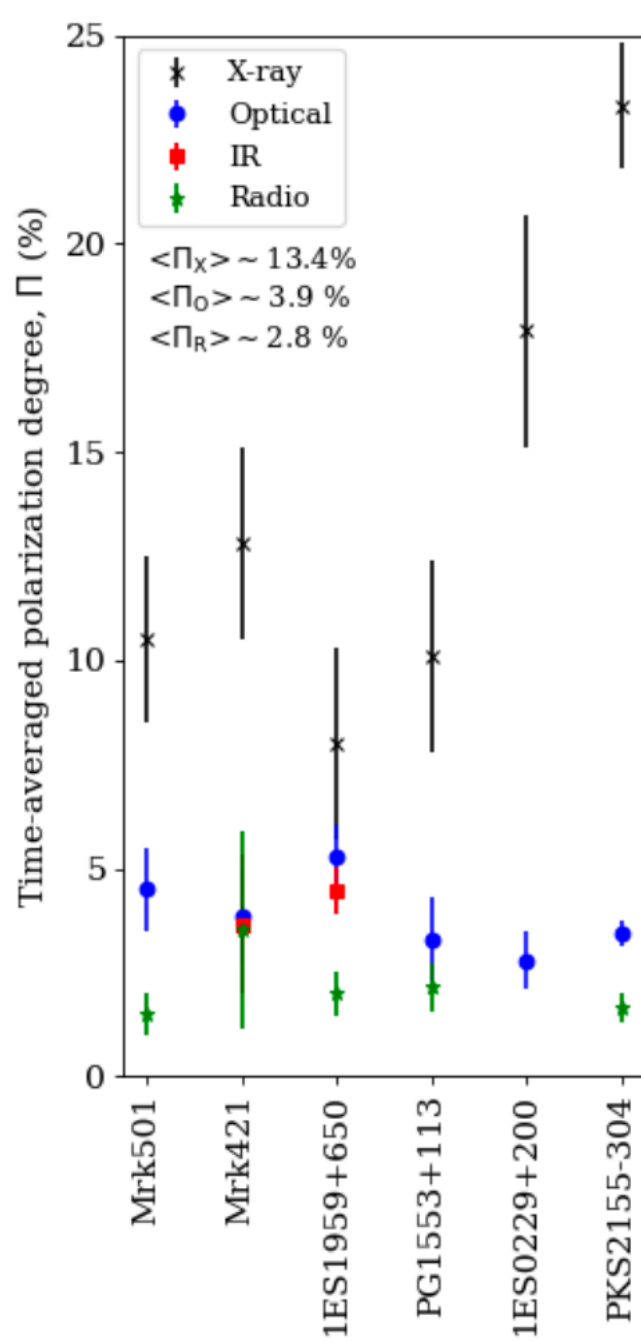
Mag. reconnection multi-cell simulation



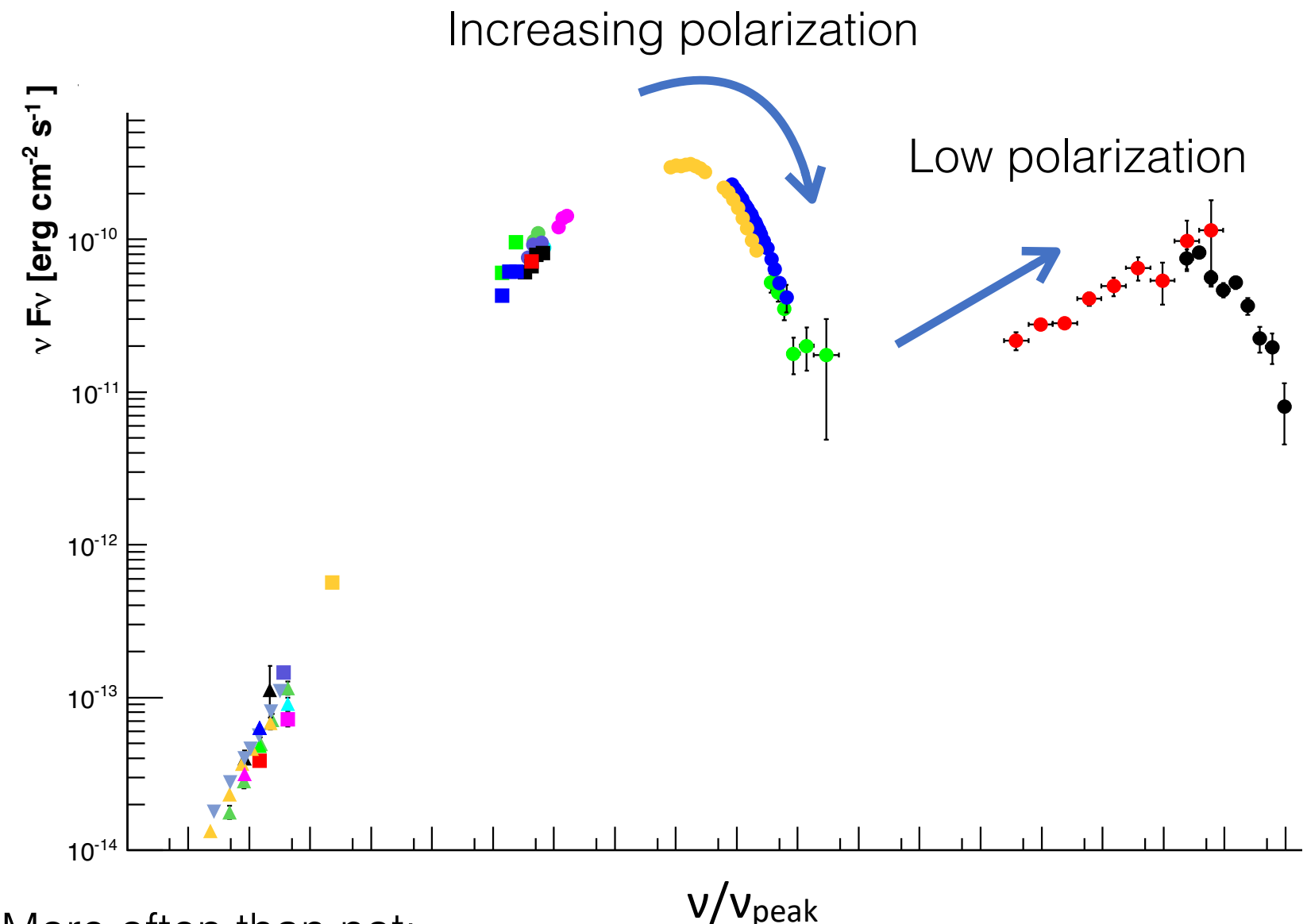
- Less compact cluster, 1/4 jet
- Reproduces light curve and pol. deg
- Pol. Angle still too steady

- Even less compact, 1/2 jet
- Pol. angle swings similar to data
- But pol. degree is too small

Summary



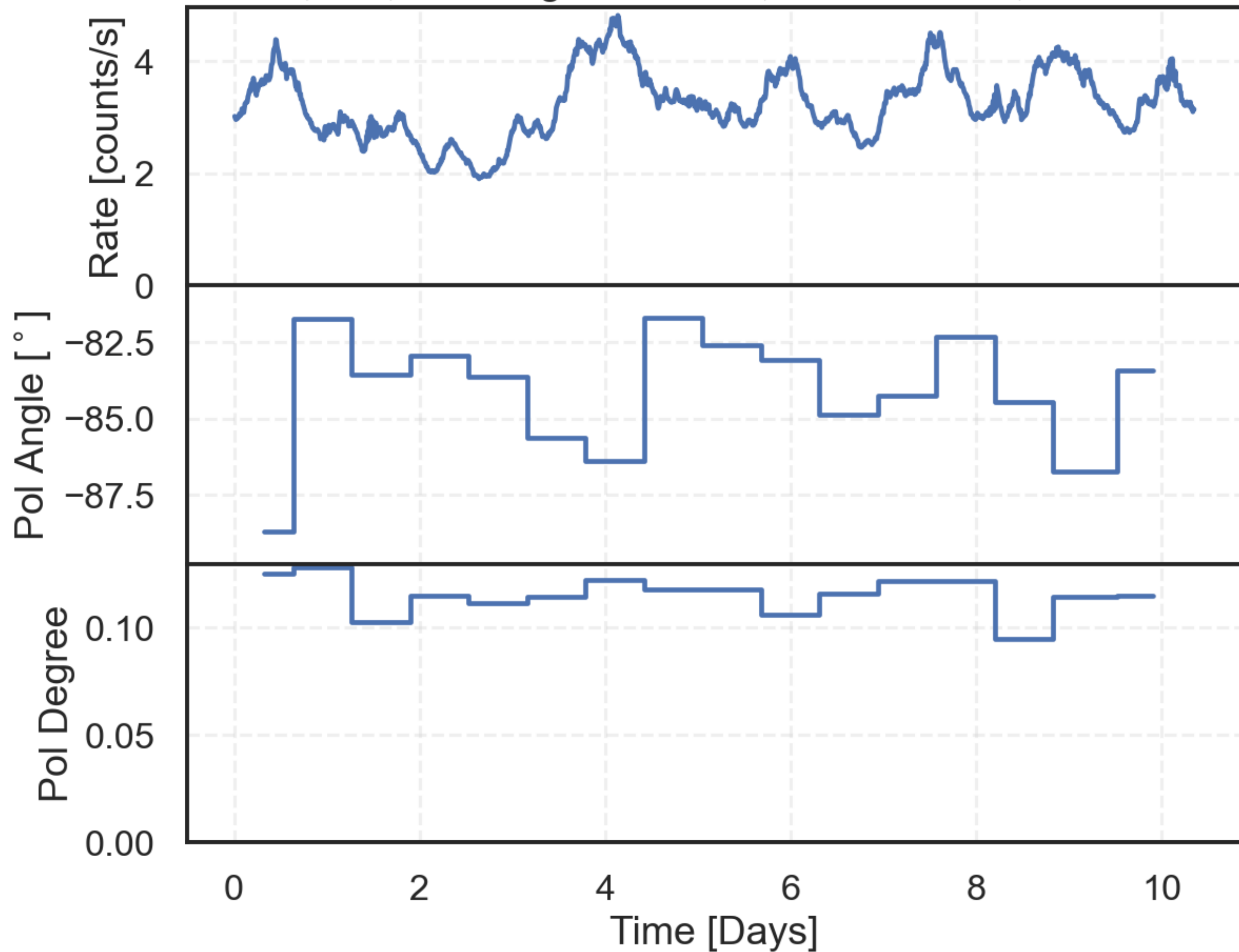
Increasing polarization → Ordered B → More compact region



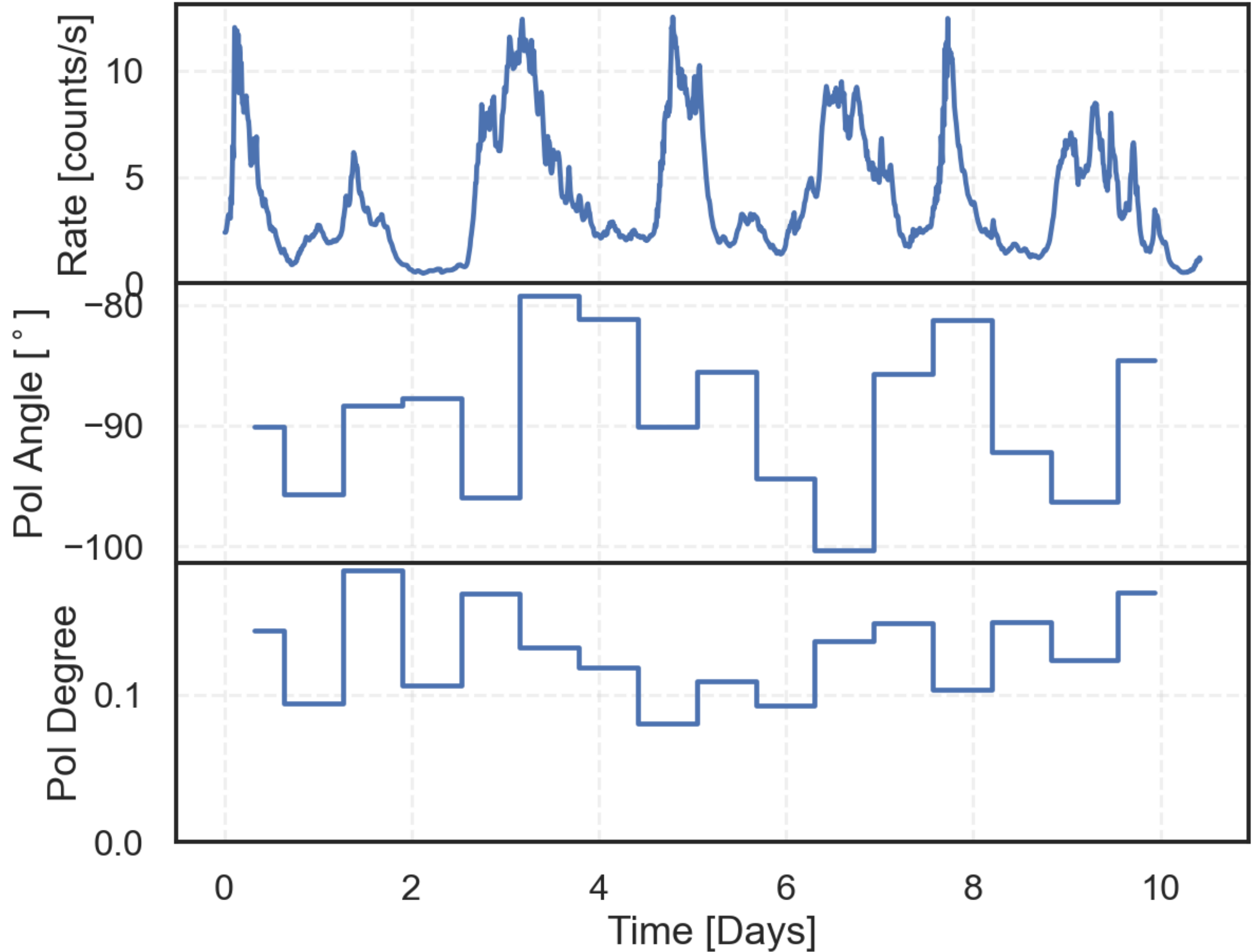
More often than not:
 EVPA is aligned with the jet direction
 X-ray polarization is higher than optical polarization
 Emission likely to originate from a localized region in the jet
 Complexity of pol. dynamics favor multi-zone emission region

Backup slides

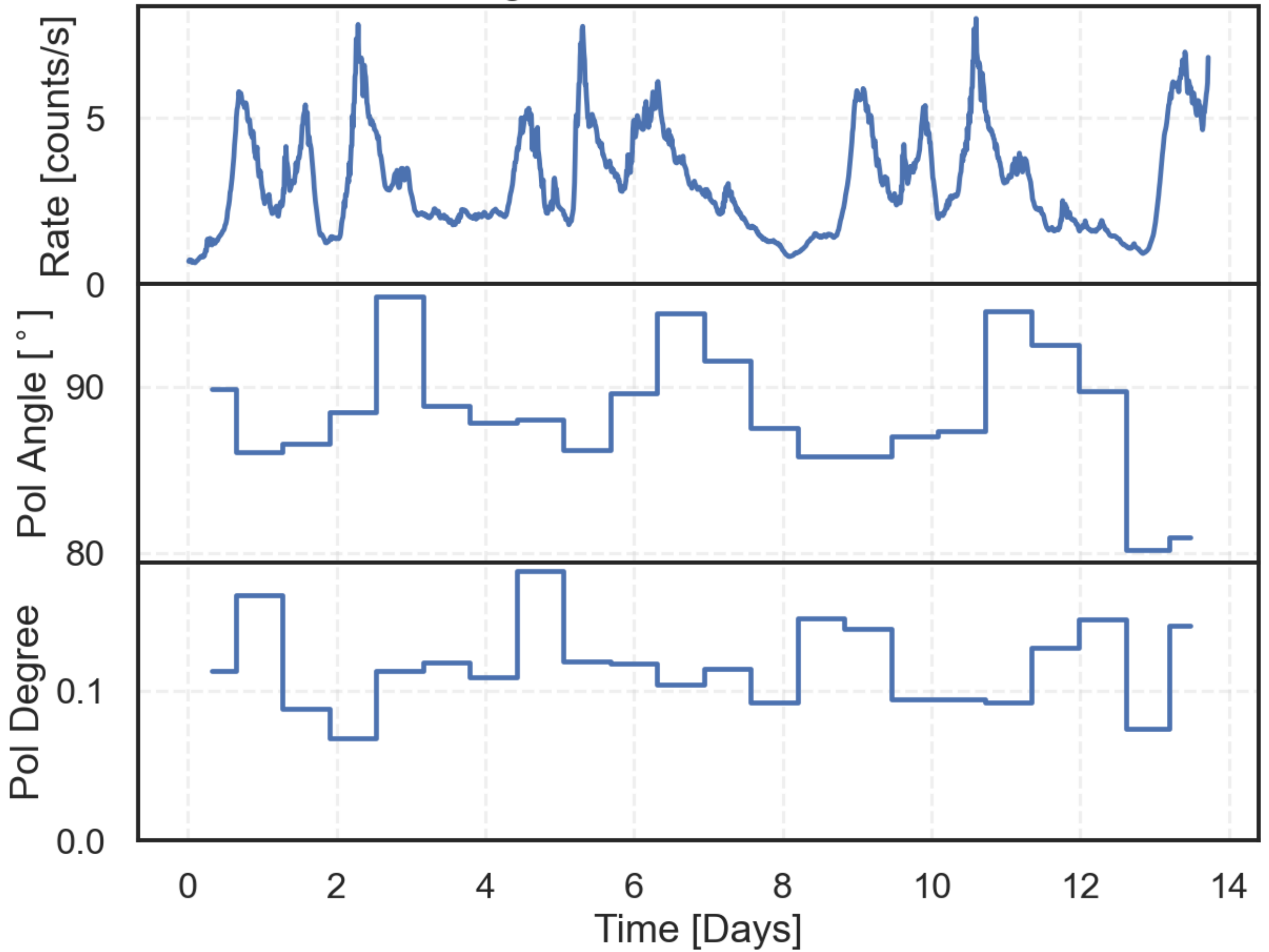
N=100, MR, Max Angle=0.79 rad, PL Index=2.5, Guide=20%



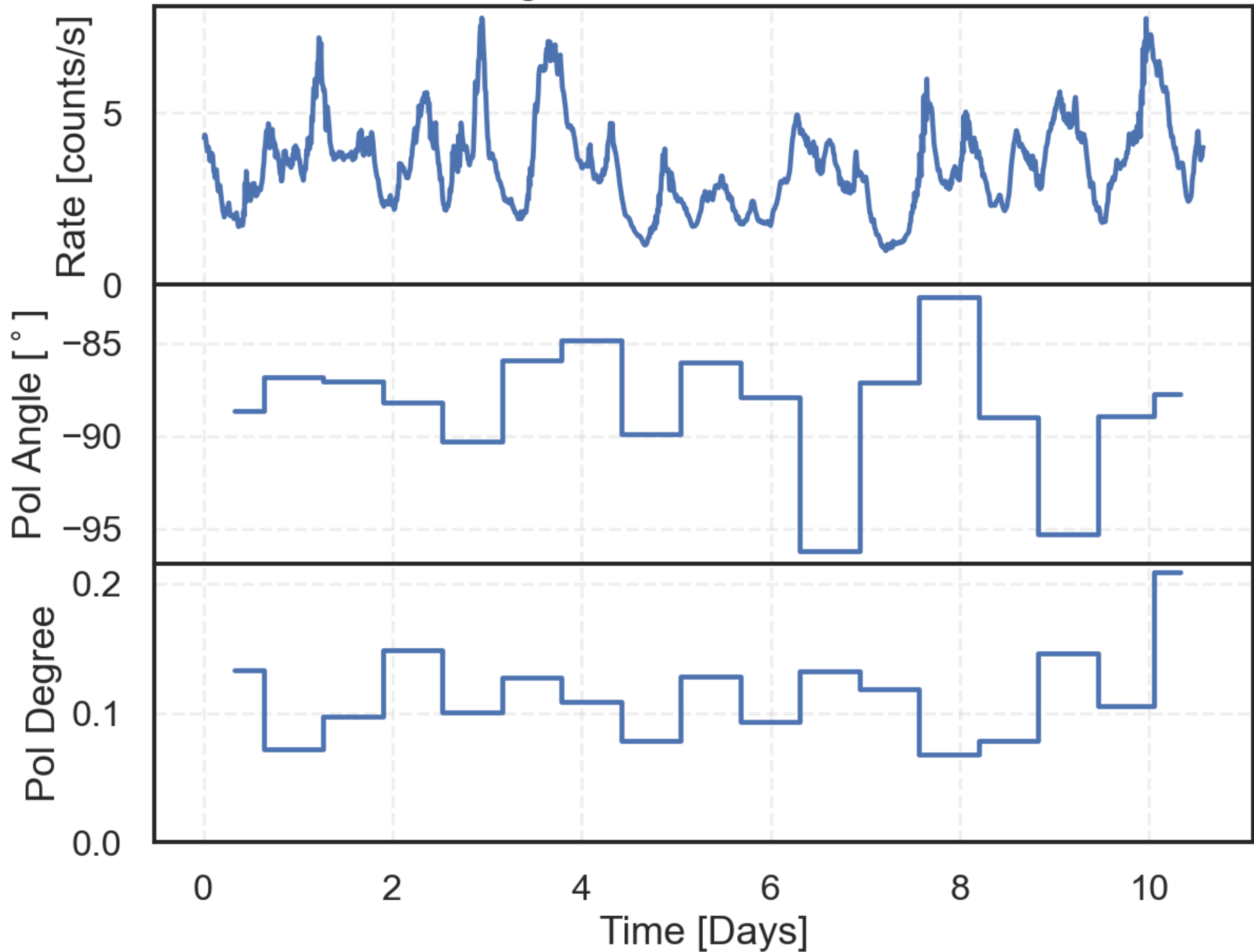
N=10, MR, Max Angle=0.393 rad, PL Index=1.5, Guide=20%



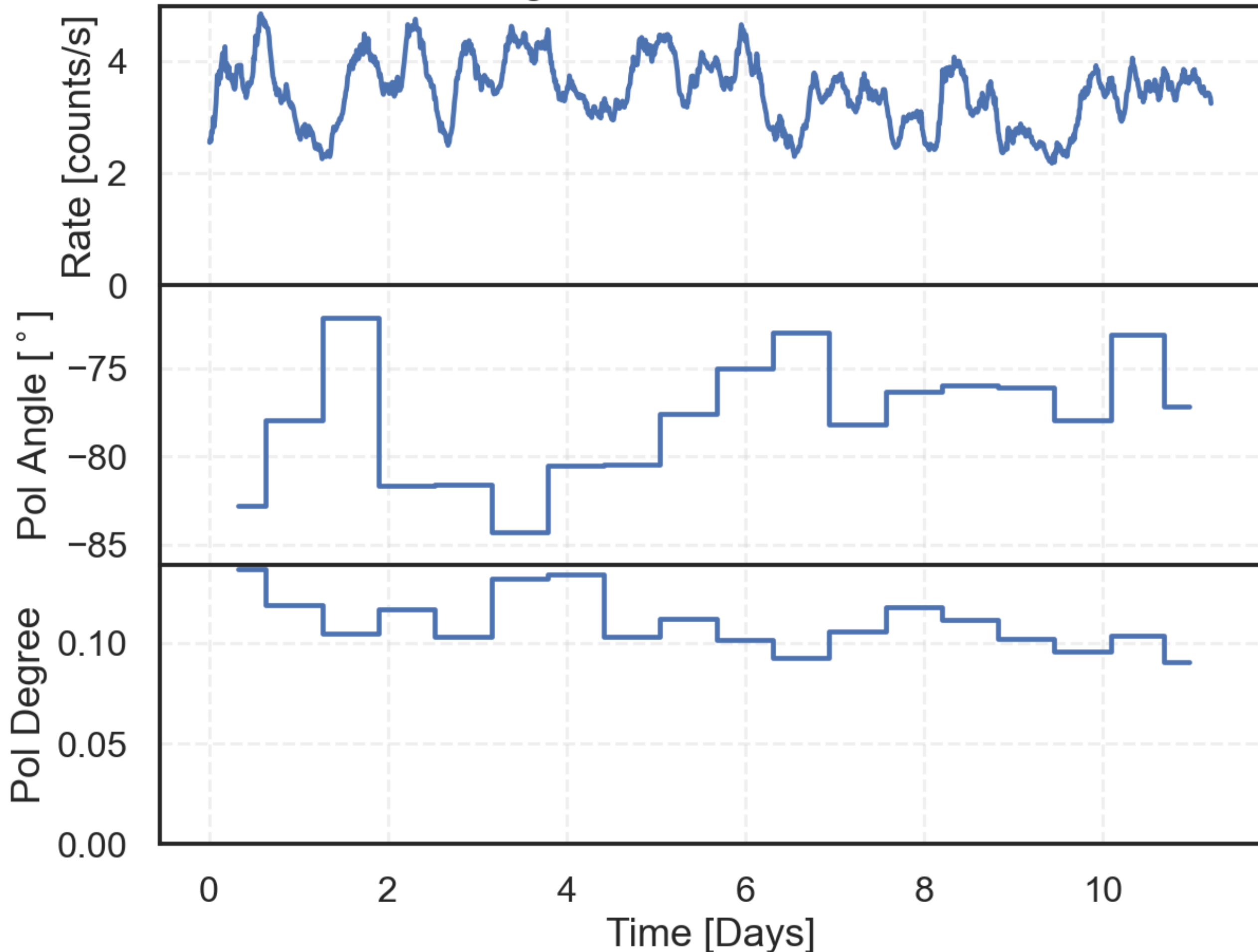
N=30, MR, Max Angle=0.393 rad, PL Index=1.5, Guide=20%



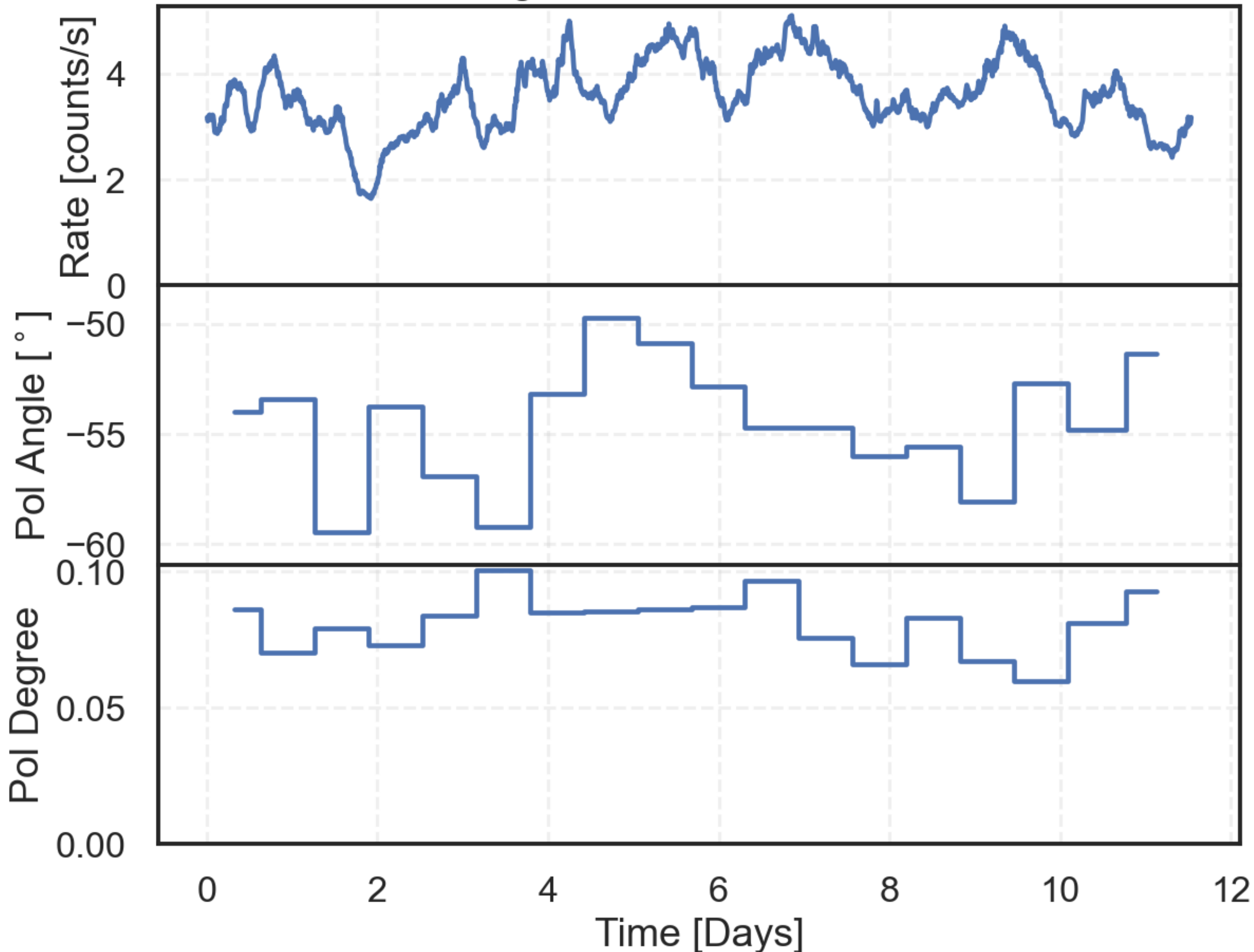
N=100, MR, Max Angle=0.393 rad, PL Index=1.5, Guide=20%



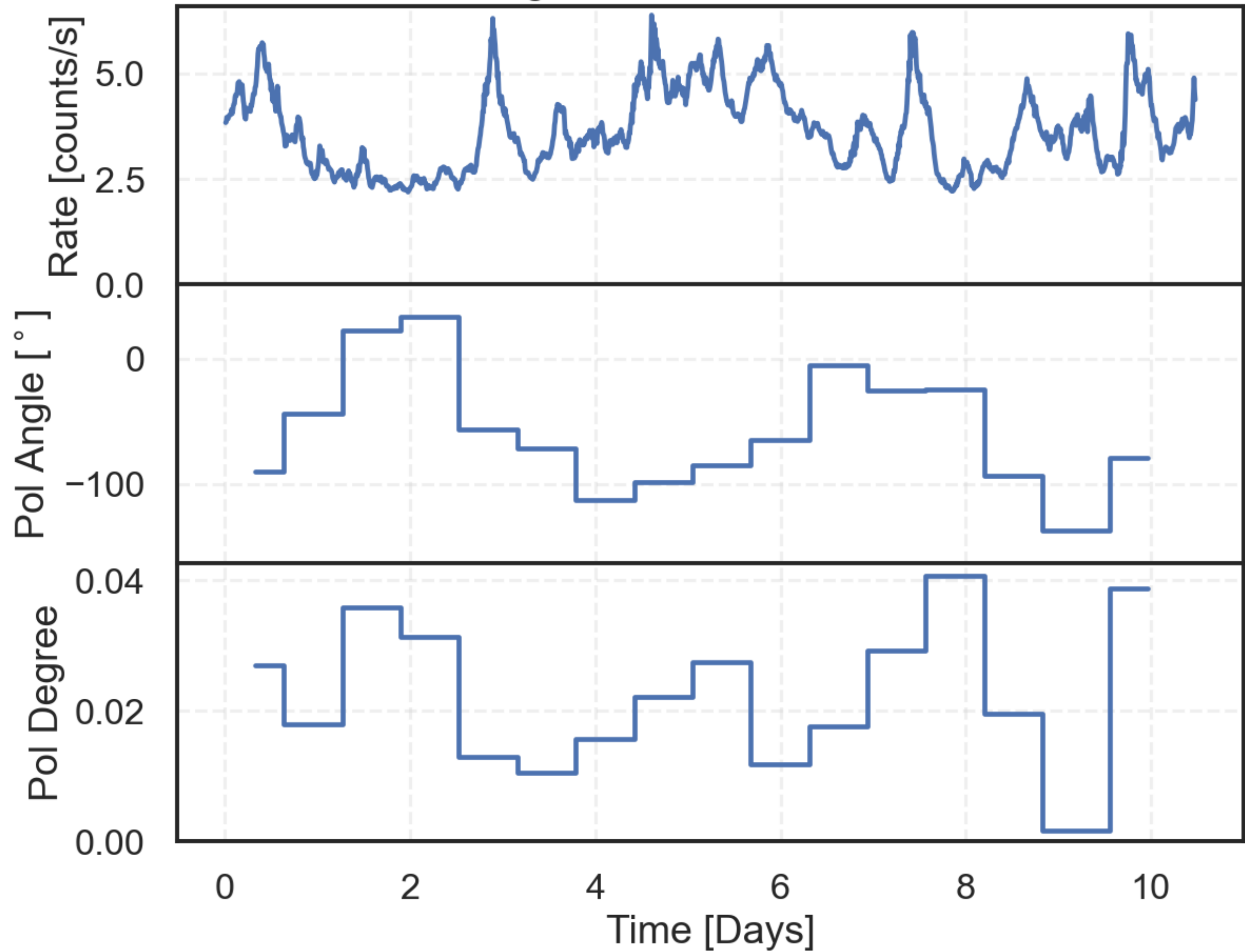
N=30, MR, Max Angle=1.57 rad, PL Index=2.5, Guide=20%

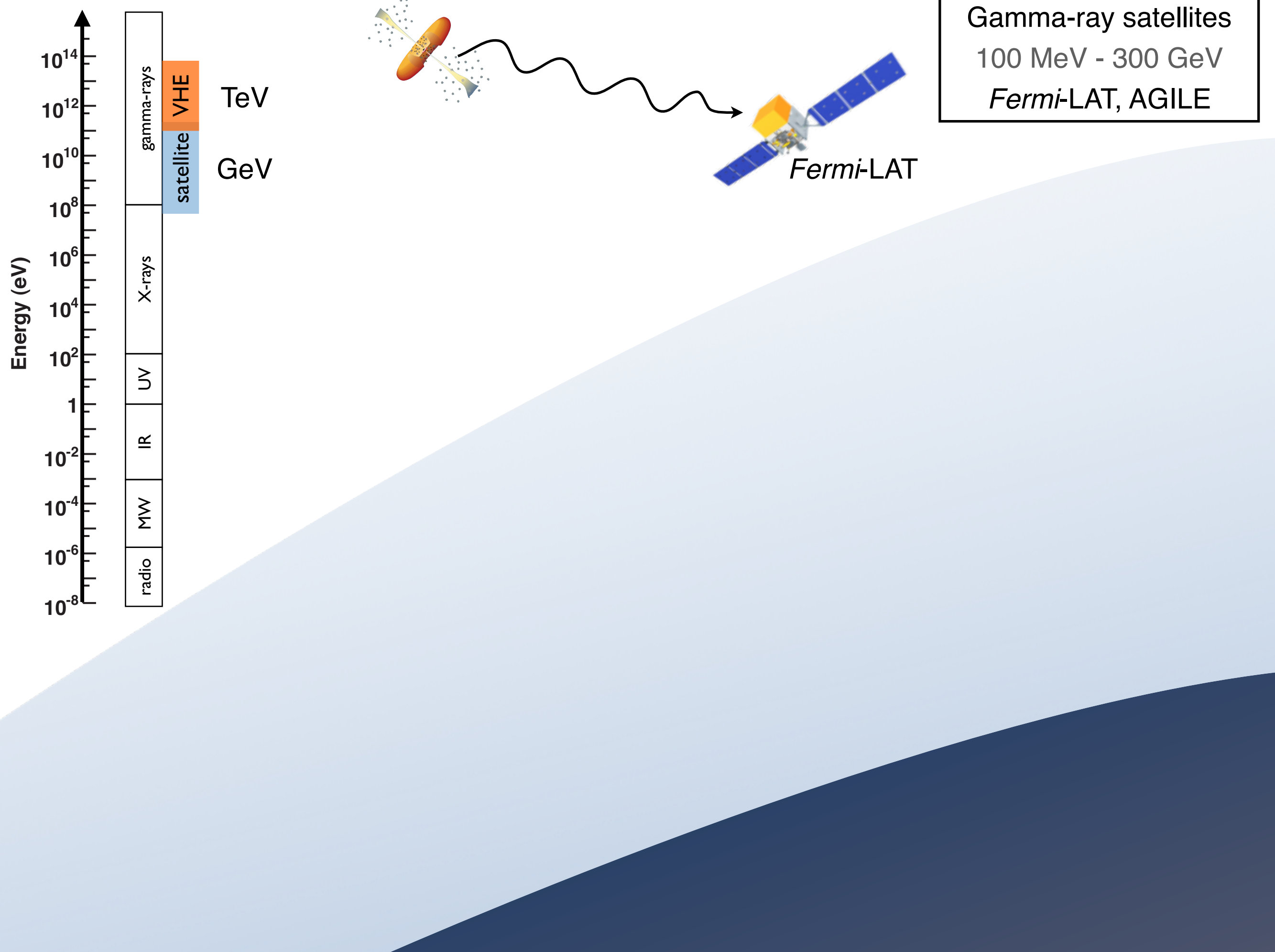


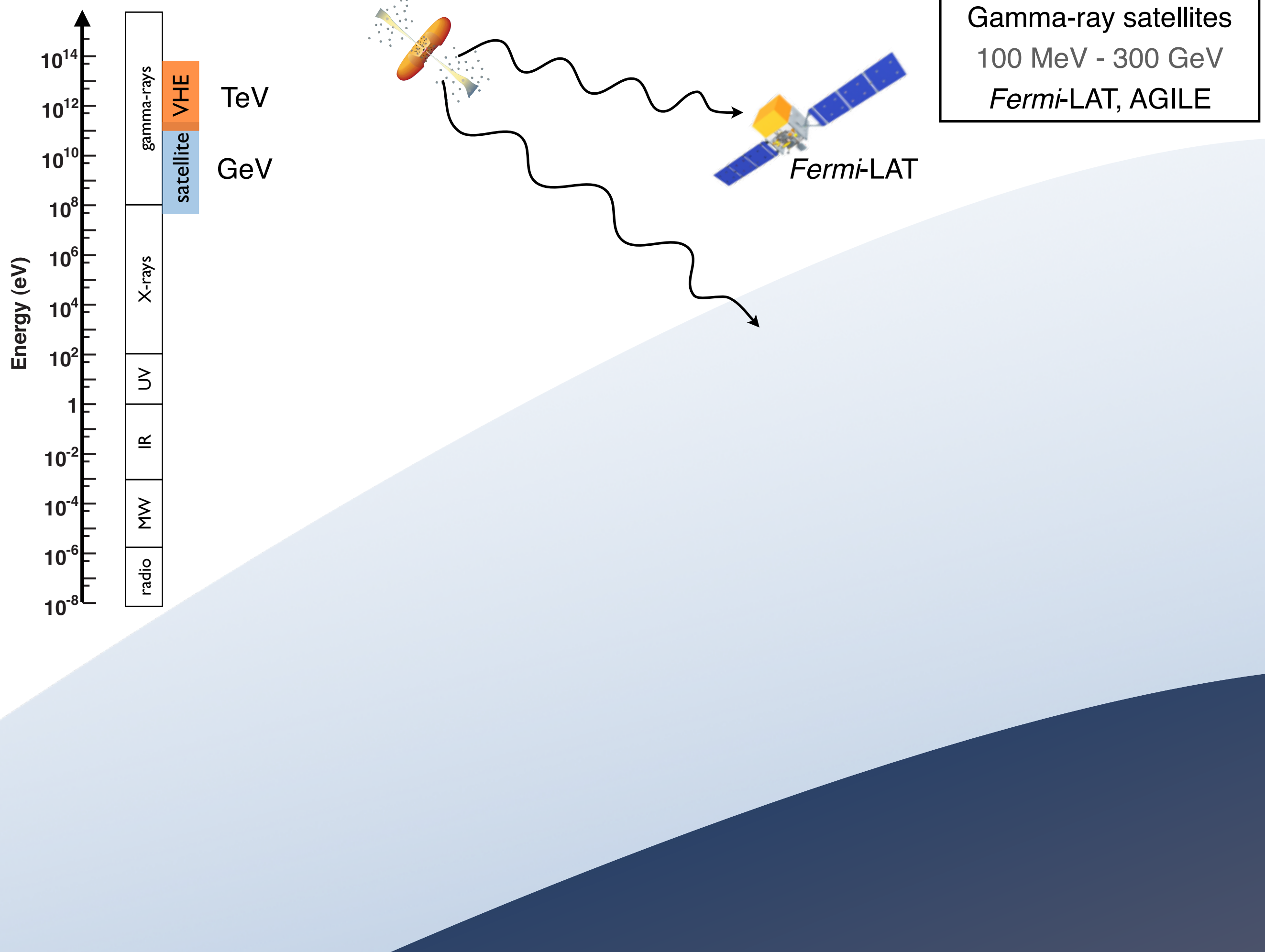
N=30, MR, Max Angle=3.14 rad, PL Index=2.5, Guide=20%

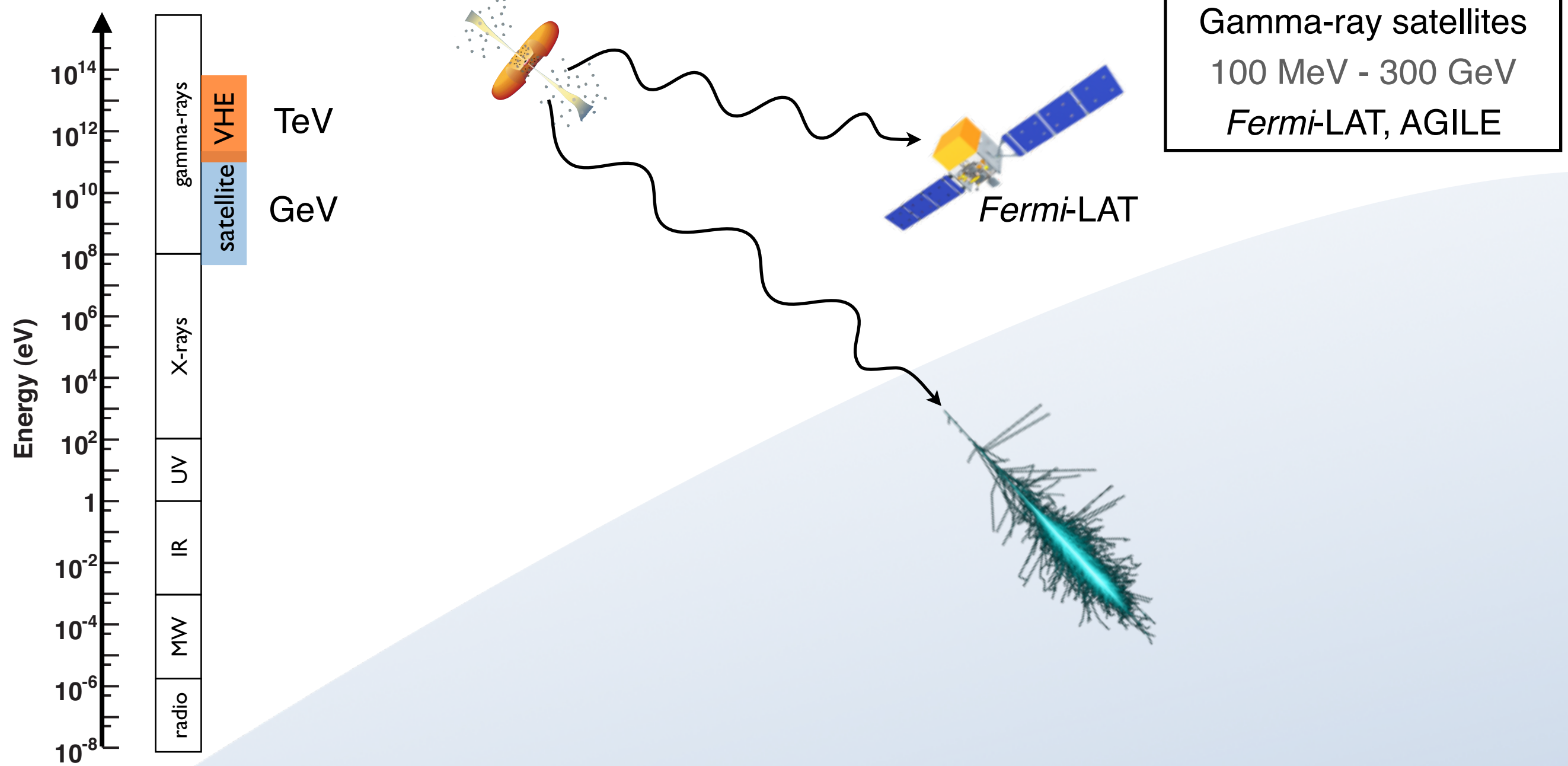


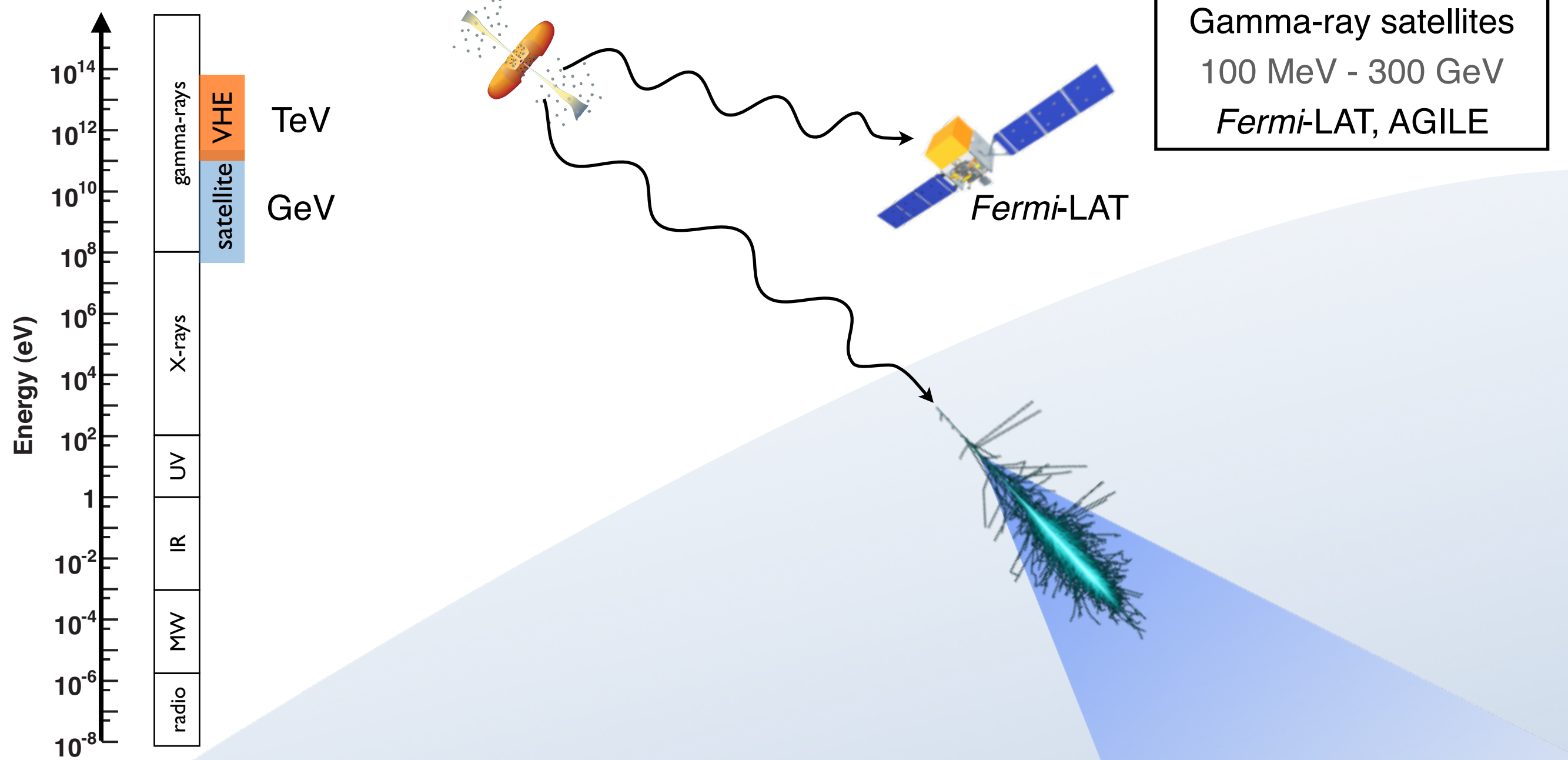
N=30, MR, Max Angle=6.28 rad, PL Index=2.5, Guide=20%

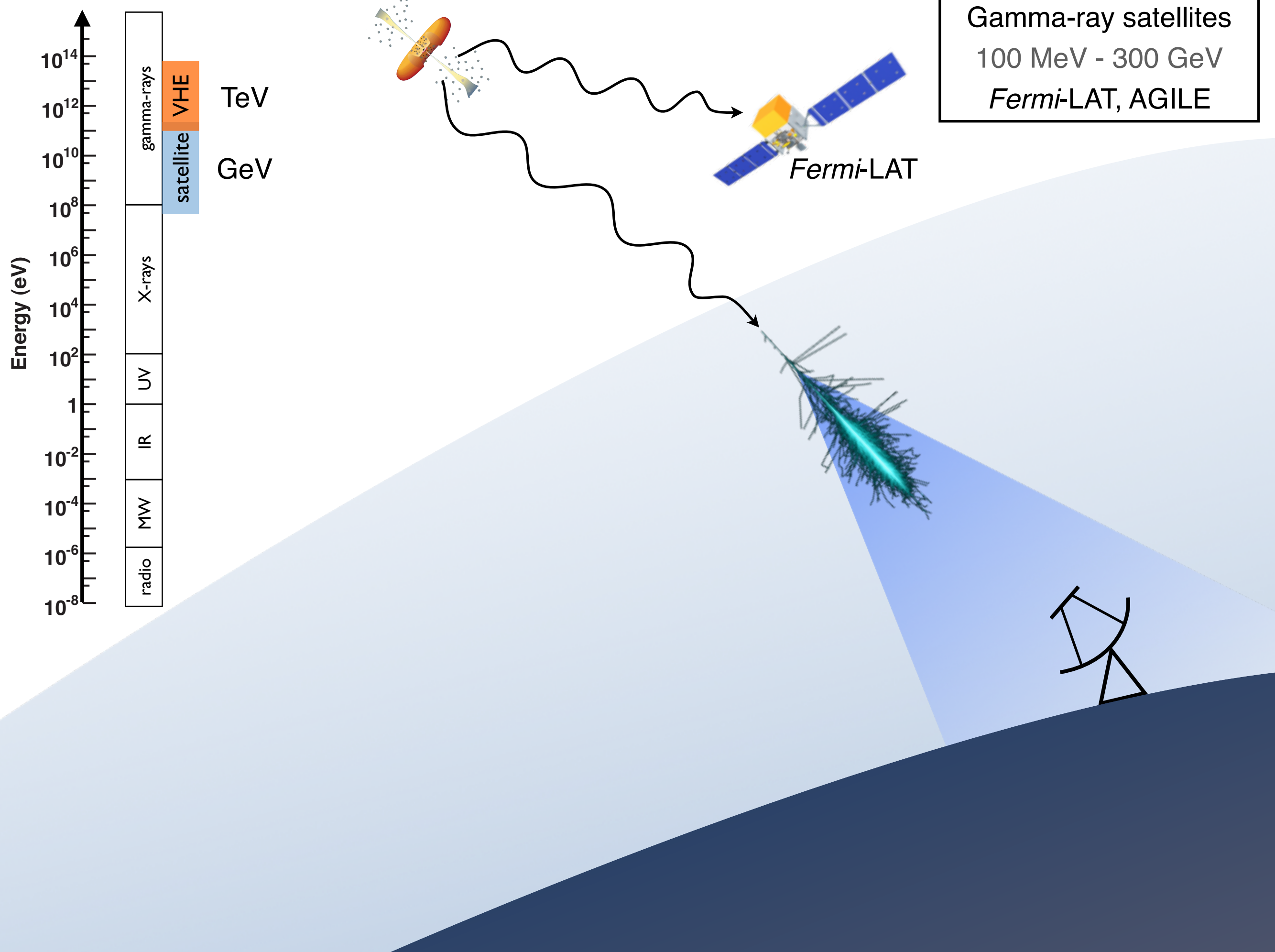


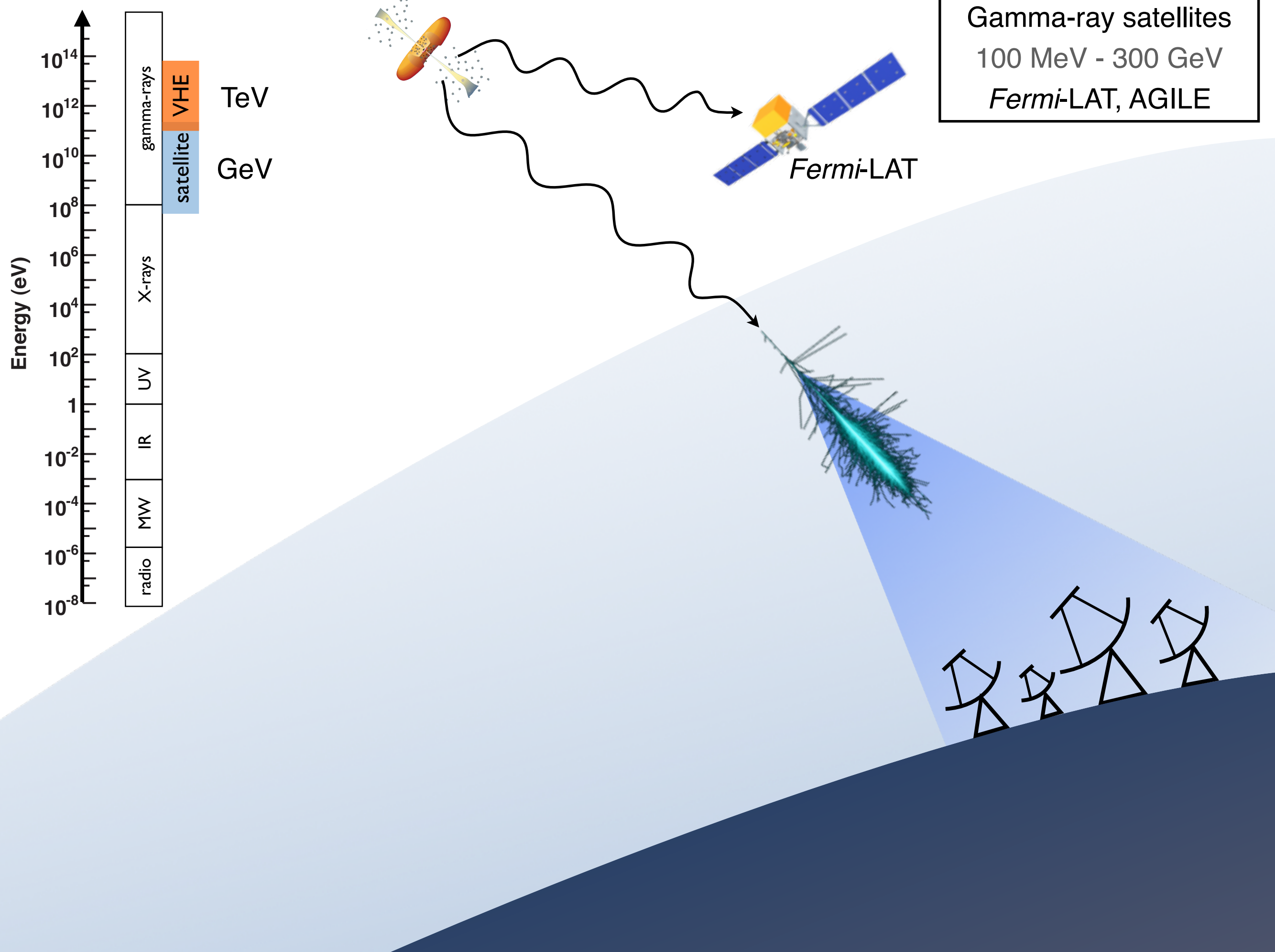


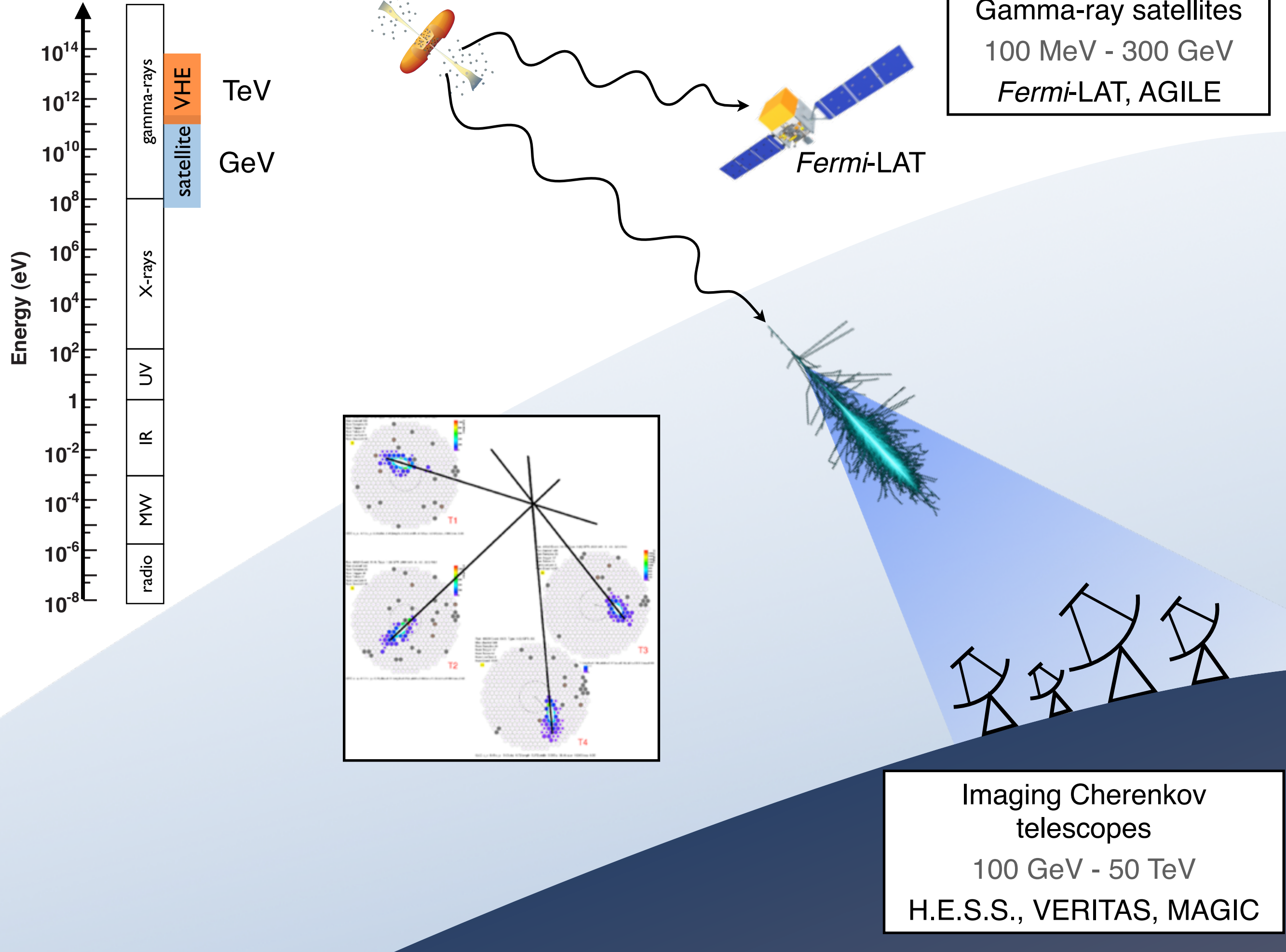




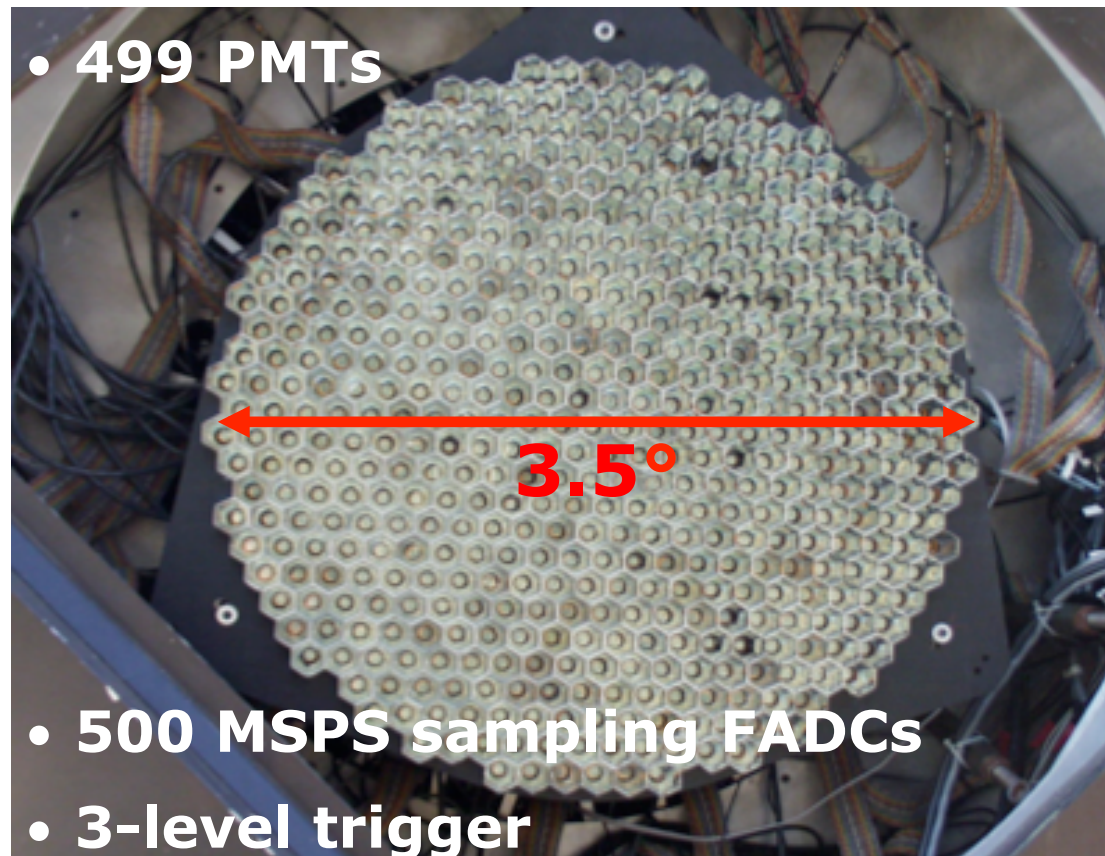
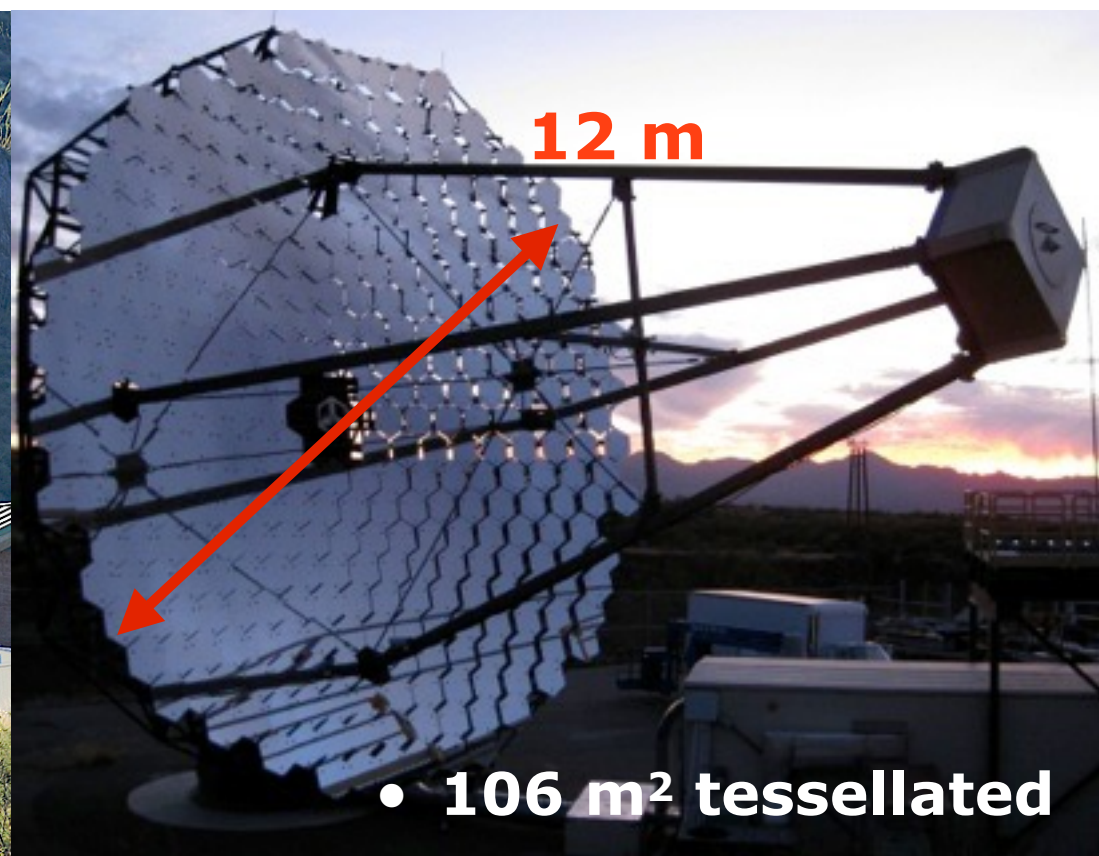




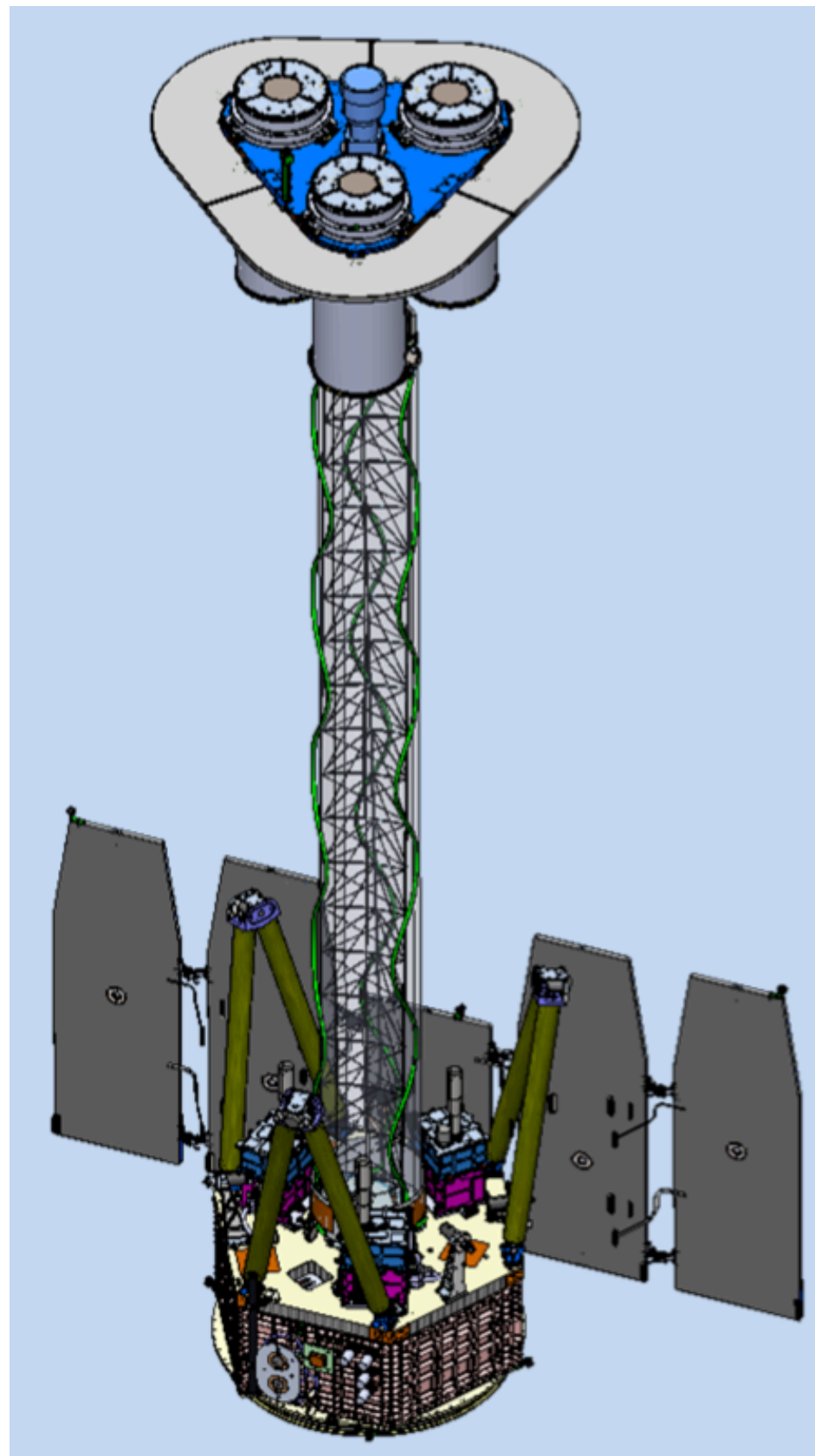




- Situated at 1280m altitude at Whipple Observatory in Arizona

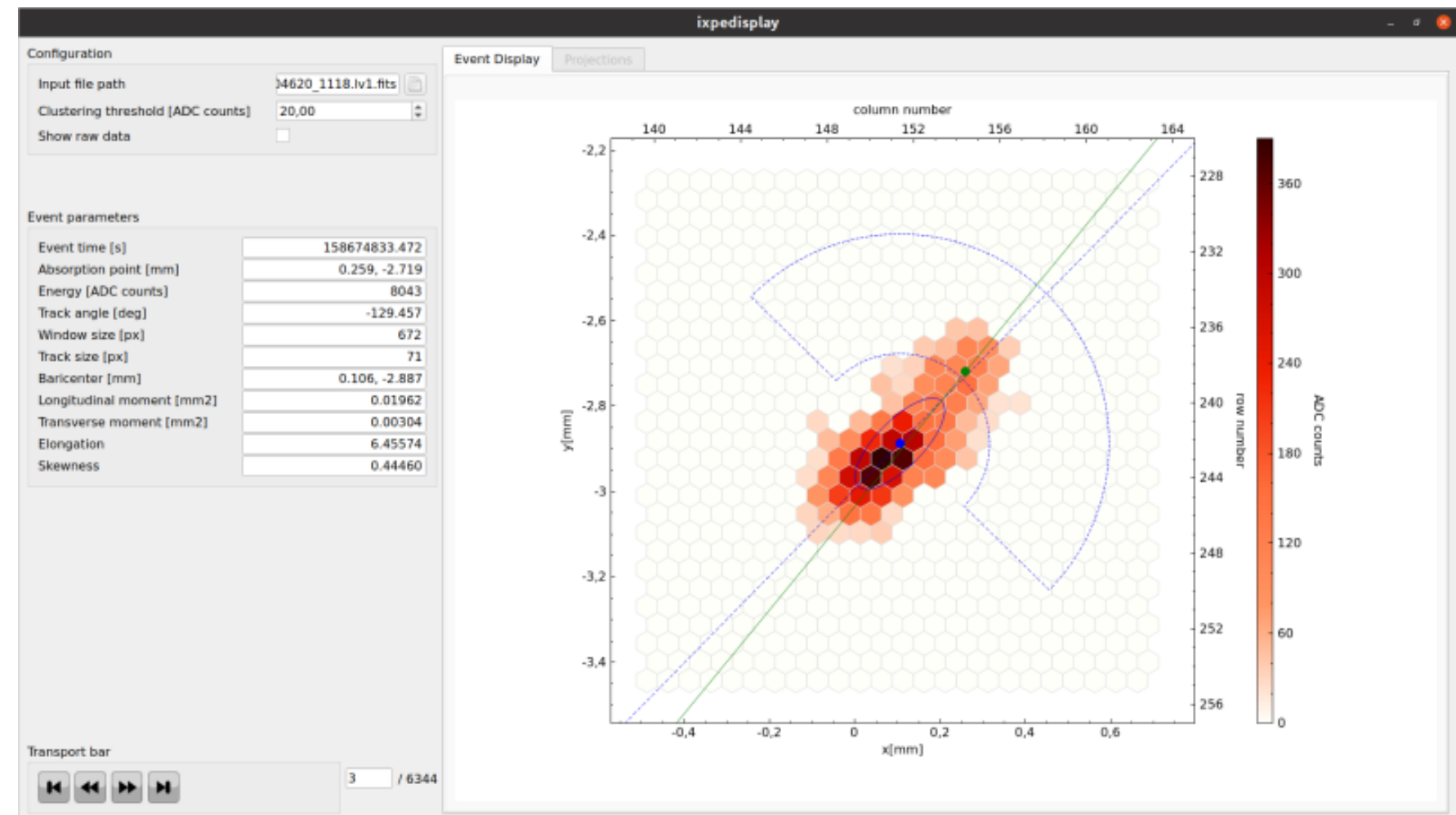
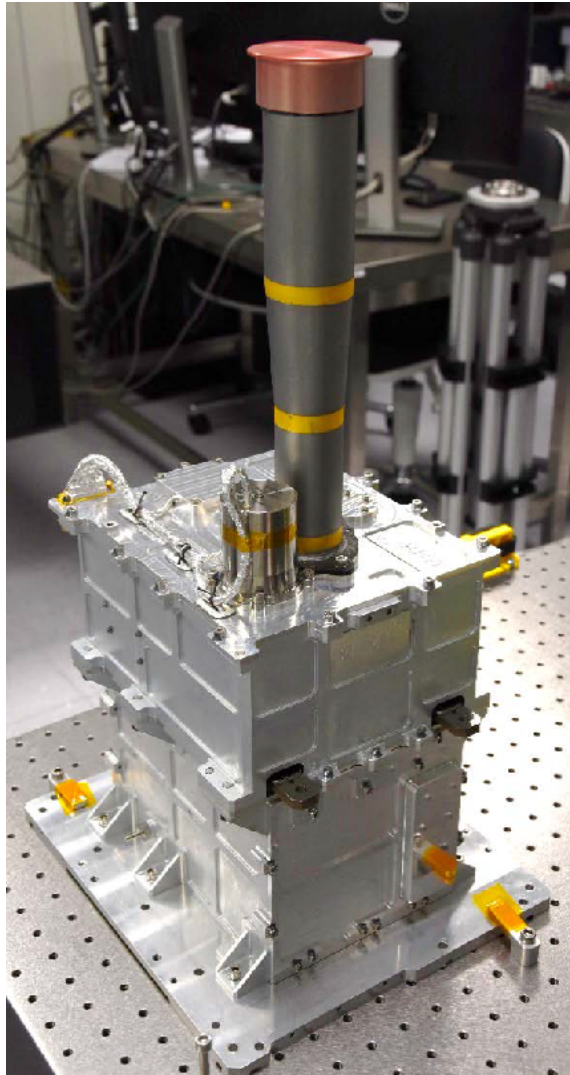


IXPE status and operations



- Launched on Dec 9th 2021.
- Boom deployed on Dec 15.
- Commissioning and calibration finished successfully.
- Science operations started Jan 11 2022.
- Sensitive to X-ray polarization in the 2-8 keV band.
- First X-ray polarimeter in space in 40 years.

X-ray polarization via the photoelectric effect



**Detector Unit
(DU)
INAF/IAPS,
INFN-PI**

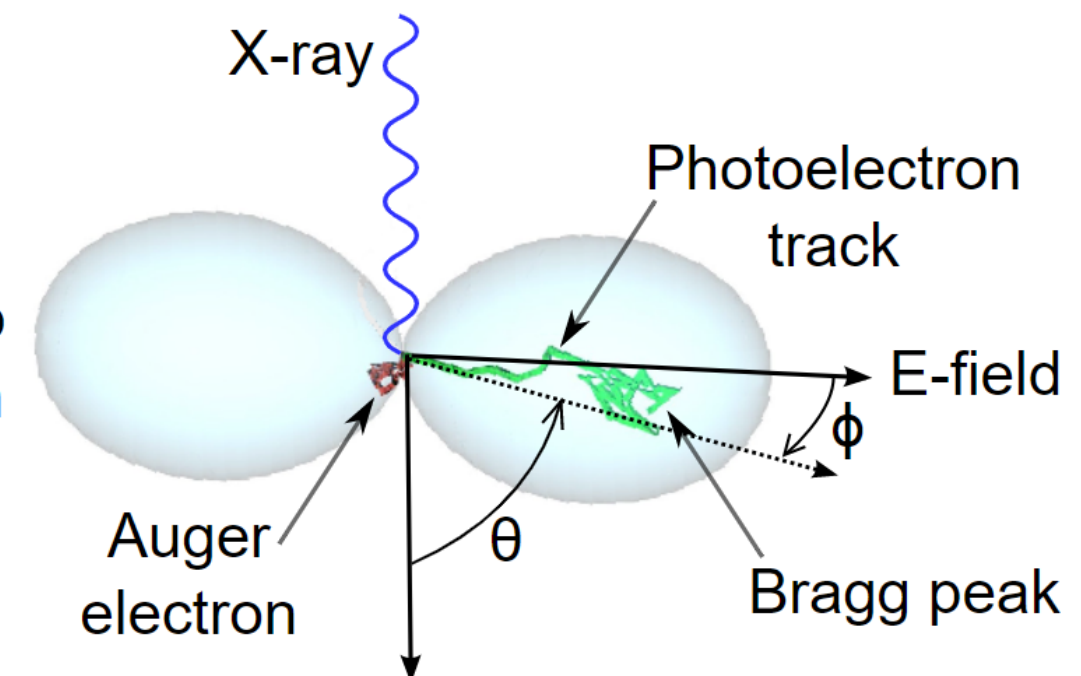
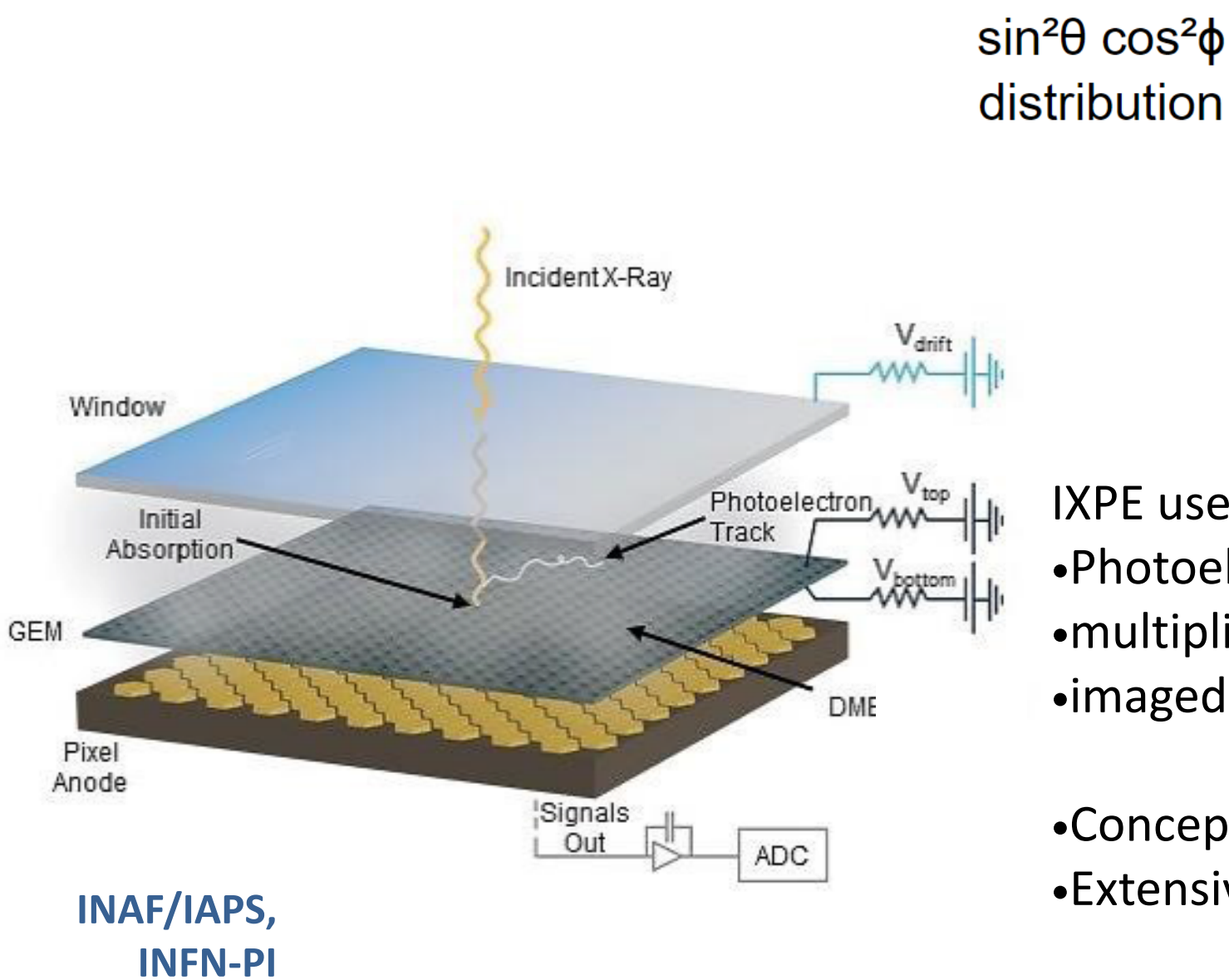
First photo-electron track obtained during IXPE science operations
SNR Cas A, 2022 January 11, initiated by 2.7-keV photon in DU1.

Key is to find photoelectron direction at interaction point.

X-ray polarization via the photoelectric effect

IXPE uses the photoelectric effect.

- Photoelectron ejected along photon E field.

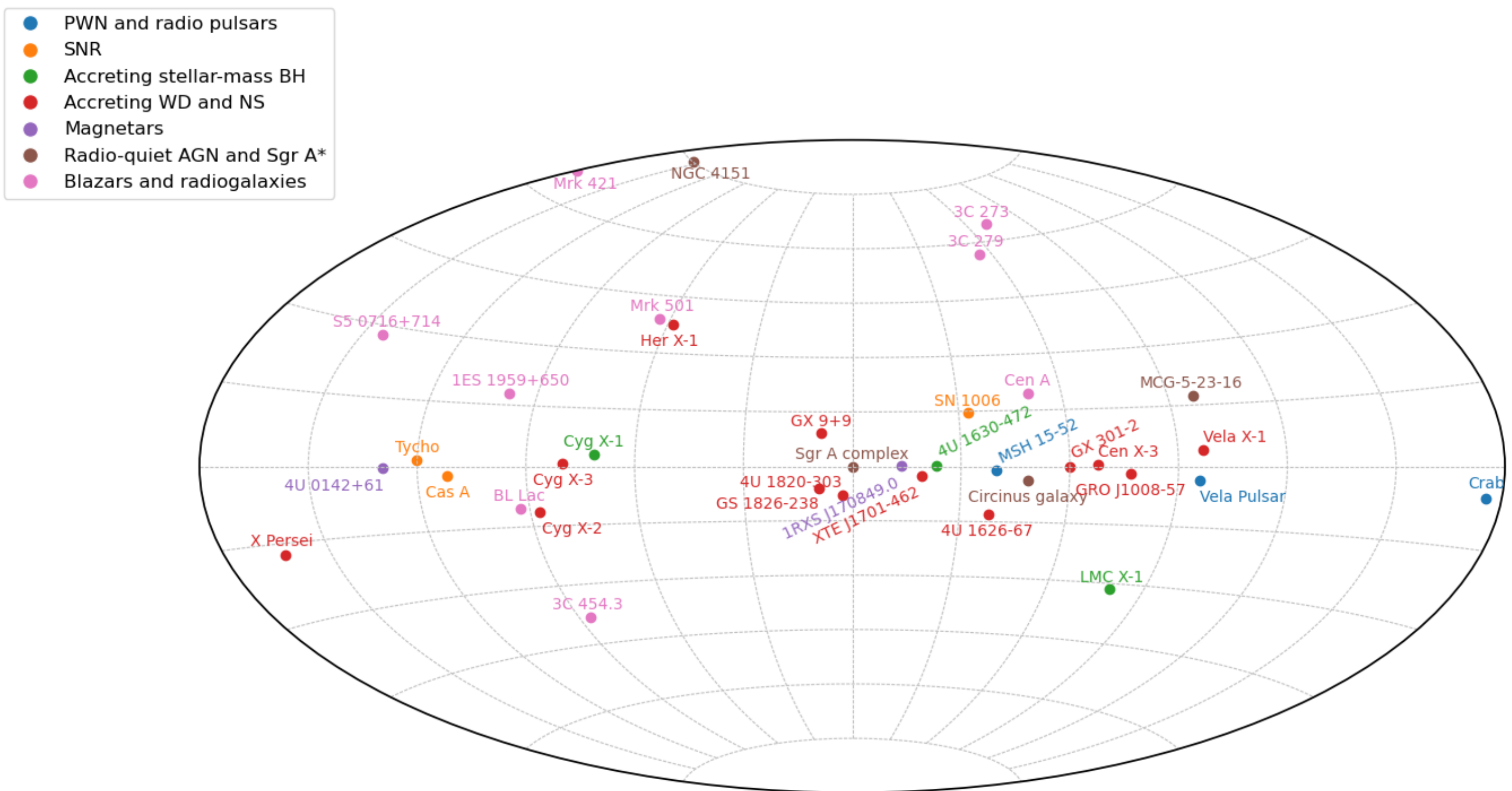


IXPE uses 'gas pixel detector' (GPD).

- Photoelectron liberates electrons in gas (DME),
- multiplied in gas electron multiplier (GEM),
- imaged with 105k hexagonal pixels 50 μ m.

- Concept from Costa et al. (2001)
- Extensive development of readout in Italy.

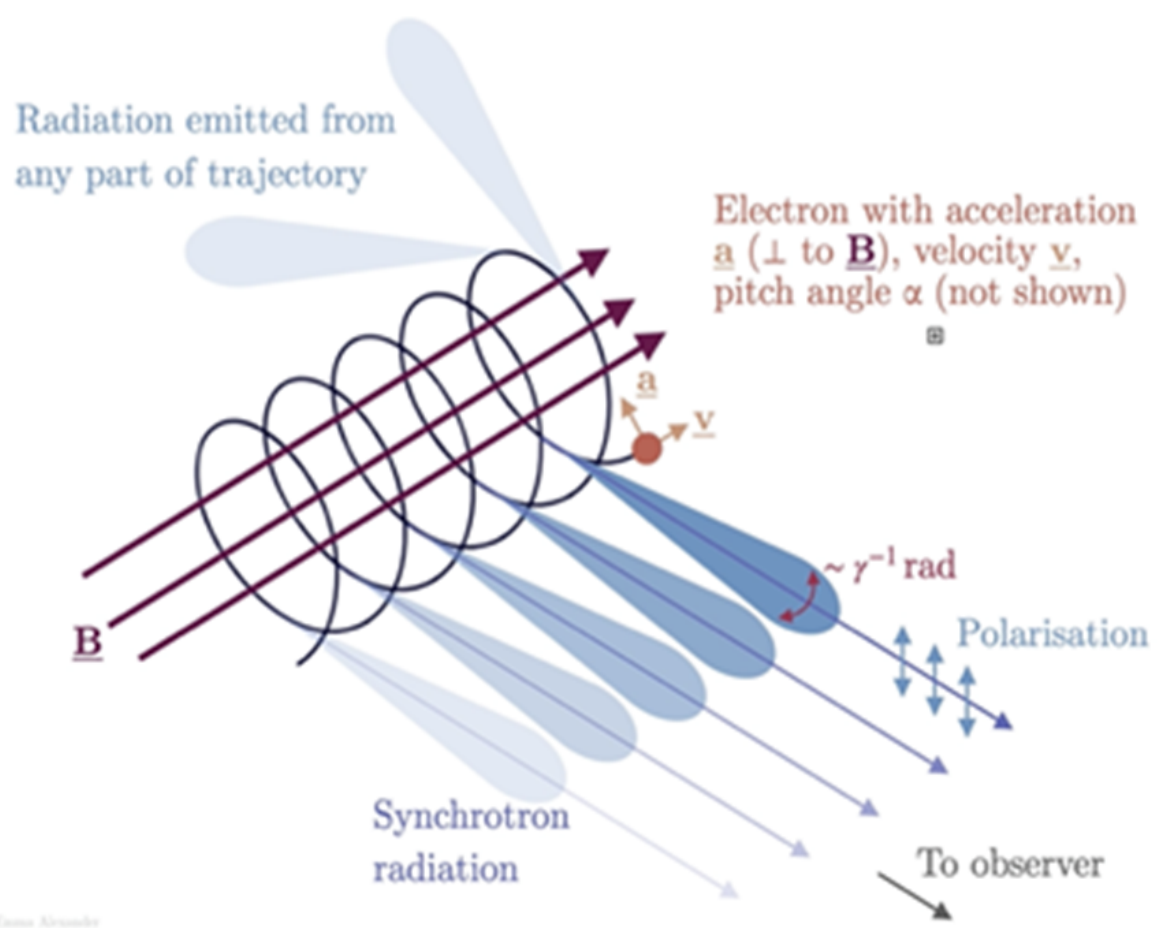
First IXPE targets



Selected IXPE science results

- Blazar jets
- Pulsar wind nebulae
- Supernova remnants
- Radio-quiet active galactic nuclei
- Echoes of Sgr A*
- Accreting stellar-mass black holes
- Accreting neutron stars (low B)
- Magnetars
- Accretion powered pulsars

Emission in first group is via synchrotron radiation



Enrico Alexander

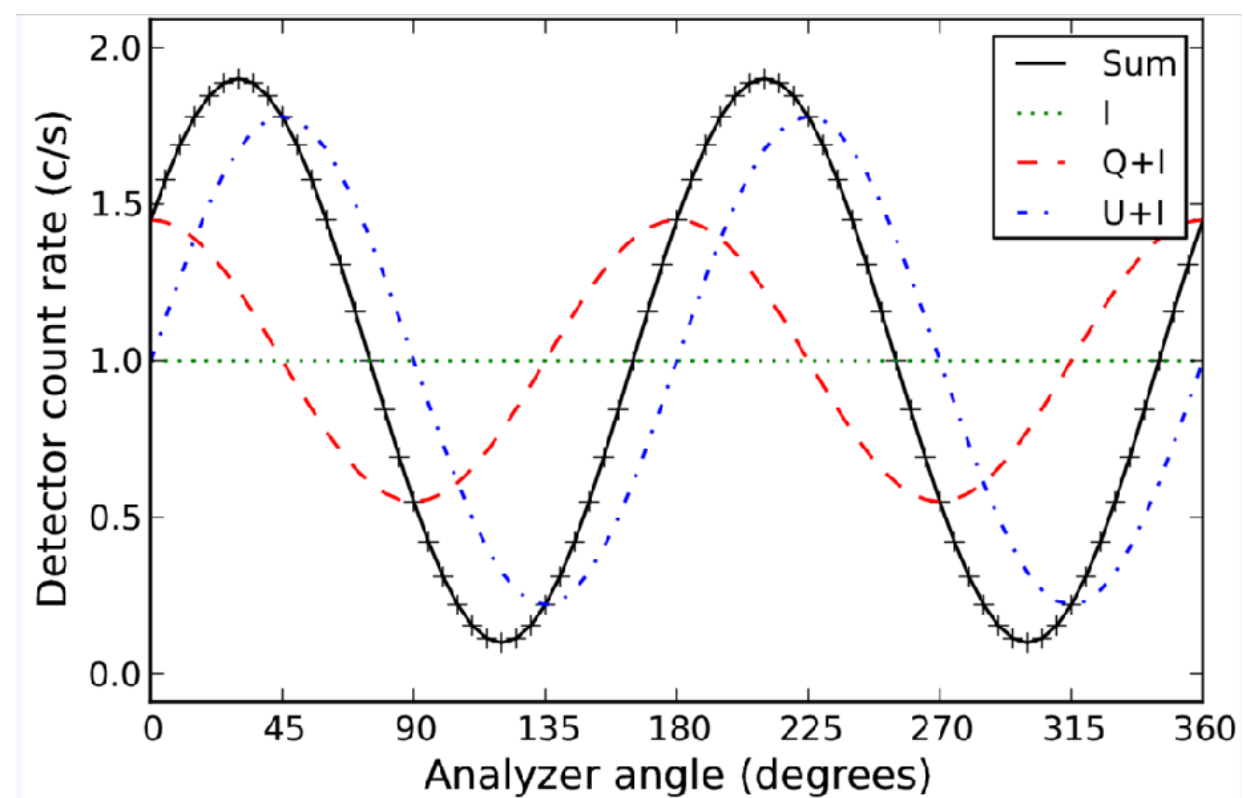
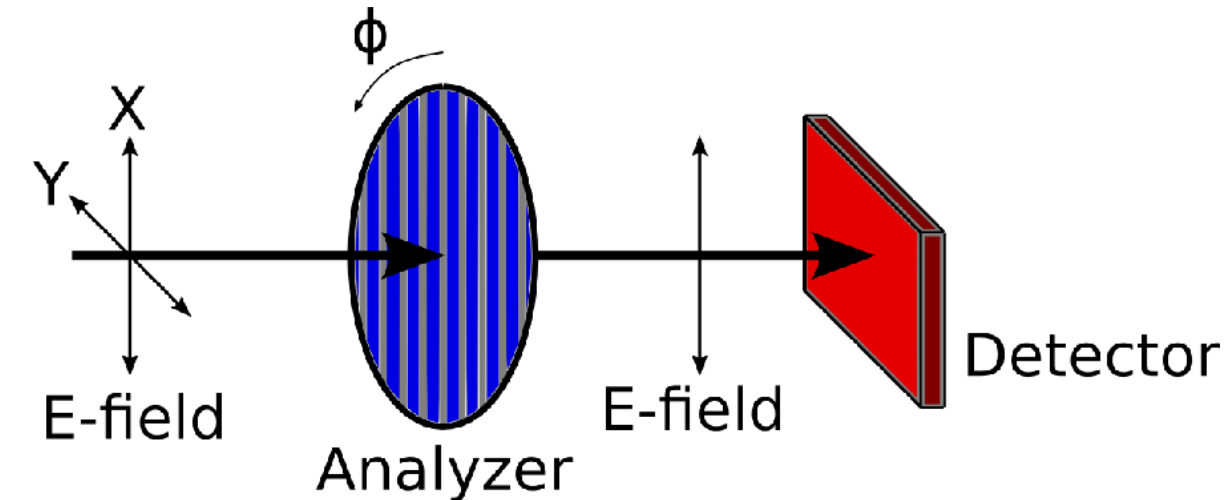
Stokes parameters and MDP

- Work in Stokes parameters
 - Independent, gaussian errors
 - Simply additive
 - No coordinate singularity at $\Pi = 0$
- Compute Stokes parameters (q_i, u_i) for each X-ray from initial direction of photoelectron
- Do spectropolarimetry (in Xspec) using spectra in Stokes I, Q, and U and ‘modulation response’.
- Minimum Detectable Polarization (MDP)

$$MDP_{99} = \frac{4.29}{\mu s} \sqrt{\frac{s+b}{T}}$$

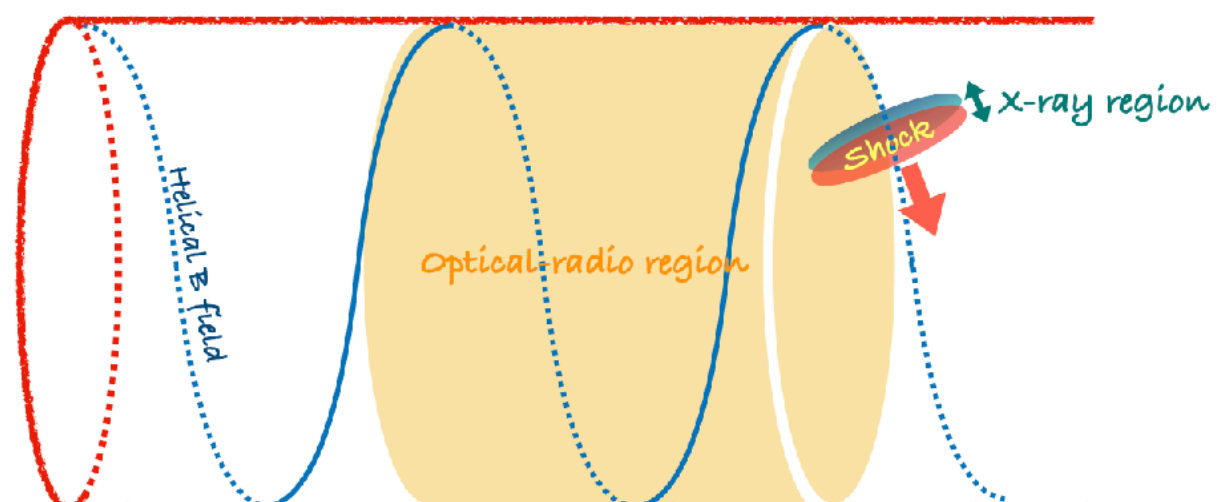
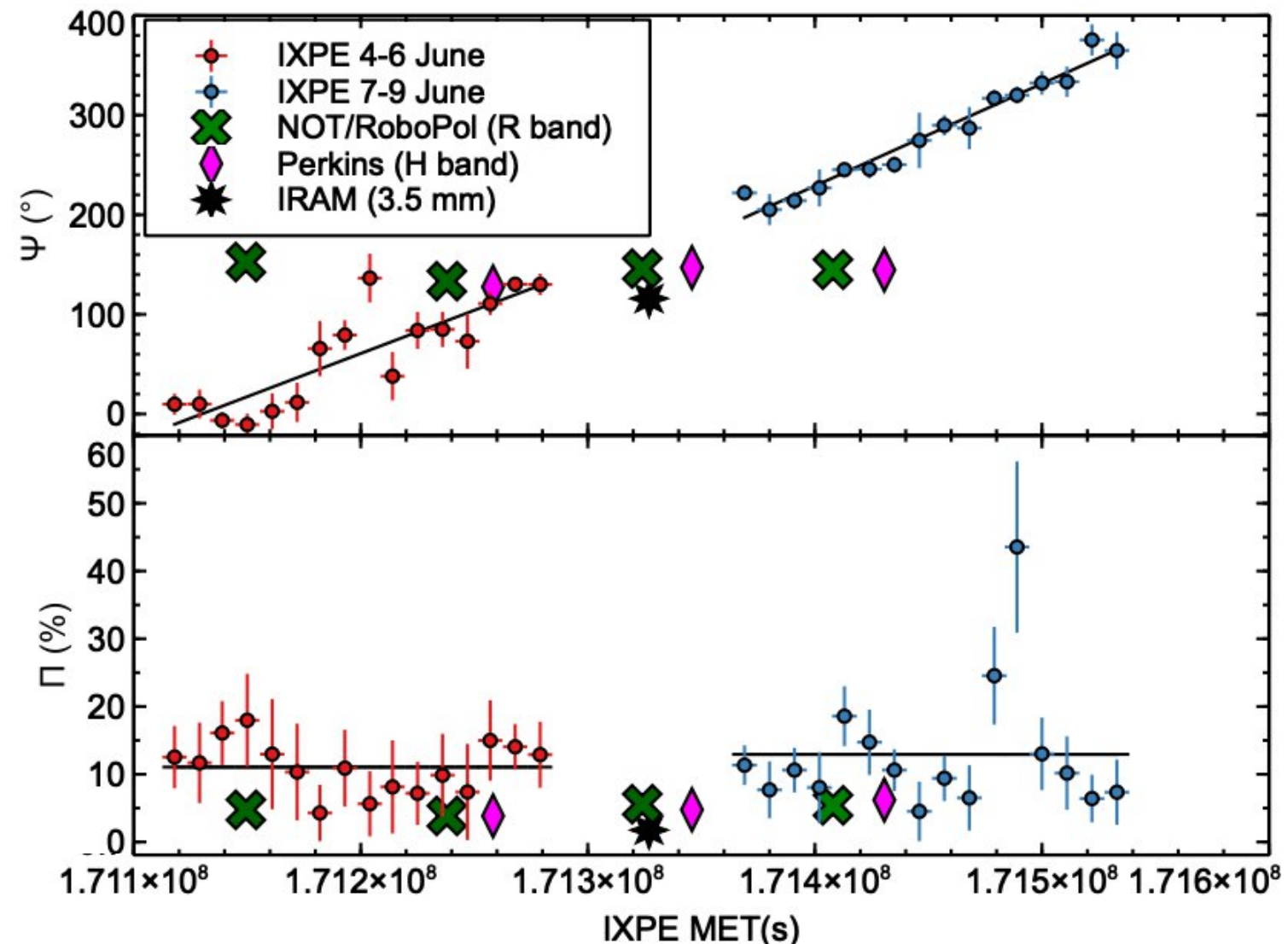
where μ = modulation factor, s = source rate, b = background rate, T = exposure time.

For $MDP = 2\%$ with $\mu = 0.4$ and $b = 0$, need 3×10^5 X-rays.

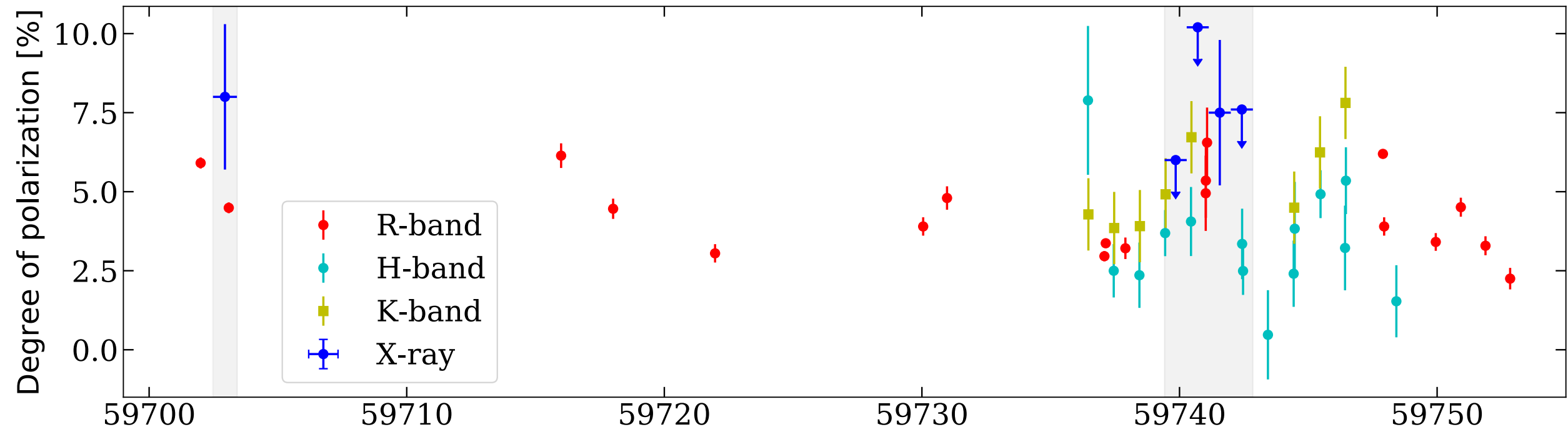


Polarization angle rotation: Mrk 421

- Rotation of the X-ray polarization angle of $\sim 85^\circ/\text{day}$.
- Compatible with compact X-ray emitting region in helical motion around the jet spine.

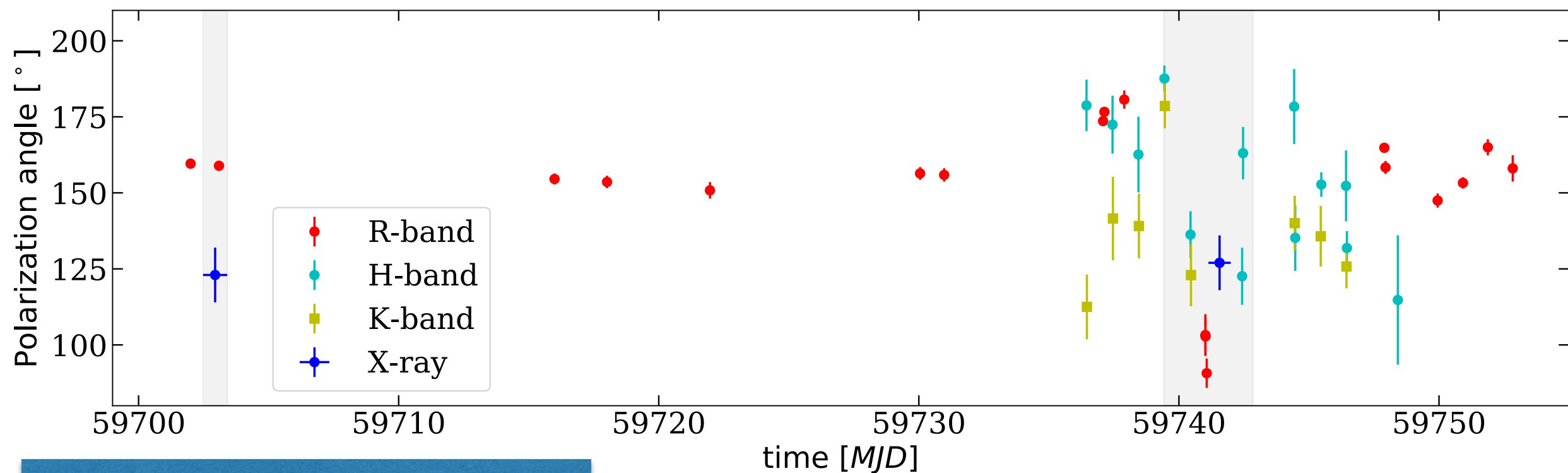
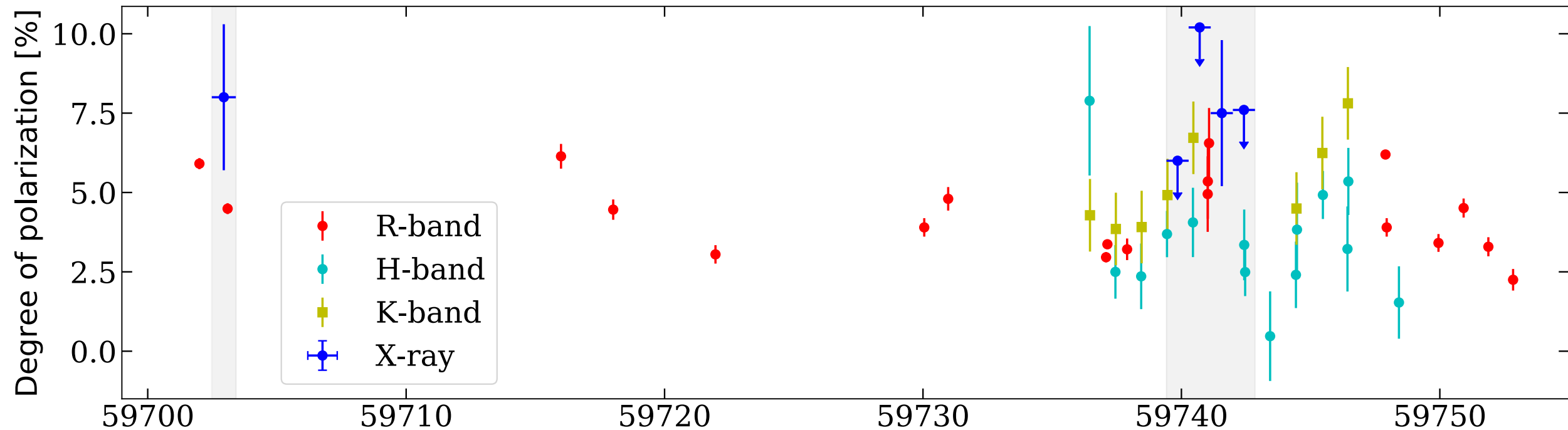


Turbulence in the jet: 1ES 1959+650

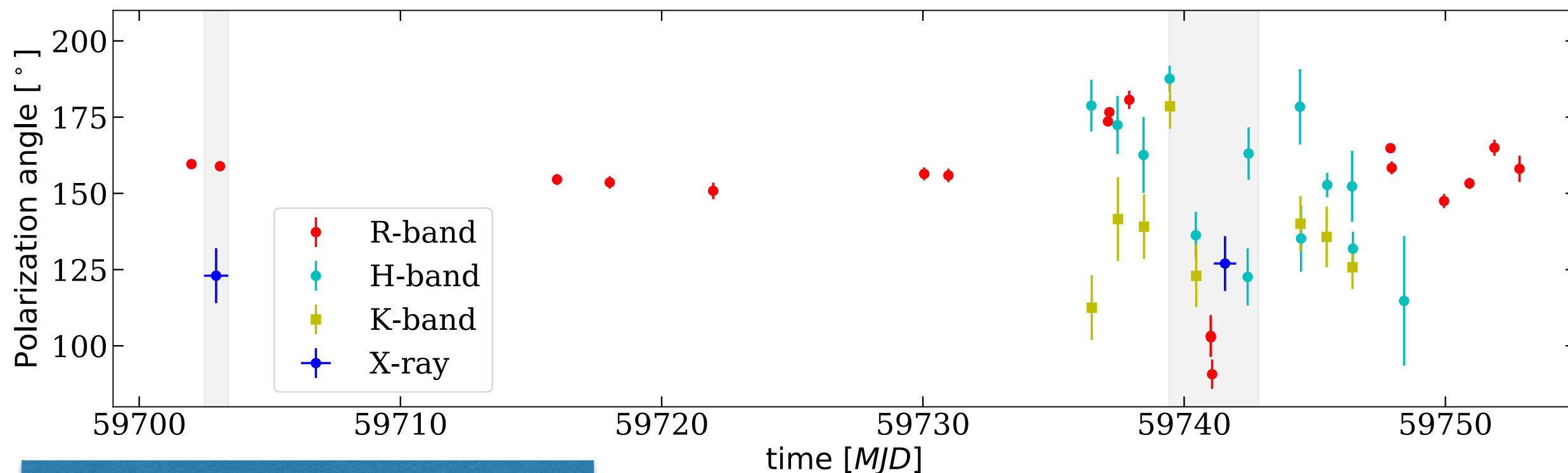
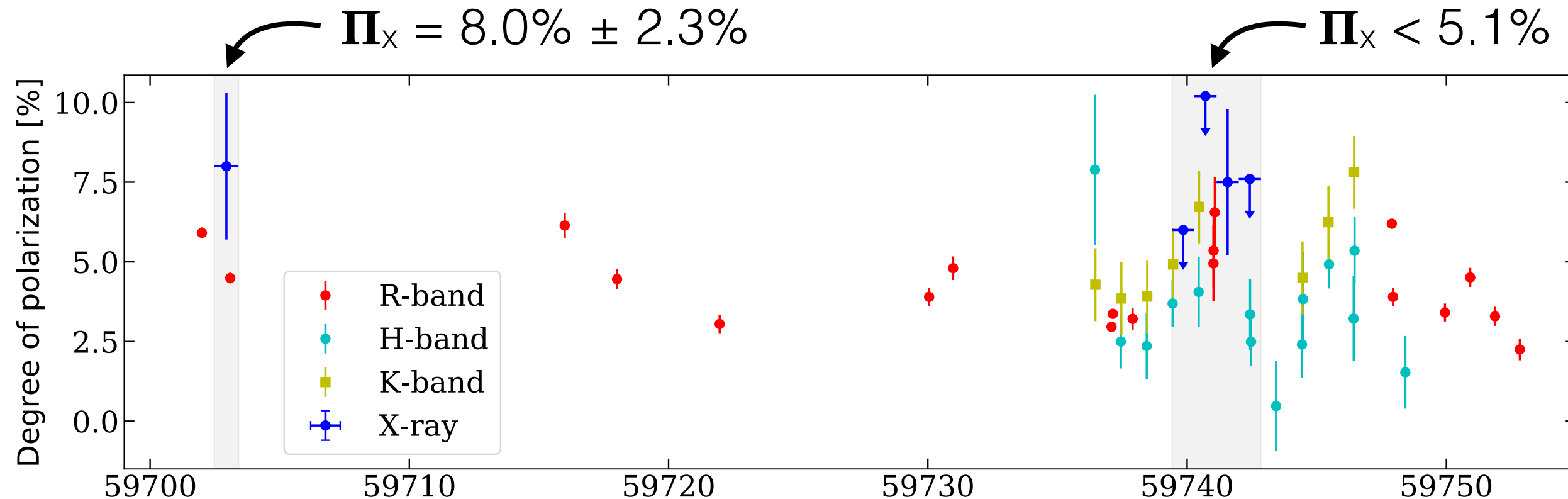


Turbulence in the jet: 1ES 1959+650

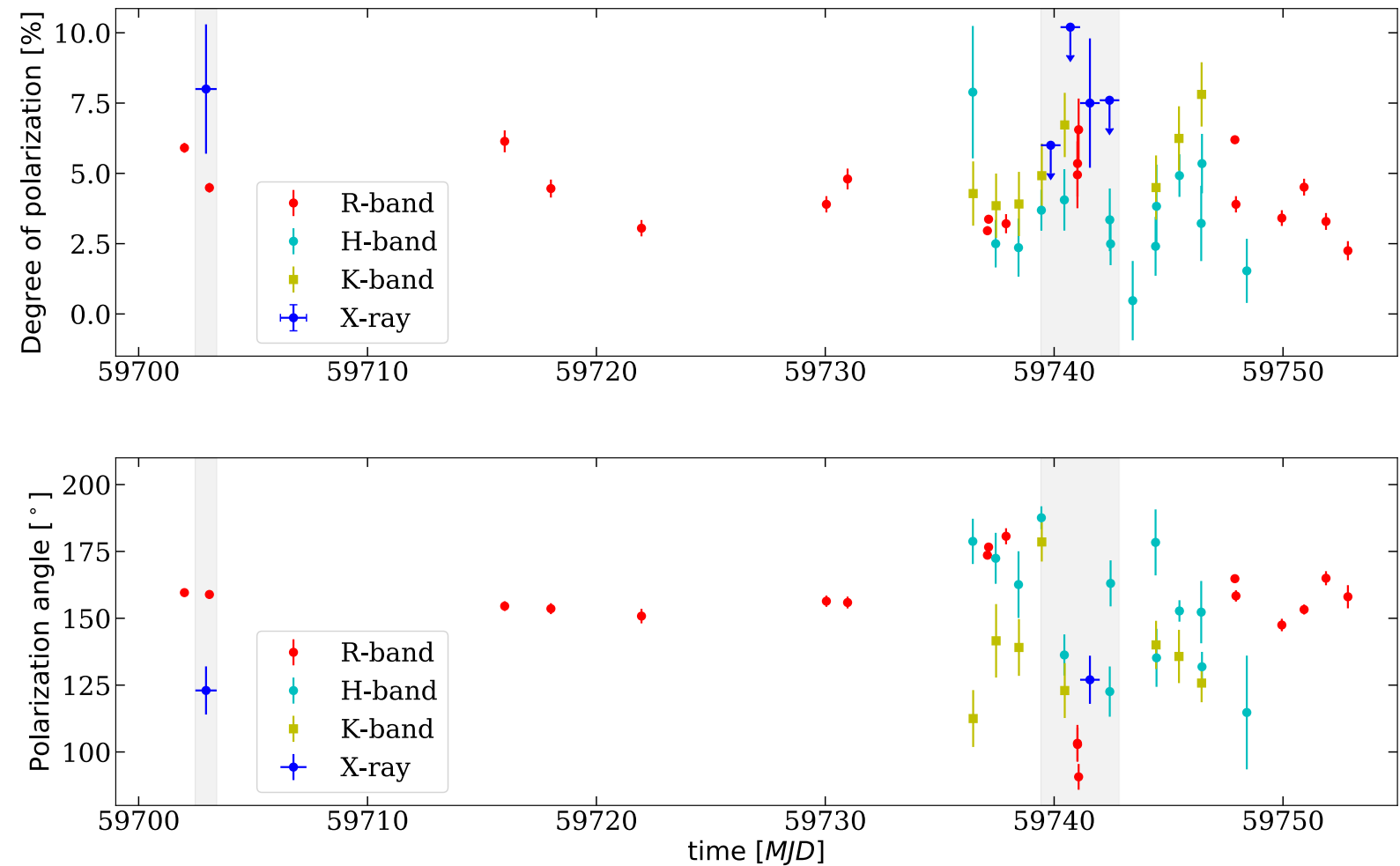
$$\Pi_x = 8.0\% \pm 2.3\%$$



Turbulence in the jet: 1ES 1959+650



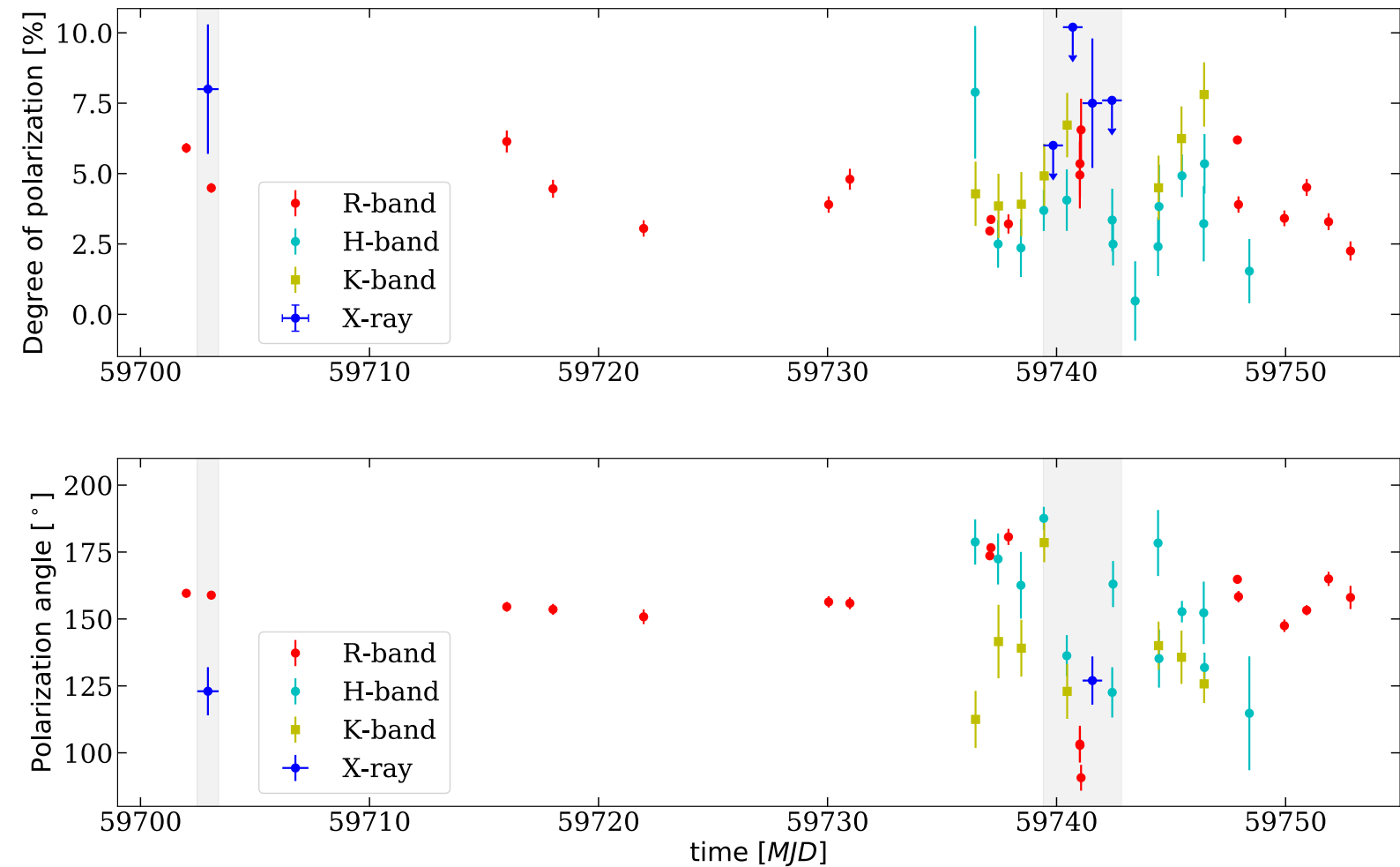
Turbulence in the jet: 1ES 1959+650



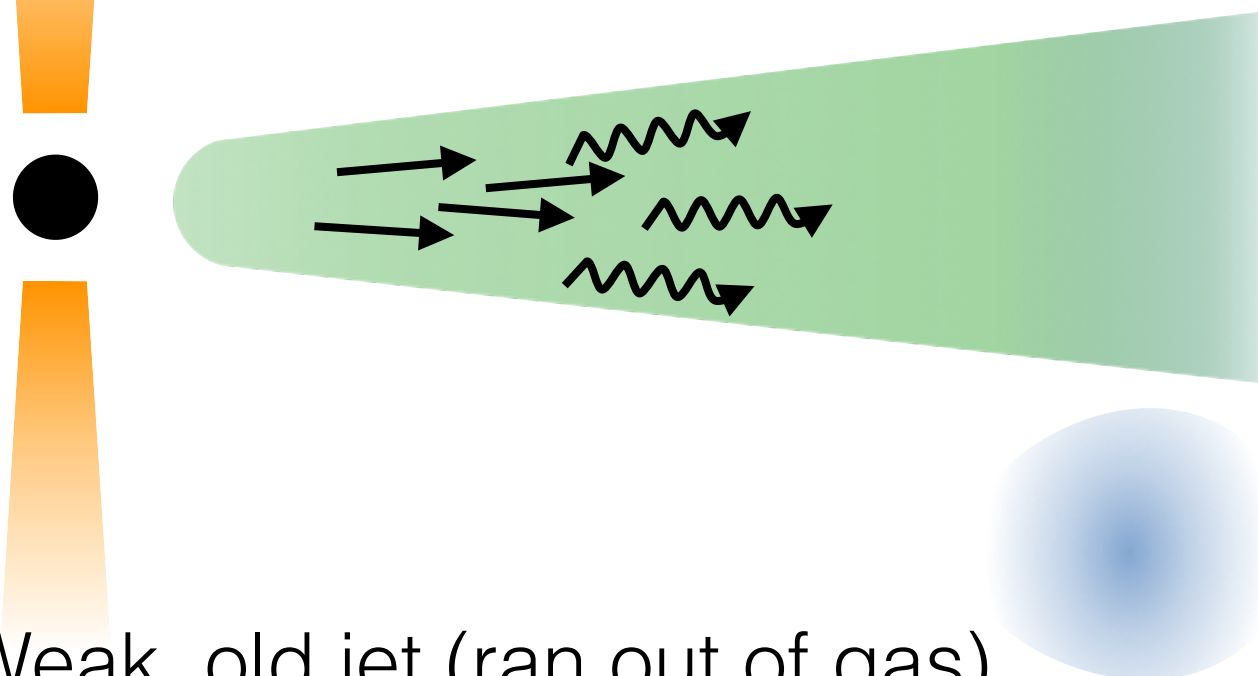
- IXPE makes a time-averaged measurement of X-ray polarization. Depending on flux level and polarization state, it takes IXPE 30-100 ksec or longer to measure the polarization state.
- Changes of X-ray polarization in timescales shorter than the IXPE integration time lead to depolarization.

Turbulence in the jet: 1ES 1959+650

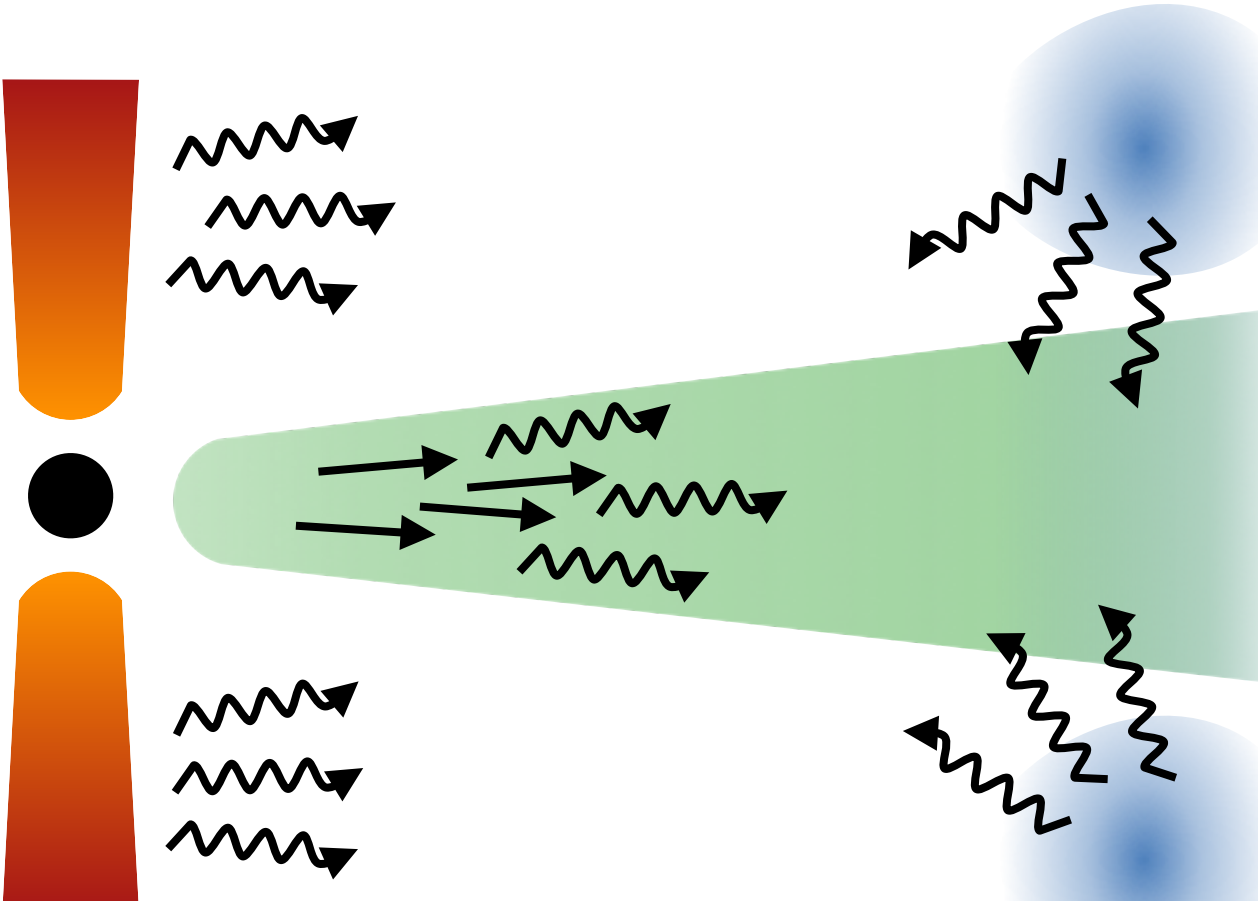
The low X-ray polarization during the second observation of 1ES 1959+650 may be attributed to turbulence in the jet flow with dynamical timescales shorter than 1 day.



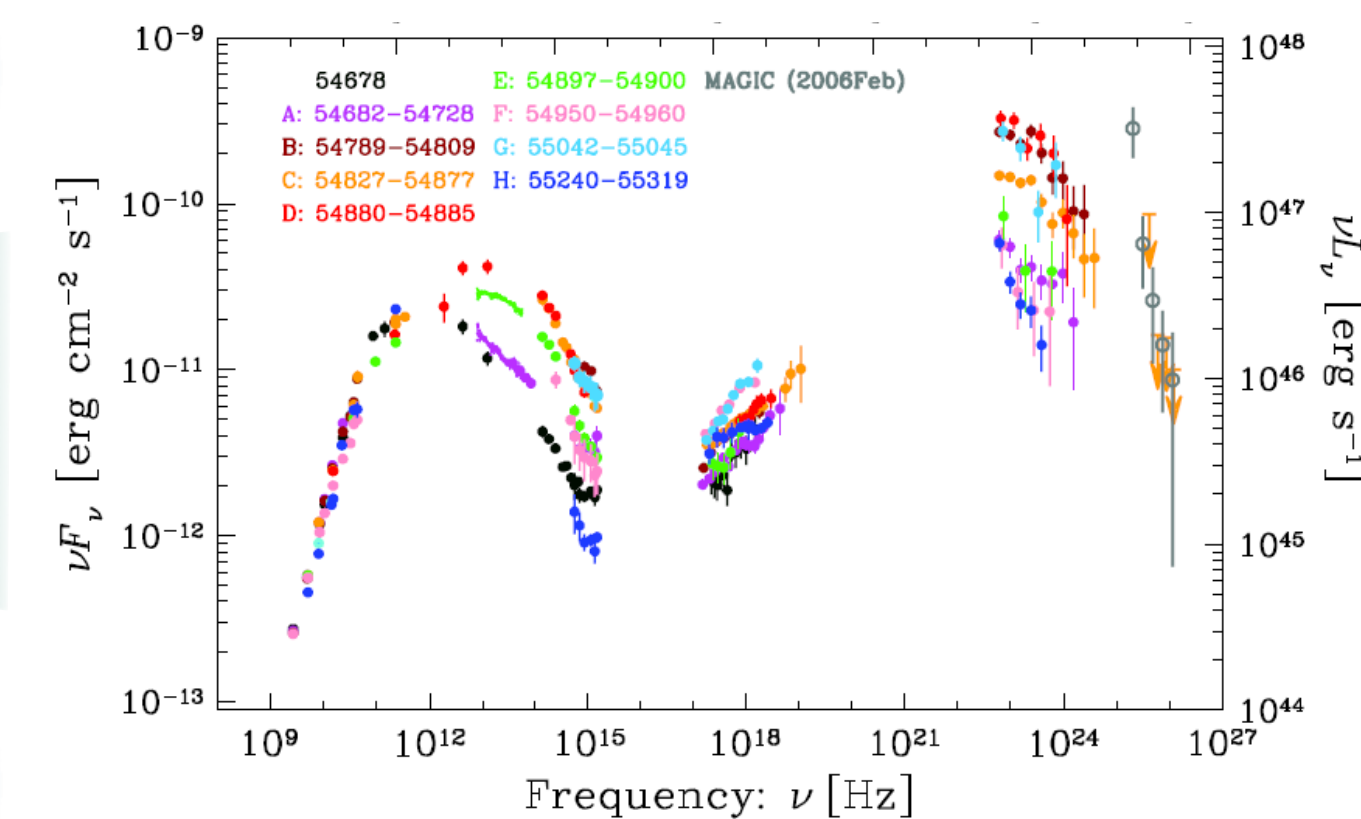
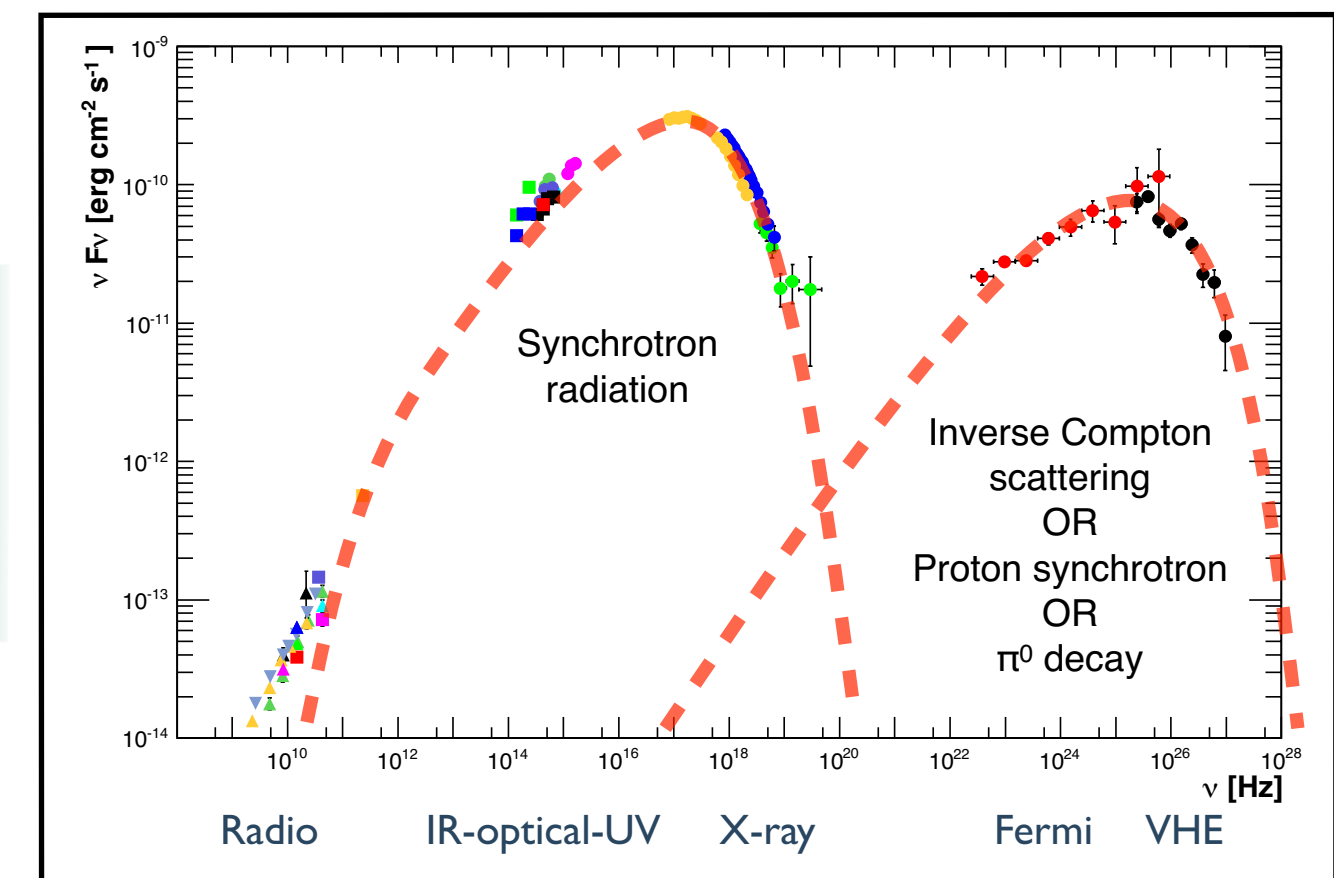
$\rightarrow e^-, e^+, p?$
 \rightsquigarrow photons



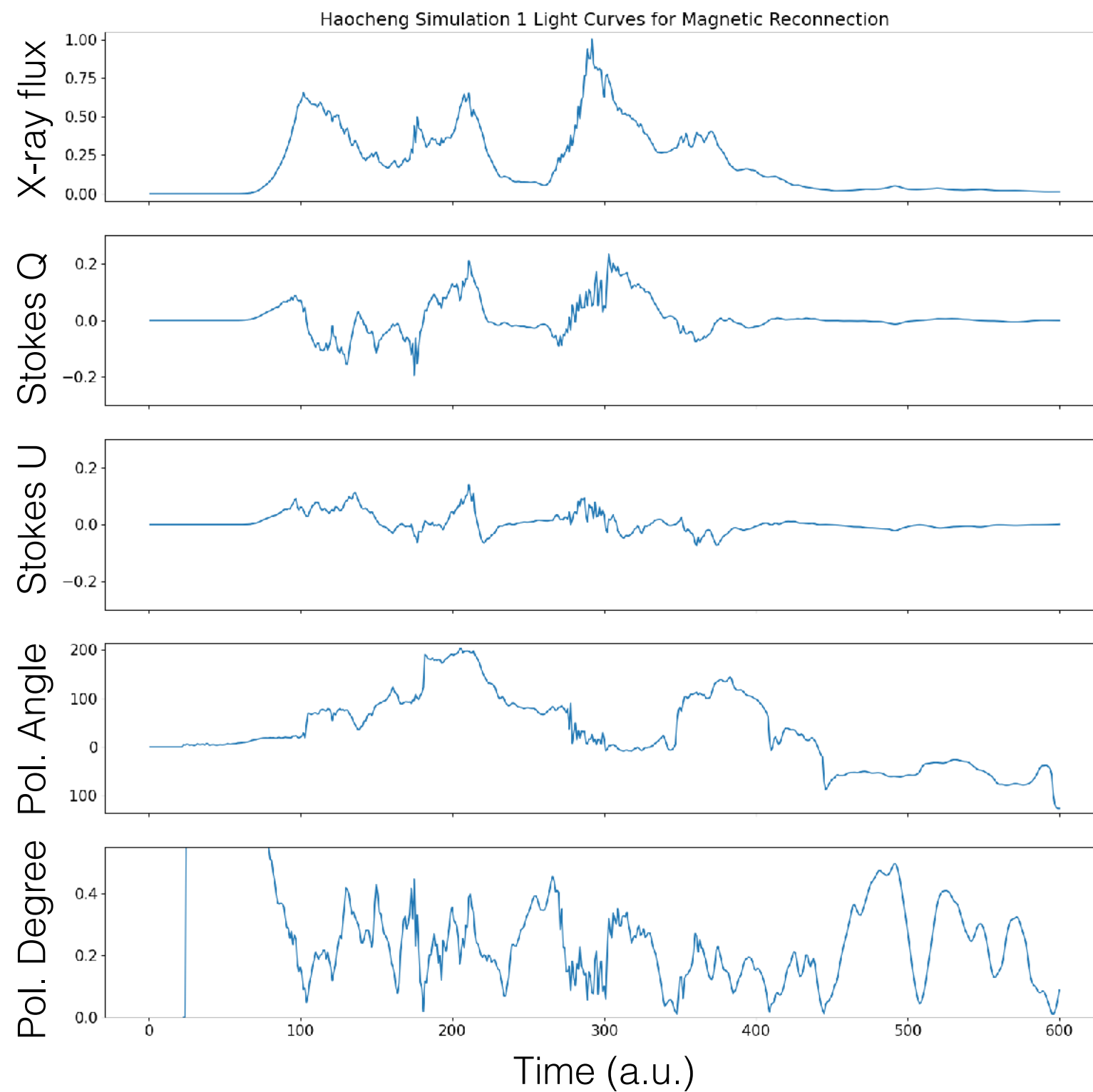
Weak, old jet (ran out of gas)



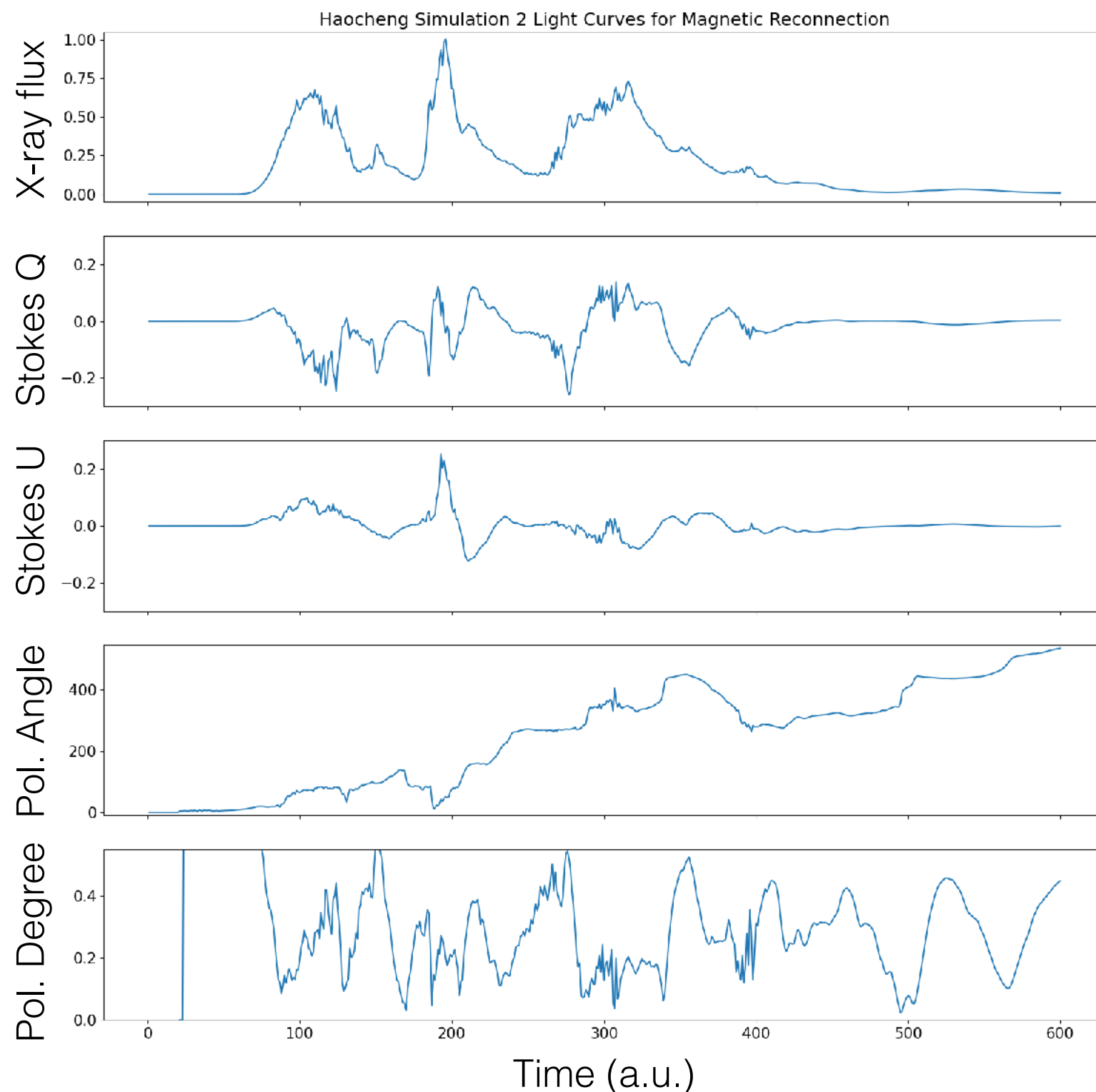
Strong, young jet (gas is available)



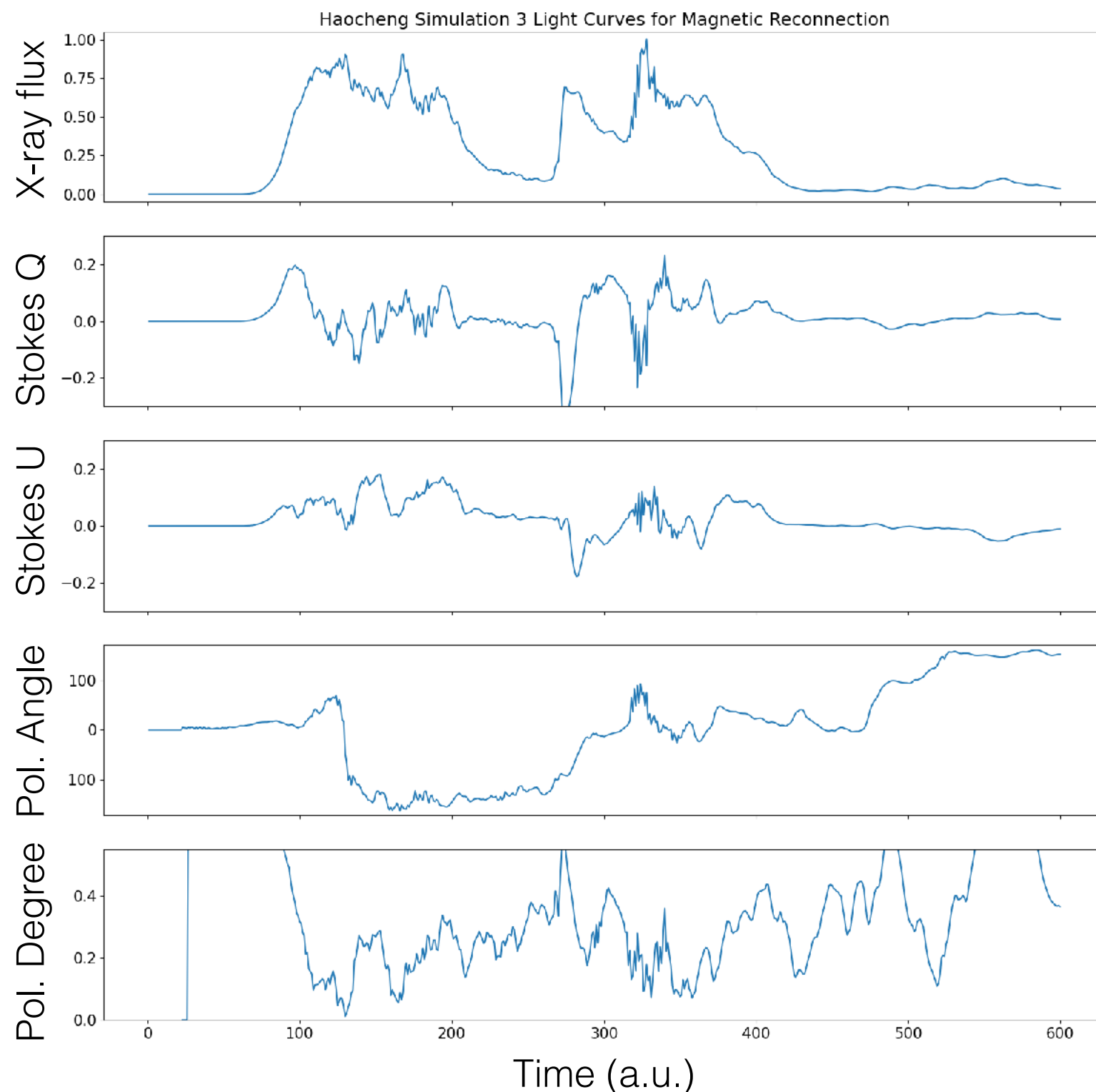
Magnetic reconnection



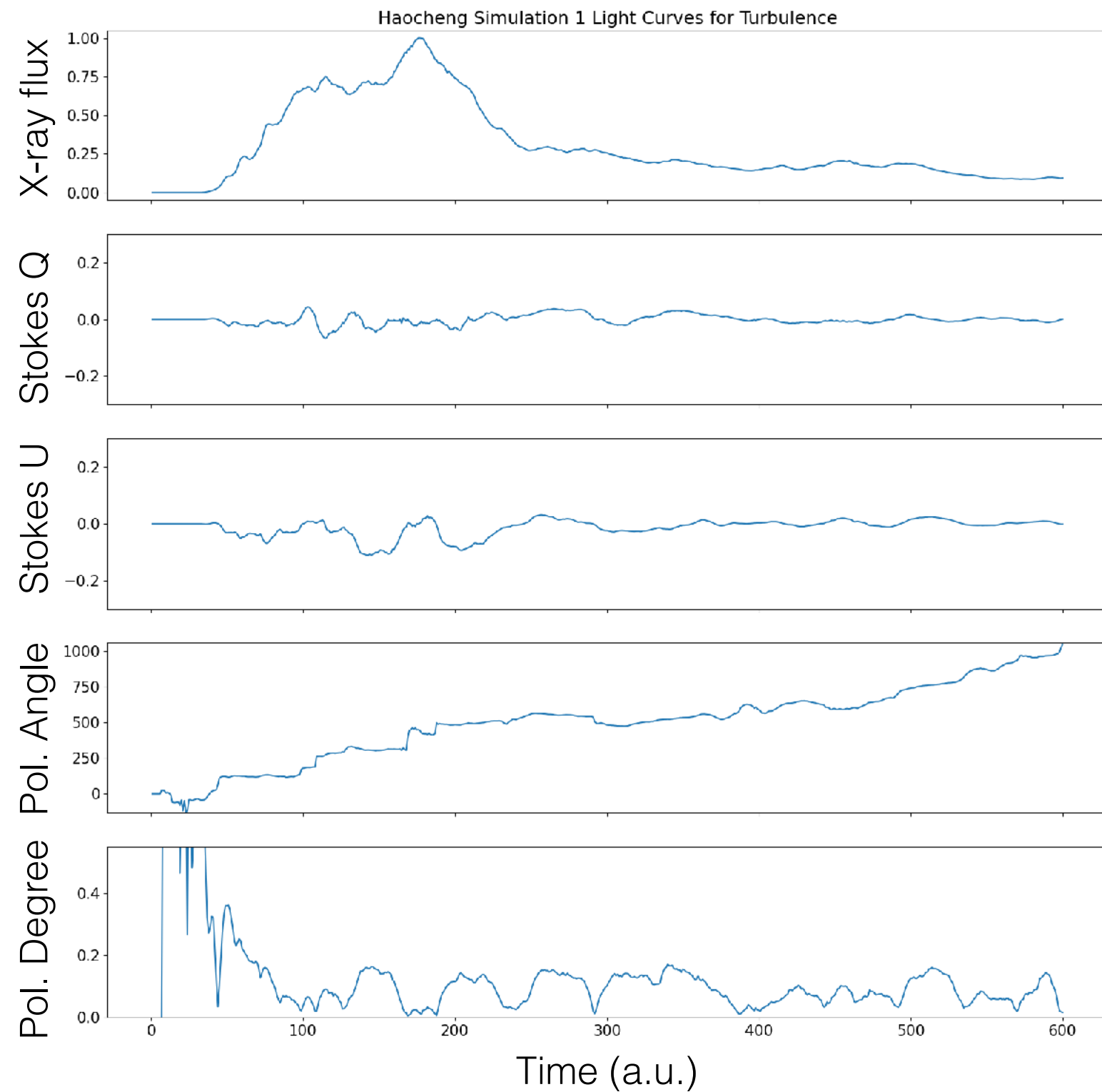
Magnetic reconnection



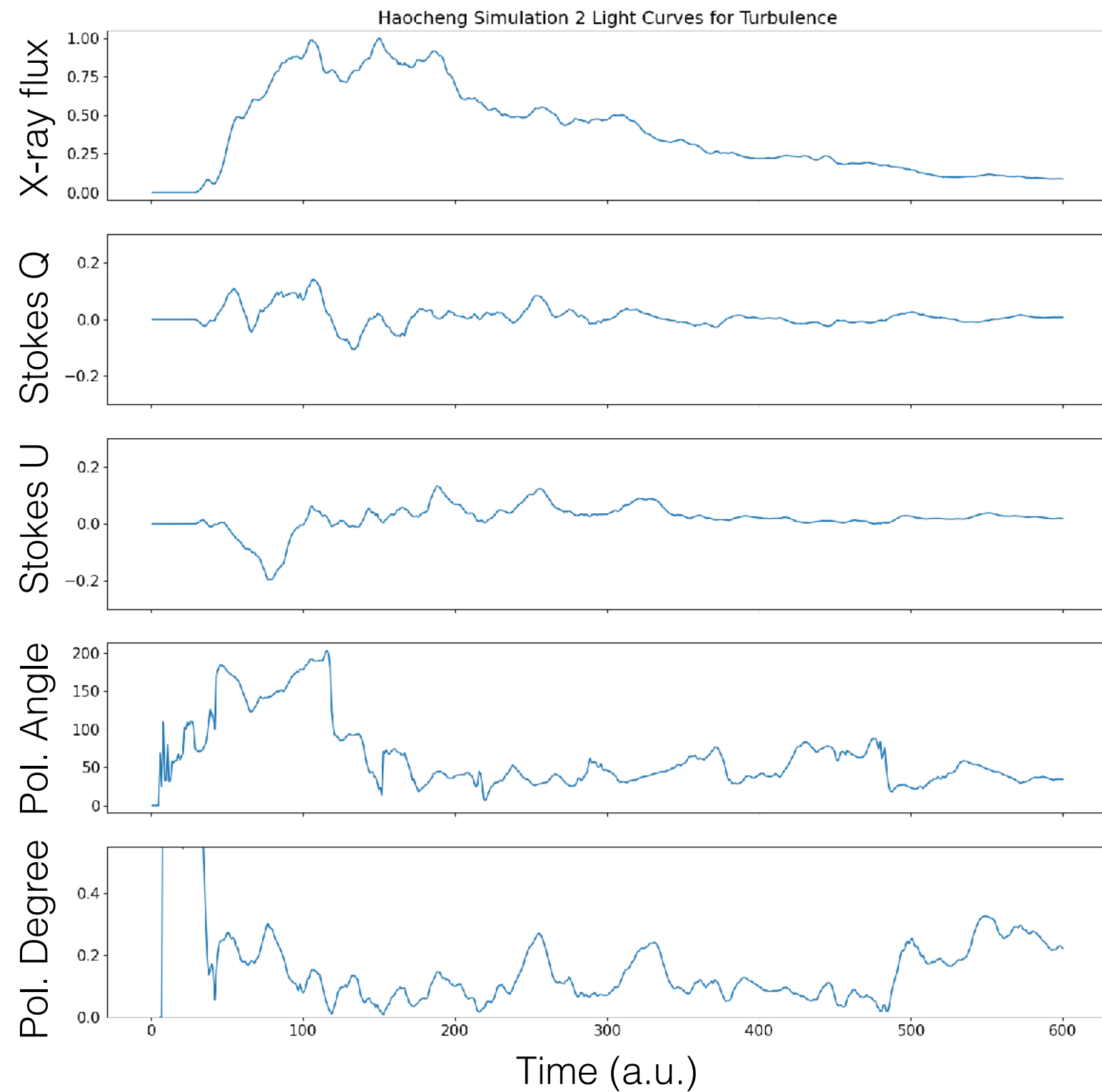
Magnetic reconnection



Turbulent shock acceleration



Turbulent shock acceleration



Turbulent shock acceleration

